DARLI MASSARDO

HISTÓRIA NATURAL E EVOLUTIVA DE *DIONE* HÜBNER, [1819]: UMA ABORDAGEM MORFOLÓGICA E MOLECULAR.

Tese apresentada ao Programa de Pós-Graduação em Biologia Animal, Instituto de Biociências da Universidade Federal do Rio Grande do Sul, como requisito parcial à obtenção do título de Doutor em Biologia Animal.

Área de Concentração: Biologia e Comportamento Animal

Orientador: Prof. Dr. Gilson R. P. Moreira

Universidade Federal do Rio Grande do Sul
Porto Alegre
2013

HISTÓRIA NATURAL E EVOLUTIVA DE

DIONE HÜBNER, [1819]:

UMA ABORDAGEM MORFOLÓGICA E MOLECULAR.

DARLI MASSARDO

Tese aprovada em: 20 de Novembro de 2013.

Prof. Dr. Luiz Alexandre Campos (UFRGS – Porto Alegre)

Prof. Dr. Eduardo Carneiro dos Santos (UFPR – Curitiba)

Profa. Dra. Danessa Schardong Boligon (UNC – Concórdia)

“O futuro pertence àqueles que acreditam na beleza de seus sonhos.”

(Elleanor Roosevelt)

Por isso, dedico esta tese àos meus queridos pais **Nérci** e **Fátima**,

à minha amada irmã **Keli** por sempre acreditarem em mim e

nunca me abandonarem em minhas decisões,

e ao meu querido afilhado **Leonardo.**

Agradecimentos

"Ser lembrado é acima de tudo um agradecimento que deve ser retribuído com um obrigado muito especial, feito de dentro para fora, do coração para o mundo."

(Vinítius Sales)

Por isso agradeço:

Ao orientador

Gilson R. P. Moreira

Aos colaboradores

Marcus R. Kronforst, Héctor A. Vargas, Paula A. Roratto, Gislene L. Gonçalves e Rodrigo Fornel.

Aos amigos do LMCI, colegas e ex-colegas que de alguma forma sempre me ajudaram

Ábner, Ana Kristina, Bruna, Carolina, Danessa, Daniel, Denis, Dirleane, Fernando, Kim, Louise, Rosângela, Sabrina.

Aos professores da Pós-Graduação em Biologia Animal

Ao Laboratório de Citogenética e Evolução

Ao Departamento de Pós-Graduação em Biologia Animal (UFRGS) e ao FAS Center for System Biology (Harvard)

Aos curadores de Lepidoptera que me receberam tão bem

Jackeline Miller (MGCL/FLMNH - Gainesville), Bob Robbins e Brian Harris (USMN - Washington) e Gerardo Lamas (MUSM - Lima), bem como aos demais curadores das outras coleções entomológicas que autorizaram o acesso e o registro dos espécimes deste estudo

Aos que me ajudaram com as fotos de museu

Juan Grados, Kim Ribeiro Barão e Rosângela Brito.

À facilitação ao acesso das borboletas utilizadas neste estudo

Héctor A. Vargas, Carolina Millán, Julian Adolfo Salazar e Sabrina Thiele.

Ao RU pelo almoço de todos os dias

Às pessoas que por um momento me receberam seus lares

Leonardo Ré Jorge (Campinas), Ari Martinez (Gainesville, Flórida), Danessa Boligon e Alexandre Machado (Porto Alegre).

Às fontes financiadoras

CAPES (Doutorado), CNPq (Doutorado Sanduíche) e PPG/BAN.

Aos amigos da UFRGS

Adriano Cavalleri, Augusto Ferrari, Ivanklin Campos-Filho e Felipe Ribeiro, bem como aos demais colegas do departamento.

Aos amigos de Boston

Simone e Christian, Francia e Francisco, Rodrigo, Davi, Yochai, Jaime e Romela, Alexandra, Scott, Kathryn, Adriana e Maria.

Aos amigos do Kronforst Lab

Marcus, Kenny, Ayse, Nicola e Krushnameg.

Aos amigos da academia

Clayton Melo e José Guedes.

Às amigas e amigos do Extremo Oeste Catarinense

Alice, Clarice, Dinara, Eliane, Lisiane, Lulo, Ricardo e Tiago. Em especial à Alice por ter me proporcionado a alegria de ser a "Dinda" do Leonardo.

Às amigas de Porto Alegre

Danessa, Daiana, Fátima e Carolzinha.

Aos amigos queridos de bares e discussões

Alexandre, Fátima, Leonardo e Thiago. Um agradecimento especial ao Alexandre por todos os ensinamentos, discussões, parceria e apoio.

Às aulas de inglês, "sessões de terapia" e claro pela sincera amizade

Patrícia Freitas

À querida amiga Danessa e ao querido amigo Denis pelos mais de 6 anos de amizade e companheirismo.

Às primas queridas

Indiana e Tais

Aos tios e tias amados

Justina e Sérgio, Selita, Marilene, em especial a minha tia Juju por ter me "alimentado" bem e me recebido sempre como filha nesses maravilhosos anos de convívio.

À minha inesquecível fiel amiga

Xaninha 

Aos que sempre em todos os momentos da minha vida me apoiaram, deram suporte, alegrias e acima de tudo muito amor

Meus pais Fátima e Nérci, minha irmã Keli e meu cunhado Alemão.

"Talvez não tenha conseguido fazer o melhor, mas lutei para que o melhor fosse feito. Não sou o que deveria ser, mas Graças a Deus, não sou o que era antes".

(Marthin Luther King)

SUMÁRIO

RESUMO

Entender as relações filogenéticas entre os organismos, como espécies compartilham uma história comum através de sua ancestralidade, é fundamental para o entendimento de processos e padrões evolutivos. Os heliconíneos, ou borboletas-do-maracujá, constituem-se num dos grupos mais conhecidos em Lepidoptera (Nymphalidae). Do ponto de vista filogenético Heliconiini é uma das tribos mais estudadas da família, sendo que seis filogenias já foram propostas, tanto de cunho morfológico quanto molecular, todas com enfoque nos gêneros mais derivados da tribo, como *Heliconius* e *Eueides*. Porém, nenhuma dessas filogenias propôs de forma robusta as relações em nível de espécie na maioria dos gêneros. Este é o caso de *Dione*, uma linhagem considerada "basal" de Heliconiini, pouco conhecida, com status filogenético ainda não bem resolvido. Tendo como objetivo aprofundar os estudos morfológicos e moleculares dentro deste gênero, neste trabalho, descreve-se e ilustra-se pela primeira vez as estruturas externas do ovo, larva e pupa *D. glycera*, única espécie do gênero ainda não contemplada neste sentido, além de fornecermos uma chave dicotômica para identificação das espécies de *Dione* nas fases de larva e pupa. Com o intuito de desenvolver trabalhos futuros em nível subespecífico e/ou calcados na genética de populações, desenvolvou-se um banco de microssatélites para a espécie *Dione moneta*, onde obteve-se 19 loci polimórficos, sendo que a maior parte desses amplificou com sucesso nas demais espécies e subespécies de *Dione*, bem como para a espécie irmã *Agraulis vanillae*. Tal resultado demonstra que estes marcadores podem ser ferramentas eficientes para estudos a respetio em *D. moneta* bem como para espécies de borboletas proximamente relacionadas. Em adição, propomos uma filogenia molecular para Heliconiini onde calculou-se o tempo de divergência entre as linhagens da tribo. Com enfoque principalmente no gênero *Dione* nossos dados demonstram que este é monofilético e grupo irmão de *Agraulis*. Também demonstramos que as espécies de *Dione* são reciprocamente monofiléticas, formam grupos

genéticos distintos e são fenotipicamente distinguíveis. Entretanto não foi possível separar as subespécies de *D. juno* e *D. moneta* através do padrão de coloração das asas, cuja validade taxonômica é questionada. O tempo de divergência estimado para o gênero (aproximadamente 30 milhões de anos) sugeriu fortemente que a especiação de *Dione* coincidiu com a ascensão de Passifloraceae e o soerguimento da Cordilheira dos Andes. Os resultados obtidos neste estudo demonstram que uma ampla cobertura geográfica e abordagens taxonômicas integrativas são ferramentas que permitem inferir com maior robustez os limites de espécies e subespécies.

APRESENTAÇÃO

Esta tese está estruturada em uma Introdução Geral com o objetivo de abranger todo o tema estudado, seguido de 3 capítulos autônomos, de forma que cada um apresenta seções independentes relativas à introdução do tema estudado, métodos empregados, resultados obtidos, discussão e referências bibliográficas.

No Capítulo I são descritos os imaturos da espécie *Dione glycera*, a única espécie do gênero que ainda não possuia tais informações. A morfologia dos imaturos de *Dione glycera* é ricamente detalhada através de microscopia eletrônica de varredura e desenhos correspondentes.

No Capítulo II é apresentado o desenvolvimento de um banco de *loci* de microssátelites para a espécie *Dione moneta* bem como a amplificação para as demais espécies do gênero *Dione* e para a espécie irmã *Agraulis vanillae*.

No Capítulo III é proposta a filogenia molecular do gênero *Dione* com uma abordagem integrativa de análises de morfometria geométrica e distribuição geográfica com o objetivo de esclarecer a história evolutiva dessa linhagem de borboletas.

Cada capítulo está formatado de acordo com as normas de publicação das revistas que os artigos foram publicados e/ou submetidos. As considerações finais sintetizam os resultados encontrados neste estudo.

1. INTRODUÇÃO GERAL

1.1 Heliconiini

Os heliconíneos, popularmente conhecidos como borboletas-do-maracujá, constituem um dos grupos mais estudados em Lepidoptera (Brown 1981; Penz 1999; Beltrán et al. 2007). Devido à coloração aposemática dos adultos, participação em anéis miméticos e a alta variabilidade genética e fenotípica, têm sido objeto de estudos taxonômicos há mais de um século (Stichel 1906; Michener 1942a; Emsley 1963; Brown & Mielke 1972; Turner 1976; Brown 1981; Brower 1994; Brower & Egan 1997; Penz 1999). A tribo também tem servido como modelo para o entendimento de coevolução entre insetos e plantas (Ehrlich & Raven 1965; Gilbert 1975; Benson et al. 1975; Brower 1997; Rodrigues & Moreira 2004; Bianchi & Moreira 2005; Kerpel et al. 2006), a base genética de determinados fenótipos (Turner 1971; Sheppard et al. 1985, Jiggins et al. 2005; Chamberlain et al. 2011; Hill et al. 2013), biologia de populações (Gilbert & Smiley 1978; Benson 1978; Mallet 1986) e conservação (Brown 1981; Gilbert 1991; Brown & Freitas 2000), especiação e hibridação (Mallet et al. 2007; Mallet 2008, 2009; Chamberlain et al. 2009; Kronforst et al. 2009; Kronforst 2012).

As espécies do grupo são reconhecidas não apenas por diferenças no padrão de coloração das asas, mas também pela morfologia da genitália e, em alguns casos, também por dados moleculares (Brower 1994; Jiggins et al. 1996; Jiggins & Davies 1998; Giraldo et al. 2008).

As subespécies são reconhecidas por raças geográficas, diferenças no padrão de coloração das asas e abundantes genótipos híbridos em zonas de contato (Holzinger & Holzinger 1994; Braby et al. 2012). Porém, muitas subespécies de heliconíneos não se encaixam na definição de subespécies como fenótipos geograficamente separados (Brown Jr.

1979; Mallet 2001). Ao contrário, em várias regiões, multiplos fenótipos co-ocorrem, e são mantidos provavelmente por mimetismo como modelos alternativos (Joron et al. 2011).

Segundo Penz & Peggie (2003), Heliconiinae encontra-se subdividida em 4 tribos: Acraeini, Heliconiini, Vagrantini e Argynnini. A tribo Heliconiini distribui-se por toda a região Neotropical e, atualmente, possui cerca de 70 espécies válidas, distribuídas em 10 gêneros, que são: *Agraulis* Boisduval & Le Conte, *Dione* Hübner, *Dryadula* Michener, *Dryas* Hübner, *Eueides* Hübner, *Heliconius* Kluk, *Laparus* Billberg, *Neruda* Turner, *Philaethria* Billberg e *Podotricha* Michener (Lamas 2004) (Figura 1).

Dentre os gêneros que compõem a tribo Heliconiini, *Heliconius* e *Eueides* são os que apresentam maior variabilidade morfológica no padrão de coloração das asas. Apenas para *Heliconius* são nominadas atualmente cerca de 50 espécies e 1500 subespécies (Holzinger & Holzinger 1994; Lamas 2004), além de ser um dos gêneros mais estudados da família Nymphalidae (Brown Jr. 1981; Brower 1994; Beltrán et al. 2007; Mallet 2009; Chamberlain et al. 2011; Hines et al. 2011; Kronforst 2012; Nadeau et al. 2012; Rosser et al. 2012). Em contraponto, os gêneros "basais" da tribo como *Agraulis*, *Dione*, *Philaethria* e *Podotricha* apresentam baixa diversidade fenotípica, porém diversas espécies e subespécies descritas, resultando em complexos agrupamentos taxonômicos de difícil identificação.

1.2 *Dione* Hübner, [1819]

O gênero *Dione* assim como *Agraulis*, *Podotricha*, *Dryadula* e *Dryas*, apresentam a venação da célula discal da asa posterior aberta, são palatáveis e o vôo é caracterizado como rápido para evitar a predação (Emsley 1963; Brown Jr. 1981).

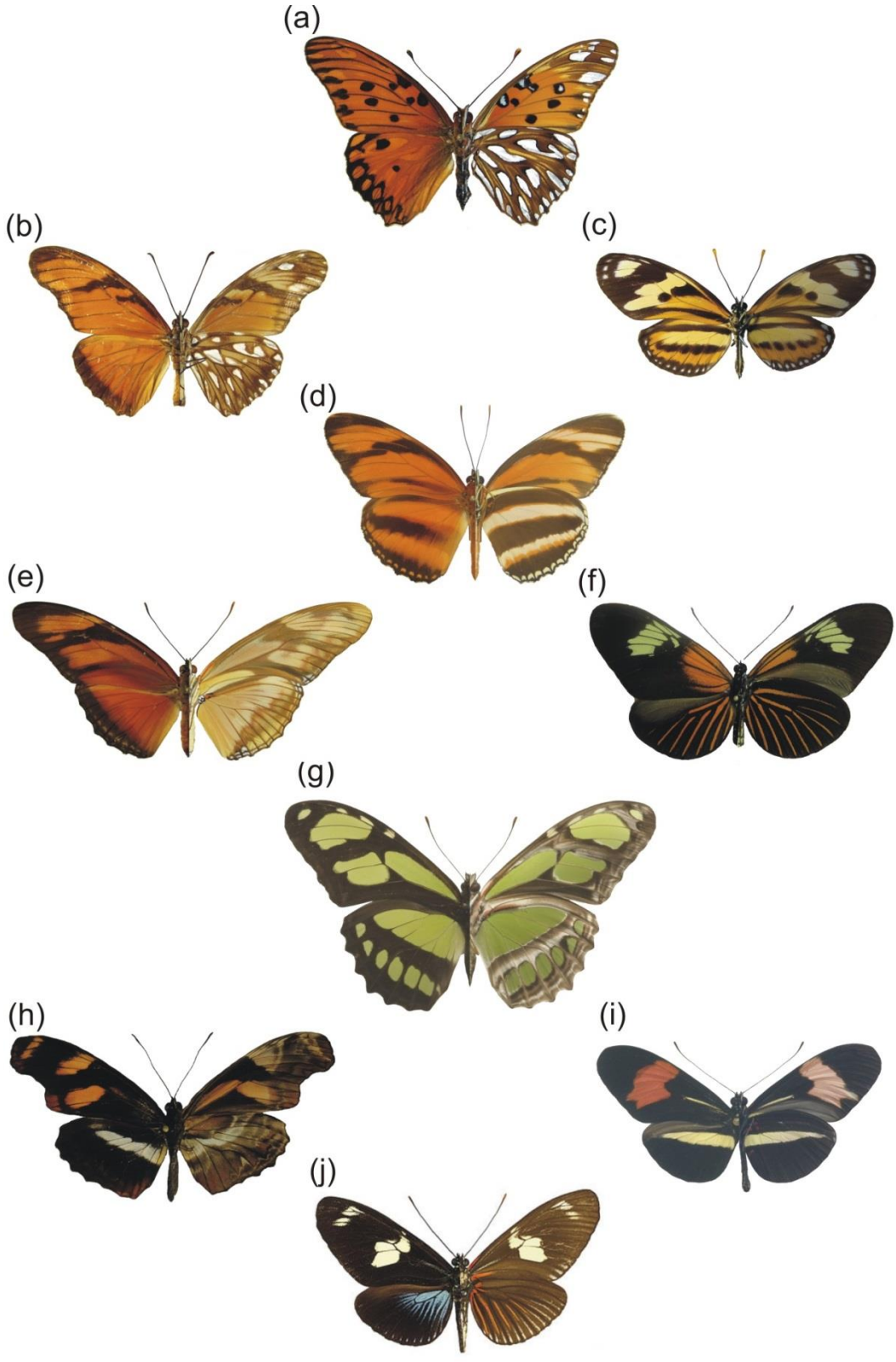

Figura 1. Representação dos gêneros que compõem a tribo Heliconiini, vistas dorsal e ventral, respectivamente. (a) *Agraulis*; (b) *Dione*; (c) *Eueides*; (d) *Dryadula*; (e) *Dryas*; (f) *Neruda*; (g) *Philaethria*; (h) *Podotricha;* (i) *Heliconius*; (j) *Laparus*. Fonte: adaptado de Silva (2010).

O gênero *Dione* é diagnosticado em relação aos demais, pela coloração de fundo laranja com manchas pretas, lado ventral com manchas em forma de pérolas prateadas, bem como pela margem distal da asa anterior recortada (irregular, esculpida) e a androcônia dos machos presentes em cinco veias da asa posterior (Emsley 1963).

Dione é composto por três espécies: *Dione juno* (Cramer 1779) (Figura 2 a-b), *Dione moneta* Hübner [1825] (Figura 2 c-d) e *Dione glycera* (C. Felder & R. Felder 1861) (Figura 2 e-f), sendo as duas primeiras compostas por subespécies; apenas *D. glycera* não possui tal diferenciação (Lamas 2004).

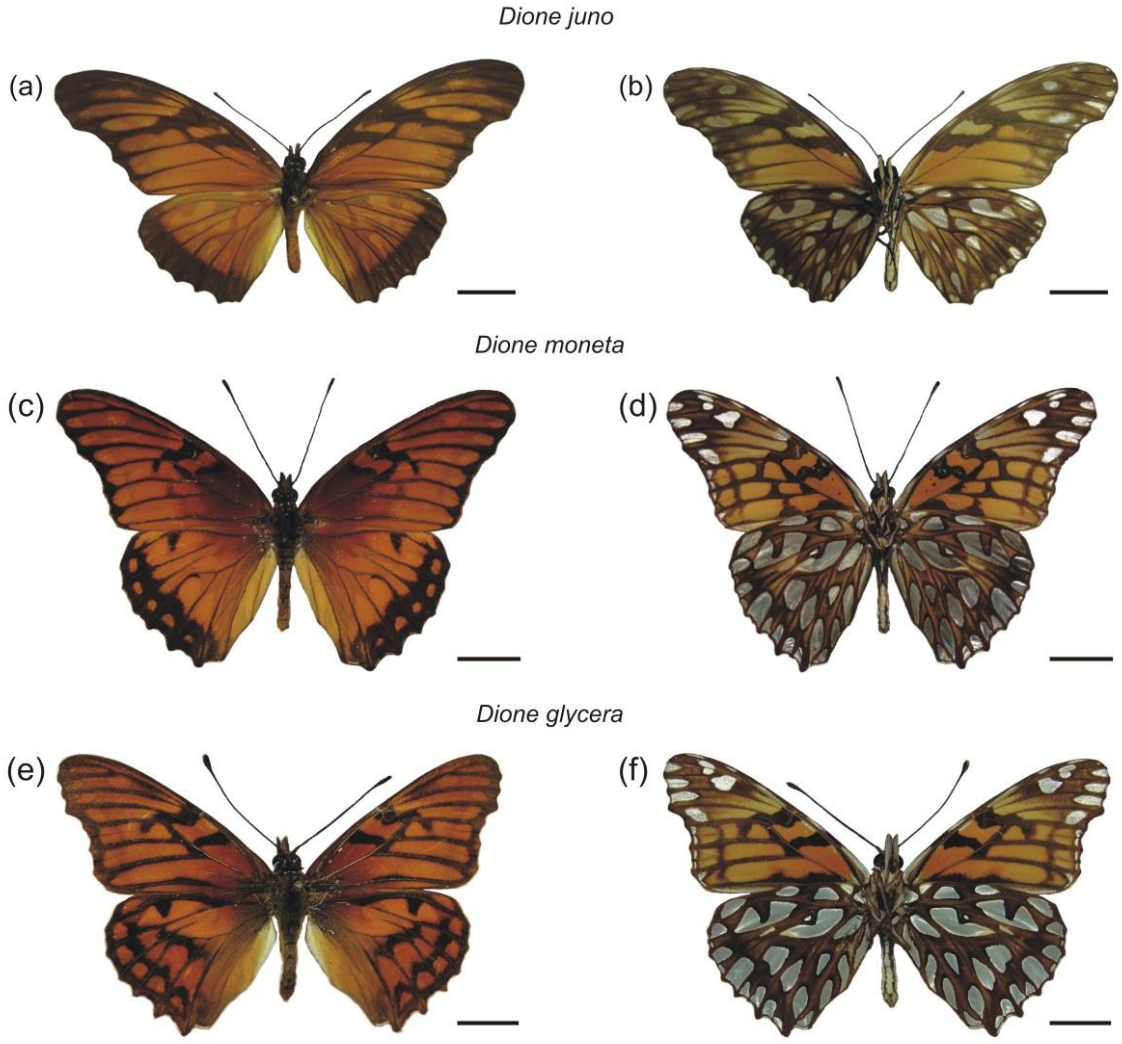

Figura 2. Adultos de *Dione* em vista dorsal e ventral respectivamente. (a-b) *Dione juno*; (c-d) *Dione moneta*; (e-f) *Dione glycera*. Barra: 1cm.

As espécies de *Dione* ocorrem no sul dos Estados Unidos, em toda América Central e em quase toda América do Sul (Emsley 1963; DeVries 1987; Brown Jr. & Mielke 1972; Rosser et al. 2012) e utilizam como planta hospedeira um grande número de espécies de *Passiflora* (Passifloraceae) (Tabela 1) (Brown Jr. & Mielke 1972; Beccaloni et al. 2008).

Tabela 1. Plantas hospedeiras utilizadas pelos imaturos das espécies de *Dione*.

Espécie	Planta hospedeira	Referência
Dione juno		
	Passiflora laurifolia	[Alexander 1961; Beccaloni et al. 2008 (ssp. *juno*)]
	P. serratedigitada	[Alexander 1961; Beccaloni et al. 2008 (ssp. *huascuma*)]
	P. auriculata	[Alexander 1961; Beccaloni et al. 2008 (ssp. *juno*)]
	P. alata	[Brown Jr. & Mielke 1972 (ssp. *suffumata*; Beccaloni et al. 2008 (ssp. *juno*)]
	P. speciosa	[Brown Jr. & Mielke 1972; Beccaloni et al.2008 (ssp. *juno*)]
	P. caerulea	[Brown Jr. & Mielke 1972 (ssp. *juno*)]
	P. edulis	[Garcias 1983 (ssp. j*uno*; ssp. *huascuma*; ssp. *andicola*; ssp. *miraculosa*)]
	P. capsularis	[Garcias 1983; Brown Jr. & Mielke 1972; Beccaloni et al. 2008 (ssp. *huascuma*)]
	P. tenuifila	[Garcias 1983 (ssp. *juno*)]
	P. misera	[Garcias 1983 (ssp. *juno*)]
	P. odontophylla	[Brown Jr. & Mielke 1972 (ssp. *juno*)]
	P. actinia	[Beccaloni et al. 2008 (ssp. *juno*)]
	P. cincinnata	[Beccaloni et al. 2008 (ssp. *juno*)]
	P. coccinea	[Beccaloni et al. 2008 (ssp. *juno*)]
	P. foetida	[Beccaloni et al. 2008 (ssp. *juno*)]
	P. ligularis	[Beccaloni et al. 2008 (ssp. *juno*; ssp. *andicola*)]
	P. microcarpa	[Beccaloni et al. 2008 (ssp. *juno*)]
	P. nitida	[Beccaloni et al. 2008 (ssp. *juno*)]
	P. pedata	[Beccaloni et al. 2008 (ssp. *juno*)]
	P. platyloba	[Beccaloni et al. 2008 (ssp. *juno*)]
	P. quadrangularis	[Beccaloni et al. 2008 (ssp. *juno*)]
	P. rubra	[Beccaloni et al. 2008 (ssp. *juno*)]

	P. seemannii	[Beccaloni et al. 2008 (ssp. *juno*)]
	P. veraguasensis	[Beccaloni et al. 2008 (ssp. *juno*)]
	P. bicornis	[Beccaloni et al. 2008 (ssp. *huascuma*)]
	P. coriacea	[Beccaloni et al. 2008 (ssp. *huascuma*)]
	P. helleri	[Beccaloni et al. 2008 (ssp. *huascuma*)]
	P. lancetillensis	[Beccaloni et al. 2008 (ssp. *huascuma*)]
	P. oerstedii	[Beccaloni et al. 2008 (ssp. *huascuma*)]
	P. salvadorensis	[Beccaloni et al. 2008 (ssp. *huascuma*)]
	P. seemannii	[Beccaloni et al. 2008 (ssp. *huascuma*)]
	P. mollisima	[Moreira & Lopez 2006 (ssp. *andicola*)]
	P. cornuta	[Brown Jr. & Mielke 1972 (ssp. *suffumata*)]
	P. suberosa	[Brown Jr. 1975 (ssp. *miraculosa*)]
Dione moneta		
	P. adenopoda	[Brown Jr. & Mielke 1972 (ssp. *poeyii*); Beccaloni et al. 2008 (ssp. *butleri*)]
	P. morifolia	[Brown Jr. & Mielke 1972; Benson et al.1975;DeVries 1987; Brown Jr. 1992; Dell'Erba et al. 2005; Beccaloni et al. 2008; (ssp. *moneta*)]
	P. violacea	[Beccaloni et al. 2008 (ssp. *moneta*)]
	P. lobata	[Brown Jr. & Mielke 1972 (ssp. *poeyii*)]
	P. oerstedii	[Beccaloni et al. 2008 (ssp. *poeyii*)]
	P. capsularis	[Brown Jr. & Mielke 1972 (ssp. *poeyii*)]
	P. edulis	[Beccaloni et al. 2008]
	P. lobata	[Beccaloni et al. 2008 (ssp. *poeyii*)]
	P. misera	[Beccaloni et al.2008]
	P. mollissima	[Beccaloni et al. 2008]
	P. serratodigitata	[Beccaloni et al. 2008]
	P. sexflora	[Beccaloni et al. 2008]
	P. violacea	[Beccaloni et al. 2008 (ssp. *moneta*]
Dione glycera		
	P. alnifolia	[Beccaloni et al.2008 (sp. *glycera*)]
	P. cyanea	[Beccaloni et al. 2008 (sp. *glycera*)]
	P. ligulares	[Beccaloni et al.2008 (sp. *glycera*)]
	P. mixta	[Beccaloni et al. 2008 (sp. *glycera*)]

P. caerulea	[Beccaloni et al.2008 (sp. *glycera*)]
P. edulis	[Beccaloni et al.2008 (sp. *glycera*)]
P. mollissima	[Beccaloni et al.2008 (sp. *glycera*)]

1.3 *Dione juno* (Cramer 1779)

Caracteriza-se por apresentar uma banda preta na asa posterior completa, sem manchas no seu interior (Emsley 1963) (Figura 2 a-b). De acordo com Lamas (2004) encontra-se representada por cinco subespécies: *D. juno juno* (Cramer 1779), *D. juno andicola* (Bates 1864), *D. juno huascuma* (Reakirt 1866), *D. juno miraculosa* (Hering 1926) e *D. juno suffumata* Brown Jr. & Mielke 1972.

Os adultos são comumente encontrados em áreas abertas e ambientes perturbados, mas podem ocorrer no dossel de florestas primárias (Emsley 1963). Ocorrem ao longo da América Central, grande parte da América do Sul e nas Antilhas (Emsley 1963; Brown Jr. & Mielke 1972; DeVries 1987; Rosser et al. 2012) (Figura 3).

A morfologia externa dos estágios imaturos de *D. juno juno* foi descrita por Tavares et al. (2002) e Bianchi & Moreira (2005) investigaram aspectos da biologia, frente ao uso de plantas hospedeiras no sul do Brasil.

1.3.1 *Dione juno juno* (Cramer 1779)

É caracterizada por possuir a margem anterior das asas anteriores escavadas e uma barra escura que atravessa a célula discal; a parte posterior das asas posteriores possui uma ampla margem preta (DeVries 1987). De acordo com Rosser et al. (2012) ocorre em praticamente toda a América do Sul (Figura 3), mas raramente ocorre acima de 1500 metros de altitude (Emsley 1963). É reconhecida pelo hábito gregário de suas larvas e por utilizar *Passiflora edulis* como um dos recursos alimentares de suas larvas, passiflorácea utilizada

mundialmente em cultivos comerciais de maracujá (Vanderplank 1991). Assim, *D. juno juno* é considerada praga desta cultura (Lara et al. 1999).

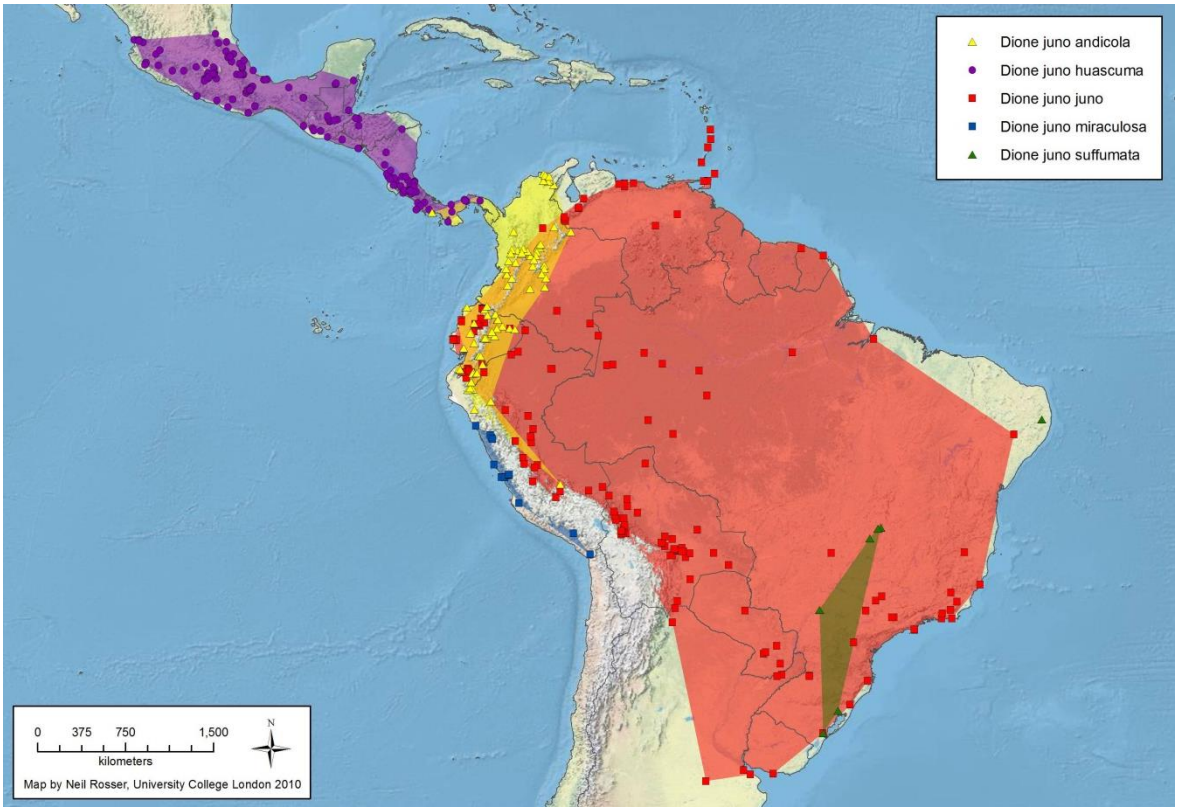

Figura 3. Distribuição das subespécies de *Dione juno* na reagião Neotropical. Fonte: Rosser et al. (2012).

1.3.2 *Dione juno huascuma* (Reakirt 1866)

Dione juno huascuma difere das demais subespécies por ser maior e possuir uma coloração mais pálida, com a margem escura da asa posterior manchada com a cor do fundo e mais variável. Apresenta um dicromatismo sexual pronunciado, onde as fêmeas apresentam uma cor mais clara e manchas escuras menos precisas. Raramente ocorre acima de 1.500 metros de altitude (Emsley 1963). Informações sobre a biologia desta subespécie foi

detalhada por Muyshondt et al. (1973). Distribui-se no norte do México, na América Central e na Colômbia (Rosser et al. 2012) (Figura 3).

1.3.3 *Dione juno andicola* (Bates 1864)

Dione juno andicola difere de *D. juno huascuma* por apresentar menor tamanho e manchas escuras mais pálidas em ambos os sexos (Emsley 1963). A biologia desta subespécie foi estudada por Molina Moreira & Arias de Lopez (2006). Distribui-se pela Cordilheira dos Andes, na Colômbia, Equador e Peru, ocorrendo abaixo de 2.200 metros de altitude (Emsley 1963; Rosser et al. 2012) (Figura 3).

1.3.4 *Dione juno miraculosa* Hering 1926

Apresenta morfologia semelhante a *D. juno juno*, sendo considerada uma subespécie diferente pelo fato de ser mais avermelhada (Brown Jr. 1975). Ocorre no nordeste do Peru e sudeste do Equador (Rosser et al. 2012). A forma típica ocorre na área de Lima e sul de Arequipa, no Peru, em uma área muito seca (Brown Jr. 1975) (Figura 3).

1.3.5 *Dione juno suffumata* Brown & Mielke 1972

É conspicuamente distinta das demais subespécies devido a extensa invasão das áreas vermelho-alaranjadas na superfície superior das bordas pretas, produzindo um ápice da asa anterior muito escuro e ampla margem preta na asa posterior (Brown Jr. 1973).

Populações isoladas foram localizadas próximas à Brasília (Distrito Federal, Brasil), podendo ocorrer também em outras áreas da região centro-sul do Brasil (Brown Jr. & Mielke 1972; Brown Jr. 1973; Rosser et al. 2012) (Figura 3).

1.4 *Dione moneta* Hübner [1825]

Em relação às demais espécies de *Dione*, a asa posterior de *D. moneta* apresenta uma banda preta com manchas alaranjadas (ocelos) menores ou iguais à metade da largura da mesma (Emsley 1963; DeVries 1987; D´Abrera 1984) (Figure 2 c-d). Três subespécies de *D. moneta* são reconhecidas por Lamas (2004): *D. moneta poeyii* Butler 1873; *D. moneta butleri* Stichel [1908]; e *D. moneta moneta* Hübner [1825].

Os adultos possuem hábito migratório, fator que pode explicar sua ampla distribuição geográfica e grandes flutuações anuais na abundância populacional (Gilbert 1969). *D. moneta* utiliza passifloráceas com tricomas em forma de gancho tais como *P. adenopoda*, *P. lobata* e *P. morifolia* ao longo de sua distribuição (Benson et al. 1975; Beccaloni et al. 2008).

Kaminski et al. (2008) descreveram a morfologia externa dos estágios imaturos de *D. moneta moneta* utilizando populações do Rio Grande do Sul e Thiele (dados inéditos) avaliou o uso de *Passiflora* e sua influência na distribuição geográfica de *D. moneta moneta* comprovando que é uma espécie monófaga e que sua distribuição é positivamente correlacionada com a de *P. morifolia*.

1.4.1 *Dione moneta moneta* Hübner [1825]

Dione moneta moneta diferencia-se das demais subespécies por ser menor em tamanho e apresentar manchas de tamanho médio com coloração de fundo na borda posterior da asa posterior (Emsley 1963). Os ovos se distinguem daqueles das demais espécies por serem depositados em *P. morifolia*, geralmente em pequenos grupos e de maneira não ordenada (Dell'Erba et al. 2005).

Na América do Sul, tem sido encontrada em populações disjuntas no Brasil, Argentina, Paraguai e Bolívia (Brown Jr. & Mielke 1972; Rosser et al. 2012) (Figura 4).

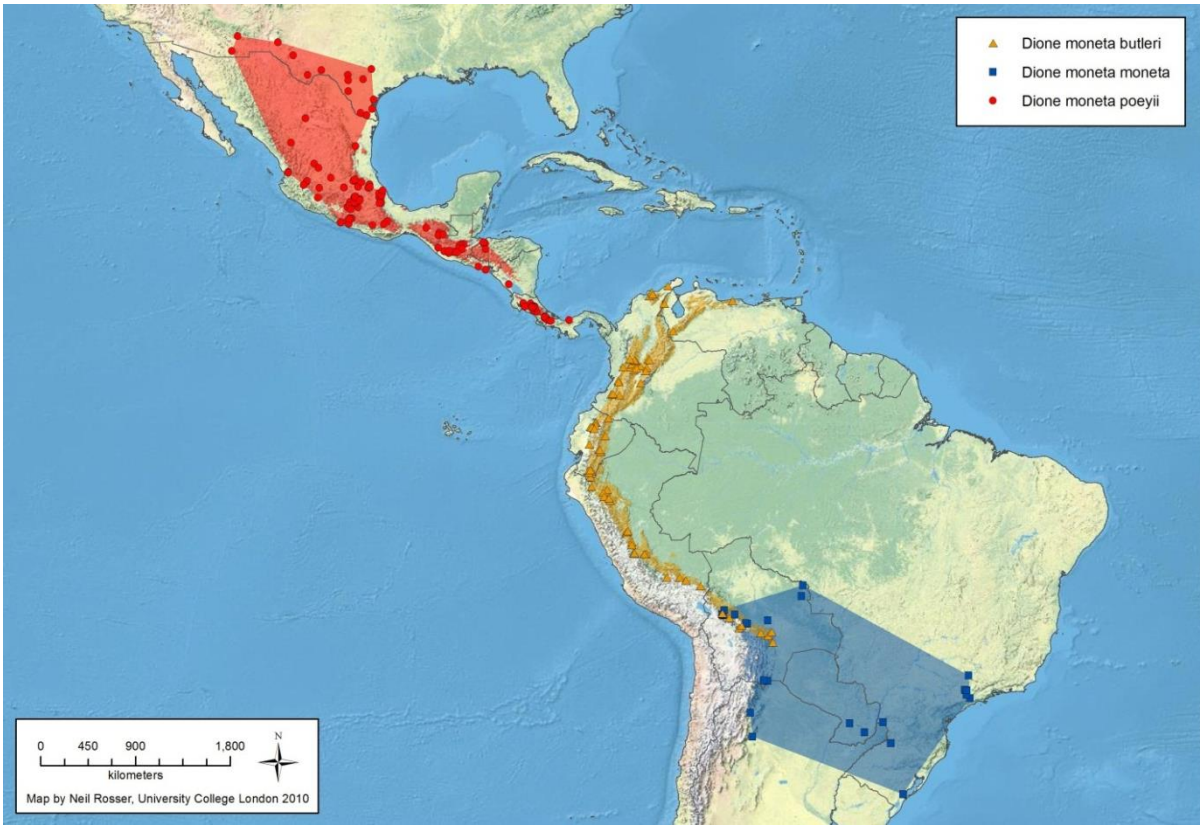

Figura 4. Distribuição das subespécies de *Dione moneta* na reagião Neotropical. Fonte: Rosser et al. (2012).

1.4.2 *Dione moneta butleri* Stichel [1908]

De tamanho intermediário entre as demais subespécies de *D. moneta*, *D. moneta butleri* apresenta manchas de coloração de fundo na borda posterior da asa posterior, estas intermediárias entre as manchas pequenas características de *D. moneta moneta* e as manchas grandes de *D. moneta poeyii* (Emsley 1963). Ocorre ao longo da Cordilheira dos Andes (Rosser et al. 2012) (Figura 4).

1.4.3 *Dione moneta poeyii* Butler 1873

Distingue-se das demais subespécies por possuir maior número de manchas prateadas na parte inferior das asas, e na parte superior uma faixa preta mediana (DeVries 1987). É a subespécie de maior tamanho em relação às demais e possui manchas de coloração de fundo na borda posterior da asa posterior (Emsley 1963). De acordo com Emsley (1963) e Rosser et

al. (2012) tem distribuição ao sul dos Estados Unidos, América Central e norte da América do Sul (Figura 4).

1.5 *Dione glycera* (C. Felder & R. Felder 1861)

Diferencia-se de *Dione moneta* por ser de menor tamanho e apresentar menos manchas pretas na região dorsal das asas (Hall 1921; Emsley 1963) (Figura 2 e-f). É encontrada em regiões montanhosas, raramente abaixo de 1.000 metros de altitude. Não são diferenciadas em subespécies (Emsley 1963). Distribui-se na América do Sul, na Cordilheira dos Andes da Venezuela a Argentina (Emsley 1963) (Figura 5).

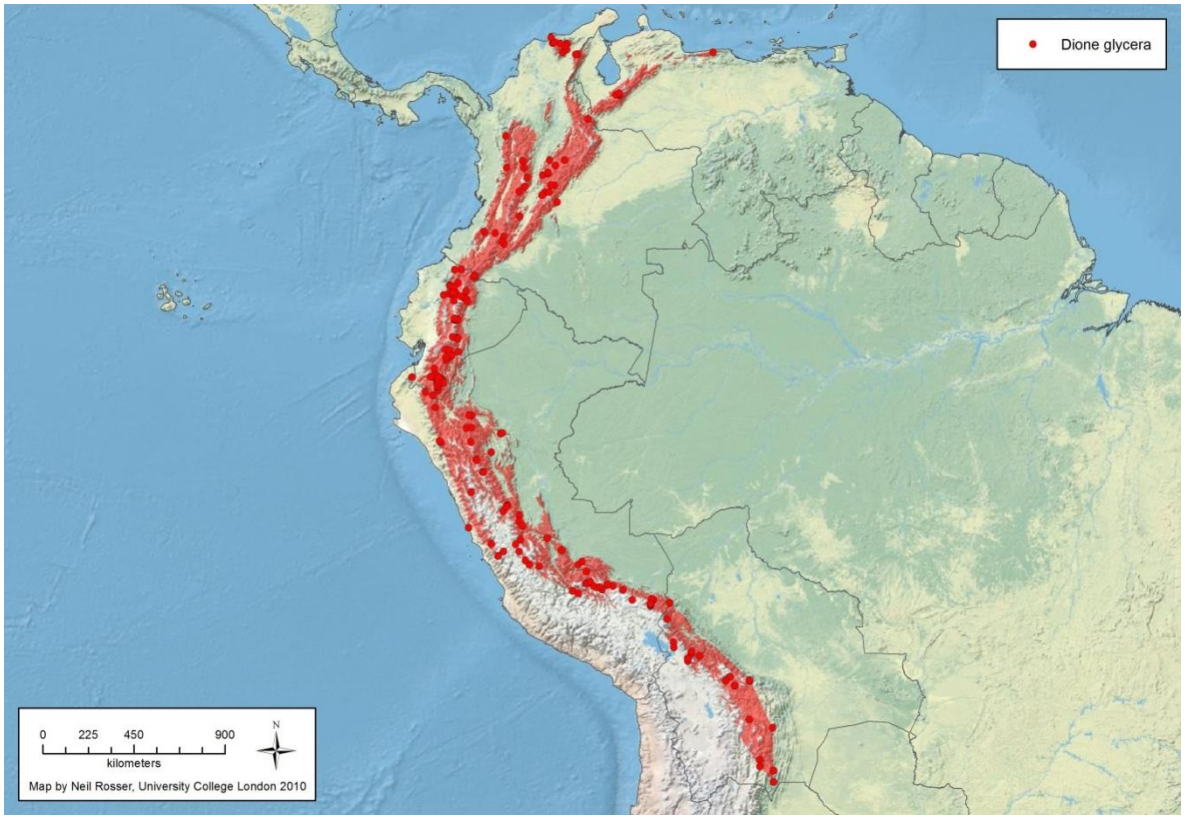

Figura 5. Distribuição de *Dione glycera* na reagião Neotropical. Fonte: Rosser et al. (2012).

Informações sobre a biologia e morfologia dos estágios imaturos de *D. glycera* resumem-se a descrições breves (ver Brown Jr. 1981). Os estudos de Beebe et al. (1960) e

Fleming (1960) sobre a morfologia dos estágios imaturos de heliconíneos não incluem *D. glycera*. Penz (1999) propôs uma filogenia para os heliconíneos baseada na morfologia dos imaturos e adultos, mas não incluiu caracteres de ovo para *D. glycera*. À exceção dos estados de caracteres utilizados por Penz (1999), a ultraestrutura externa dos imaturos ainda é desconhecida do ponto de vista morfológico, o que será aqui motivo de estudo (Capítulo I).

1.6 Relações filogenéticas

Para compreender processos e padrões evolutivos é fundamental caracterizar as relações filogenéticas entre os organismos, ou seja, como espécies compartilham uma história comum através de sua ancestralidade (Desluc et al. 2005). A representação filogenética através de diagrama em forma de árvore surgiu a partir da teoria da evolução apresentada no livro de Charles Darwin, A Origem das Espécies (Desluc et al. 2005). Quase um século depois Willi Hennig propôs a "Sistemática Filogenética", método de reconstrução das relações de parentesco entre os grupos de organismos (Hennig 1950), onde os organismos que compartilham caracteres com condições derivadas (ou apomórficas) podem ser hipotetizados como sendo descendentes da espécie ancestral na qual a condição primitiva (ou plesiomórfica) passa à condição derivada (Miyaki et al. 2001).

O objetivo central da sistemática filogenética é organizar o conhecimento sobre a diversidade biológica a partir das relações de parentesco entre grupos, bem como conhecer a evolução de características, sejam elas morfológicas, comportamentais, ecológicas, fisiológicas, citogenéticas ou moleculares, interpretando os padrões e processos evolutivos (Miyaki et al. 2001).

As classificações biológicas, quando organizadas, são fontes sintéticas de informações sobre a ordem que se pode perceber na diversidade biológica, colocando em destaque o grupo em estudo e permitindo compreende–lo como um todo, quanto à evolução de uma

característica, ou um conjunto de características compartilhadas por espécies desse grupo (Amorim 2002).

Heliconiini é um dos grupos em Lepidoptera mais trabalhados do ponto de vista filogenético. As principais contribuições até o presente momento foram de Michener (1942a), Emsley (1963), Brown Jr. (1981), Brower (1994), Brower & Egan (1997), Penz (1999) e Beltrán et al. (2007). Apenas os quatro últimos utilizaram métodos cladísticos, baseando-se também em dados moleculares. Utilizando análise morfológica somente dos adultos, Michener (1942a) propôs diagnoses e uma chave de identificação para sete gêneros de Heliconiini, sendo o marco divisório para a sistemática desse grupo. Emsley (1963), também através de caracteres morfológicos dos adultos, foi o primeiro a propor uma filogenia para as borboletas-do-maracujá. Estabeleceu um nível basal a partir do qual todos os heliconíneos teriam divergido. Nesta filogenia o gênero *Dione* é considerado grupo irmão de *Agraulis* ocupando uma posição basal na tribo Heliconiini. Brown Jr. (1981), utilizando dados morfológicos e caracteres ecológicos, baseou-se na filogenia de Emsley (1963) para sustentar as relações filogenéticas entre os heliconíneos. O gênero *Dione* mais uma vez foi considerado grupo irmão de *Agraulis*. Brower (1994) utilizou seqüencias de DNA mitocondrial (COI e COII) e métodos cladísticos para analisar a filogenia de Heliconiini. Nesta proposta, o gênero *Dryas* foi considerado o grupo mais basal de Heliconiini e *Dione* foi considerado grupo irmão de *Podotricha*.

Usando a combinação de seqüências de DNA mitocondrial (COI, COII) e do gene nuclear *Wingless*, Brower & Egan (1997) revisaram a filogenia de Brower (1994). De acordo com esta análise combinada de seqüências, *Agraulis* foi considerado o gênero mais basal e *Dione* o grupo irmão dos demais Heliconiini.

Penz (1999), com base em caracteres morfológicos dos estágios imaturos, incluindo a morfologia do ovo, do primeiro e quinto instar larval, da pupa e do estágio adulto, analisou as

relações filogenéticas entre 24 espécies de heliconíneos, representantes dos 10 gêneros. Nesta análise *Dione* foi considerada o grupo irmão de *Agraulis*, e também o gênero mais basal do grupo.

Beltrán et al.(2007), através da análise de sequências de genes mitocondriais (Citocromo Oxidase e 16S) e nucleares (*Elongation factor*-1α, *Apterous*, *Decapentaplegic* e *Wingless*) reavaliaram as relações filogenéticas de 60 espécies de Heliconiinae. Nesta filogenia, *Dione* e *Agraulis* também formaram um grupo irmão e ainda ocupam a posição mais basal de Heliconiini. *D. moneta* foi a mais basal em relação à *D. juno* e *D. glycera*, as quais formaram um grupo irmão entre si. Tal cenário não é corroborado pela filogenia proposta por Penz (1999), onde *D. juno* é considerada espécie irmã do clado formado por *D. moneta* e *D. glycera*. Assim, no presente estudo, com base no uso integrado de marcadores moleculares, medidas calcadas na morfometria linear e geométrica, bem como num extenso número de espécimes preservados em museu e/ou criados em laboratório, distribuídos por toda a região Neotroical, aborda-se a história evolutiva do gênero *Dione*, fazendo inferências quanto ao tempo de divergência deste em relação aos demais heliconíneos, respectiva filogenia e validação taxonômica correspondente tanto em nível específico quanto subespecífico (Capitulo III).

1.7 Morfologia

Historicamente, a descrição dos organismos baseia-se principalmente em suas características morfológicas externas, em um ou mais caracteres qualitativos ou quantitativos, sendo estes, a base para o estudo de qualquer espécie animal (Wiens 2007). Especificamente em Heliconiini grande parte das descrições de espécies até o momento é de cunho morfológico externo, baseado apenas nos adultos (Michener 1942a,b Emsley 1963; Brown Jr. 1976; D'Abrera 1984; Holzinger & Holzinger 1994).

O conhecimento morfológico dos estágios imaturos de Heliconiini ainda é escasso. Trabalhos clássicos de morfologia de imaturos como Fleming (1960) e Beebe et al. (1960) abordam apenas espécies de heliconíneos da ilha de Trinidad. Outros estudos abordam a morfologia dos imaturos de algumas espécies da tribo (Brown Jr. 1944, 1970; Rickard 1968; Brown Jr. & Holzinger 1973; Brown Jr. & Benson 1975; Mallet & Longino 1982; Penz 1995; Ajmat de Toledo 1991a,b). Em estudos recentes, porém, a morfologia geral e ultraestrutural externas dos primeiros estágios ontogenéticos foi contemplada em detalhes; tais estudos incluíram espécies de ocorrência no RS (Antunes et al. 2002; Kaminski et al. 2002, 2008; Tavares et al. 2002; Paim et al. 2004; Dell'Erba et al. 2005; Silva et al. 2006, 2008; Barão & Moreira 2010).

Grande parte da evolução morfológica pode ser descrita através de alterações na forma e/ou tamanho de uma ou mais características individuais de um organismo. Tais mudanças podem ser expressas matematicamente como uma alteração na duração ou na taxa de crescimento de uma dimensão do corpo em relação à outra (Alberch 1980; Klingenberg 1998; Zelditch et al. 2000; Webster & Zelditch 2005).

1.8 Morfometria

Diferenças na forma entre indivíduos ou suas partes podem significar funções diferentes de estruturas homólogas, respostas diferentes às mesmas pressões seletivas, bem como diferenças no crescimento e morfogênese (Zelditch et al. 2004). O estudo analítico da forma encontra-se em crescente expansão, sobretudo devido aos avanços técnicos da morfometria geométrica (Bookstein 1991, 1996; Monteiro & Reis 1999; Roth & Mercer 2000).

A morfometria tem sido amplamente utilizada em estudos referentes, por exemplo, na detecção de processos heterocrônicos (Klingenberg & Spence 1993; Vinicius & Lahr 2003), caracterização de dimorfismo sexual (Adams & Funk 1997), compreensão da trajetória

ontogenética de dada estrutura (Rodrigues et al. 2005) e delimitação de espécies (Mutanen & Pretorius 2007; Fernandes et al. 2009; Mérot et al. 2013; Barão *et al*. 2014), dentre outras aplicações.

As abordagens morfométricas, lineares e geométricas, também podem ser empregadas como métodos de delimitação de espécies, pois permitem identificar espécies crípticas de maneira mais acurada do que o método tradicional de identificação visual (Mutanen & Pretorius 2007). Por exemplo, as asas de Insecta têm sido utilizadas com sucesso na discriminação e delimitação de espécies crípticas desse grupo de organismos (Imasheva et al. 2000; Villemant et al. 2007; Ludoski et al. 2008; Mérot et al. 2013).

Segundo Roth & Mercer (2000), a vantagem da descrição quantitativa da forma (morfometria), em relação à descrição qualitativa (morfologia) unicamente, é a precisão em determinar variações morfológicas sutis dentro de uma amostra aparentemente homogênea. Assim, permite reconhecer formas intermediárias, bem como determinar precisamente graus de similaridades ou dissimilaridades morfológicas. No caso dos heliconíneos, pode se tornar uma ferramenta taxonômica importante, principalmente na diferenciação das subespécies, as quais, conforme já explicitado, são reconhecidas apenas pelo padrão de coloração das asas.

1.9 Marcadores Moleculares

A sistemática tem incorporado caracteres de origem de DNA para aprimorar as filogenias baseando-se nos processos evolutivos moleculares (Cho et al. 1995; Caterino & Sperling 1999; Whinnett et al. 2005; Wiens 1999). O emprego da genética molecular, através da utilização de marcadores, tem permitido a identificação de populações, raças e/ou espécies crípticas associadas às plantas hospedeiras (Drès & Mallet 2002).

A crescente aplicação dos dados moleculares revolucionou a taxonomia, mas a validade e os aspectos práticos desta abordagem molecular tem sido objeto de diversas críticas relativas a aspectos da herdabilidade dos genes mitocondriais e suas taxas evolutivas;

e a falta de integração com outros marcadores nucleares e caracteres morfológicos (Lipscomb et al. 2003; Will & Rubinoff 2004; Wheeler 2005; Brower 2006; Elias et al. 2007; Dasmahapatra et al. 2010). Com a atual compreensão das diferenças entre árvores de genes e árvores de espécies (Brower et al. 1996; Nichols 2001) há a demanda de se utilizar diversos tipos de marcadores moleculares e em grande escala para gerar hipóteses sobre as relações filogenéticas, o que também foi abordado no Capítulo III desta tese.

Atualmente, as informações obtidas com seqüências de mtDNA têm sido contrastadas com diversos genes nucleares (Wahlberg et al. 2009) e marcadores genômicos de co-dominância, como microssatélites e AFLP ("Amplified Fragment Lenght Polymorphism") para obter hipóteses filogenéticas que sejam mais robustas e confiáveis (Orsini et al. 2004; Pellmyr et al. 2007; Rout et al. 2008; Dasmahapatra et al. 2009; Mendelson & Wong 2010). Os microssatélites em particular, a semelhança de AFLPs tem sido usado no contexto subespecífico, principalmente em comparações em nível populacional. Em relação às borboletas do maracujá, entretanto, a existência desse tipo de marcador é restrita ao gênero *Heliconius* (Flanagan et al. 2002; Mavárez & González 2006). Assim, neste estudo (Capítulo II) foram isolados microssatélites para *Dione moneta*, e testados quanto a validade do uso correspondente para as demais espécies do gênero e para o gênero *Agraulis*.

1.10 Referências*

Adams DC, Funk DJ (1997) Morphometric inferences on sibling species and sexual dimorphism in *Neochlamisus bebbianae* leaf beetles: multivariate applications of the thin-plate spline. Systematic Biology 46: 180-194

Ajmat de Toledo ZD (1991a) Fauna del noroeste argentino. Contribucion al conocimiento de los lepidópteros argentinos. IX. *Dione juno* (Cramer) (Lepidoptera, Rhopalocera, Heliconiidae). Acta Zoologica Lilloana 40: 109-117

Ajmat de Toledo ZD (1991b) Fauna del noroeste argentino. Contribucion al conocimiento de los lepidópteros argentinos. X. *Agraulis vanillae maculosa* (Stichel) (Lepidoptera, Rhopalocera, Heliconiidae). Acta Zoologica Lilloana 40: 21-31

Alberch P (1980) Ontogenesis and morphological diversification. American Zoology 20: 653-667

Amorim DS (2002) Fundamentos de Sistemática Filogenética, Holos, Ribeirão Preto

Antunes FA, Menezes AO Jr, Tavares M, Moreira GRP (2002) Morfologia externa dos estágios imaturos de heliconíneos neotropicais: I. *Eueides isabella dianasa* (Hübner 1816). Revista Brasileira de Entomologia 46: 601–610

Barão KR, Moreira GRP (2010) External morphology of the immature stages of Neotropical heliconians: VIII. *Philaethria wernickei* (Röber) (Lepidoptera, Nymphalidae, Heliconiinae). Revista Brasileira de Entomologia 54: 406-418

Barão KR, Gonçalves GL, Mielke OHH, Kronforst MR, Moreira GRP Species boundaries in *Philaethria* butterflies: an integrative taxonomic analysis based on genitalia ultrastructure, wing geometric morphometrics, DNA sequences and AFLPs. *Zoological Journal of the Linnean Society*, (no prelo).

*Normas adotadas de acordo com a Conservation Genetics Resource.

Beccaloni GW, Viloria AL, Hall SK, Robinson GS (2008) A catalog of the hostplants of the Neotropical butterflies. Zaragoza, The Natural History Museum

Beebe W, Crane J, Fleming H (1960) A comparison of eggs, larvae and pupae in fourteen species of Heliconiine butterflies from Trinidad, W. I. Zoologica 45: 111-154

Beltrán M, Jiggins CD, Brower AVZ, Bermingham E, Mallet J (2007) Do pollen feeding, pupal-mating and larval gregariousness have a single origin in *Heliconius butterflies*?

Inferences from multilocus DNA sequence data. Biological Journal of the Linnean Society 92: 221-239

Benson WW (1978) Resource partitioning in passion-vine butterflies. Evolution 32: 493-518

Benson WW, Brown Jr KS, Gilbert LE (1975) Coevolution of plants and herbivores: passion flowers butterflies. Evolution 29: 659-680

Bianchi V, Moreira GRP (2005) Preferência alimentar, efeito da planta hospedeira e da densidade larval na sobrevivência e desenvolvimento de *Dione juno juno* (Cramer) (Lepidoptera, Nymphalidae). Revista Brasileira de Zoologia 22: 43-50

Bookstein FL (1991) Morphometrics tools for landmark data: geometry and biology. New York, Cambridge University Press

Bookstein FL (1996) Biometrics, biomathematics and the morphometric synthesis. Bulletin of Mathematical Biology 58: 313-365

Braby MF, Eastwood R, Murray N (2012) The subspecies concept in butterflies: has its application in taxonomy and conservation biology outlived its usefulness? Biological Journal of the Linnean Society, 106: 699–716

Brower AVZ (1994) Rapid morphological radiation and convergence among races of the butterfly *Heliconius erato* inferred from patterns of mitochondrial DNA evolution. Proceedings of the National Academy of Sciences of the USA 91: 6491-6495

Brower AVZ (2006) Problems with DNA barcodes for species delimitation: 'ten species' of *Astraptesfulgerator* reassessed (Lepidoptera: Hesperiidae). Systematics and Biodiversity 4: 127-132

Brower AVZ, Desalle R, Vogler AP (1996) Gene trees, species trees, and systematics: a cladistic perspective. Annual Review of Ecology and Systematics 27: 423-450

Brower AVZ, Egan MG (1997) Cladistic analysis of *Heliconius* butterflies and relatives (Nymphalidae: Heliconiiti): a revised phylogenetic position for *Eueides* based on sequences from mtDNA and a nuclear gene. Proceedings of the Royal Society B 264: 969-977

Brown FM (1944) The egg, larva and chrysalis of *Dione moneta* Hübner. Bulletin of the Brooklyn Entomological Society 39: 132-134

Brown KS (1979) *Ecologia Geográfica e Evolução nas Florestas Neotropicais*. Campinas: Universidade Estadual de Campinas

Brown KS Jr (1970) Rediscovery of *Heliconius nattereri* in eastern Brazil. Entomological News 81: 129-140

Brown KS Jr (1973) The Heliconians of Brazil (Lepidoptera: Nymphalidae). Part V. Three new subspecies from Mato Grosso and Rondônia. The Allyn Museum of Entomology 13: 1-19

Brown KS Jr (1975) Geographical patterns of evolution in neotropical Lepidoptera. Systematics and derivation of known and new Heliconiini (Nymphalidae: Nymphalinae). Journal of Entomology Series B 44: 201-242

Brown KS Jr (1976) An illustrated key to the silvaniform *Heliconius* with descriptions of new subspecies. Transactions of the American Entomological Society 102: 373-484

Brown KS Jr (1981) The biology of *Heliconius* and related genera. Annual Review of Entomology 26: 427-456

Brown KS Jr, Benson WW (1975) The heliconians of Brazil (Lepidoptera: Nymphalidae). Part VI. Aspects of the biology and ecology of *Heliconius demeter*, with descriptions of four new subspecies. Bulletin of the Allyn Museum 26: 1-19

Brown KS Jr, Freitas AVL (2000) Atlantic Forest butterflies: indicators for landscape conservation. Biotropica 32: 934-956

Brown KS Jr, Holzinger H (1973) The Heliconians of Brazil. Part IV. Systematics and biology of *Eueides tales* Cramer, withed scription of a new subspecies from Venezuela.Zeitschr der Arbeitsgemeinschaft Österreichischer Entomologen 24: 44-65

Brown KS Jr, Mielke OHH (1972) The Heliconians of Brazil (Lepidoptera: Nymphalidae). Part II. Introduction and general comments, with a supplementary revision of the tribe.Zoologica 57: 1-40

Caterino S, Sperling FAH (1999) *Papilio* phylogeny based on Mitochondrial Cytochrome Oxidase I and II genes. Molecular Phylogenetics and Evolution 11: 122–137

Chamberlain NL, Hill RI, Kapan DD, Gilbert LE, Kronforst MR (2009) Polymorphic butterfly reveals the missing link in ecological speciation. Science 326: 847-850

Chamberlain NL, Hill RI, Baxter SW, Jiggins CD, Kronforst MR (2011) Comparative population genetics of a mimicry locus among hybridizing *Heliconius* butterfly species. Heredity 107: 200-204

Cho S, Mitchell A, Regier JC, Mitter C, Poole RW, Friedlander TP, Zhao S (1995) A highly conserved nuclear gene for low-level phylogenetics: Elongation Factor-1 Alpha recovers morphology-based tree for Heliothine moths. Molecular Biology and Evolution 12: 650-656

D'Abrera B (1984) Butterflies of the Neotropical region. Part II. Danaidae, Ithomiidae, Heliconidae & Morphidae. Victoria, Hill House 7:173–384

Dasmahapatra KK, Elias M, Hill RI, Hoffman JI, Mallet J (2010) Mitochondrial DNA barcoding detects some species that are real, and some that are not. Molecular Ecology Resources 10: 264-273

Dasmahapatra KK, Hoffman JI, Amos W (2009) Pinniped phylogenetic relationships inferred using AFLP markers. Heredity 103: 168-77

Dell'Erba R, Kaminski LA, Moreira GRP (2005) O estágio de ovo dos Heliconiini (Lepidoptera, Nymphalidae) do Rio Grande do Sul, Brasil. Iheringia Série Zoologia 95: 29-46

Desluc F, Brinkmann H, Philipe H (2005) Phylogenomics and the Reconstruction of the Tree of Life. Nature Reviews Genetics 6: 361-375

DeVries PJ (1987) The butterflies of Costa Rica and their natural history. Papilionidae, Pieridae, Nymphalidae. Princeton, Princeton University

Drès M, Mallet J (2002) Host races in plant-feeding insects and their importance sympatric speciation. Phil. Trans.: Biological Sciences 357: 471-492

Ehrlich PR, Raven PR (1965) Butterflies and plants: a study in coevolution. Evolution 18: 586-618

Elias M, Hill RI, Willmott KR, Dasmahapatra KK, Brower AVZ Mallet J (2007) Limited performance of DNA barcoding in a diverse community of tropical butterflies. Proceedings of the Royal Society B 274: 2881-2889

Emsley M (1963) A morphological study of imagine Heliconiinae (Lepidoptera, Nymphalidae) with a consideration of the evolutionary relationships within the group. Zoologica 48: 85-129

Fernandes FA, Fornel R, Cordeiro-Estrela P, Freitas TRO (2009) Intra- and interspecific skull variation in two sister species of the subterranean rodent genus Ctenomys (Rodentia,

Ctenomyidae): coupling geometric morphometrics and chromosomal polymorphism. Zoological Journal of the Linnean Society 155: 220-237

Flanagan NS, Blum MJ, Davison A, Alamo M, Albarrán R, Faulhaber K, Peterson E, McMillan WO (2002) Characterization of microsatellite loci in neotropical Heliconius butterflies. Molecular Ecology Notes 2:398–401

Fleming H (1960) The first instar larvae of the Heliconiinae (Butterflies) of Trinidad, W.I. Zoologica 45: 91-110

Garcias GL (1983) Aspectos da biologia de cinco espécies de heliconíneos do anel mimético "laranja" (Lepidoptera: Nymphalidae). Dissertação de Mestrado. Porto Alegre, UFRGS

Gilbert LE (1969) On the ecology of natural dispersal: *Dione moneta poeyii* in Texas (Nymphalidae). Journal of the Lepidopterists' Society 23: 177–185

Gilbert LE (1975) Ecological consequences of a coevolved mutualism between butterflies and plants. In: Gilbert LE, Raven PR (eds). Coevolution of Animals and Plants. Austin, University of Texas Press, pp 210-240

Gilbert LE (1991) Biodiversity of a Central American *Heliconius* community: pattern, process, and problems. In: Price PW (ed). Plant-animal interactions.Chichester, Wiley, pp 403-427

Gilbert LE, Smiley JT (1978) Determinants of local diversity in phytophagous insects: host specialists in tropical environments. In: Mound LA, Waloff N (eds) Diversity of insect faunas. London, Blackwell, pp 89-104

Giraldo N, Salazar C, Jiggins C, Bermingham E, Linares M (2008) Two sisters in the same dress: *Heliconius* cryptic species. BMC Evolutionary Biology 8:324

Hall A (1921) Notes on the synonymy of *Dione moneta*, Hübn. And *D. glycera*, Feld. Entomologist, 54(703): 276-278

Hennig W (1950) Grundzugeeiner Theorie der phylogenetischen Systematik, Deuscher Zentralverlag, Berlim

Hill RI, Gilbert LE, Kronforst MR (2013) Cryptic genetic and wing pattern diversity in a mimetic *Heliconius* butterfly. Molecular Ecology 22: 2760-2770

Hines HM, Counterman BA, Papa R et al (2011) Wing patterning gene redefines the Mimetic history of *Heliconius* butterflies. Proceedings of the National Academy of Sciences 108: 19666–19671

Holzinger H & Holzinger R (1994) *Heliconius* and related Genera. Vennette, France: Sciences Nat

Imasheva AG, Moreteau B, David JR (2000) Growth temperature and genetic variability of wing dimensions in *Drosophila*: opposite trends in two sibling species. Genetical Research 76: 237-247

Jiggins C, Davies N (1998) "Genetic evidence for a sibling species of *Heliconius charithonia* (Lepidoptera; Nymphalidae)." Biological Journal of the Linnean Society 64 (1): 57-67

Jiggins C, Mavarez J, Beltrán M, McMillan W, Johnston J, Bermingham E (2005) "A genetic linkage map of the mimetic butterfly *Heliconius melpomene*." Genetics 171 (2): 557

Jiggins C, McMillan W, Neukirchen W, Mallet J (1996) "What can hybrid zones tell us about speciation? The case of *Heliconius erato* and *H. himera* (Lepidoptera: Nymphalidae)." Biological Journal of the Linnean Society 59 (3): 221-242

Joron M, Frezal L, Jones RT, Chamberlain NL et al (2011) Chromosomal rearrangements maintain a polymorphic supergene controlling butterfly mimicry. Nature 477: 203–206

Kaminski LA, Dell'erba R, Moreira GRP (2008) Morfologia externa dos estágios imaturos de heliconíneos neotropicais: VI. *Dione moneta moneta* Hübner (Lepidoptera, Nymphalidae, Heliconiinae). Revista Brasileira de Entomologia 52: 13–23

Kaminski LA, Tavares M, Ferro VG, Moreira GRP (2002) Morfologia externa dos estágios imaturos de heliconíneos neotropicais. III. *Heliconius erato phyllis* (Fabricius) (Lepidoptera, Nymphalidae, Heliconiinae). Revista Brasileira de Zoologia 19: 977-993

Kerpel SM, Soprano E, Moreira GRP (2006) Effect of nitrogen on *Passiflora suberosa* L. (Passifloraceae) and consequences for larval performance and oviposition in *Heliconius erato phyllis* (Fabricius) (Lepidoptera: Nymphalidae). Neotropical Entomology 35: 192-200

Klingenberg CP (1998) Heterochrony and allometry: the analysis of evolutionary significance in relation to mimicry. Journal of Zoology 155: 311–325

Klingenberg CP, Spence JR (1993) Heterochrony and allometry: lessons from the water strider genus *Limnoporus*. Evolution 47: 1834-1853

Kronforst MR (2012) Mimetic butterflies introgress to impress. PLoS Genetics 8: e1002802

Kronforst MR, Salazar CA, Linares M, Gilbert LE (2009) No genomic mosaicism in a putative hybrid butterfly species. Proceedings of the Royal Society of London 274: 1255-1264

Lamas G (2004) Checklist: Part 4A. Hesperioidea - Papilionoidea. In: J. B. Heppner (ed.). Atlas of Neotropical Lepidoptera. Volume 5A. Gainesville, Association for Tropical Lepidoptera, Scientific Publishers

Lara FM, Boiça AL Jr, Barbosa JC (1999) Preferência alimentar de *Dione juno juno* (Cremer, 1779) (Lepidoptera: Nymphalidae) por genótipos de maracujazeiro e avaliação do uso de extratos aquosos. Scientia Agricola 56: 665-671

Lipscomb D, Platnick N, Wheeler QD (2003) The intellectual content of taxonomy: a comment on DNA taxonomy. Trends in Ecology and Evolution 18: 65-68

Ludoski J, Francuski L, Vujic A, Milankov V (2008) The *Cheilosia canicularis* group (Diptera: Syrphidae): species delimitation and evolutionary relationships based on wing geometric morphometrics. Zootaxa 1825: 40-50

Mallet J (1986) Dispersal and gene flow in a butterfly with home range behavior: *Heliconius erato* (Lepidoptera: Nymphalidae). Oecologia 68: 210-217

Mallet J (2001) Gene flow. In: Woiwod IP, Reynolds DR, Thomas CD (eds) Insect Movement: Mechanisms and Consequences. CAB International, Wallingford, UK, pp 337-360

Mallet J (2008) Hybridization, ecological races and the nature of species: empirical evidence for the ease of speciation. Philosophical Transactions of the Royal Society B 63: 2971-2986

Mallet J (2009) Rapid speciation, hybridization and adaptive radiation in the *Heliconius melpomene* group. In: Butlin RK, Bridle JR, Schluter D (eds) Speciation and patterns of diversity. Cambridge, Cambridge University Press, pp 177-194

Mallet J, Beltrán M, Neukirchen W, Linares M (2007) Natural hybridization in heliconiine butterflies: the species boundary as a continuum. BMC Evolutionary Biology 7: 28

Mallet JLB, Longino JT (1982) Host plant records and descriptions of juvenile stages for two rare species of *Eueides* (Nymphalidae). Journal of the Lepidopterists' Society 36: 136-144

Mavárez J, González M (2006) A set of microsatellite markers for *Heliconius melpomene* and closely related species. Molecular Ecology Notes 6:20–23

Mendelson TC, Wong MK (2010) AFLP phylogeny of the snubnose darters and allies (Percidae: Etheostoma) provides resolution across multiple levels of divergence. Molecular Phylogenetics and Evolution 57:1253-1259

Mérot C, Mavárez J, Evin A, Dasmahapatra KK, Mallet J, Lamas G, Joron M (2013) Genetic differentiation without mimicry shift in a pair of hybridizing *Heliconius* species (Lepidoptera: Nymphalidae). Biological Journal of the Linnean Society 109: 830-847.

Michener CD (1942a) A generic revision of the Heliconiinae (Lepidoptera, Nymphalidae). American Museum Novitates 1197: 1-8

Michener CD (1942b) A review of the subspecies of *Agraulis vanillae* (Linnaeus). Lepidoptera: Nymphalidae. American Museum Novitates 1215: 1-7

Miyaki CY, Russo CAM, Pereira SL (2001) Reconstrução Filogenética. Introdução e o Método de Máxima Parcimônia. In: Matioli, S.R. Biologia Molecular e Evolução. Holos: Ribeirão Preto, pp 202

Monteiro LR, Reis SF (1999) Princípios de morfometria geométrica. São Paulo, Holos

Mutanen M, Pretorius E (2007) Subjective visual evaluation vs. traditional and geometric morphometrics in species delimitation: a comparison of moth genitalia. Systematic Entomology 32:371–386

Nadeau NJ, Whibley A, Jones RT et al. (2012) Genomic islands of divergence in hybridizing *Heliconius* butterflies identified by large-scale targeted sequencing. Philosophical Transactions of the Royal Society B 367: 343-353

Nichols R (2001) Gene trees and species trees are not the same. Trends in Ecology & Evolution 16: 358-364

Orsini L, Huttunen S, Schlötterer C (2004) A multilocus microsatellite phylogeny of the *Drosophila virilis* group. Heredity 93: 161-165

Paim AC, Kaminski LA, Moreira GRP (2004) Morfologia externa dos estágios imaturos de heliconíneos neotropicais. IV. *Dryas iulia alcionea* (Lepidoptera: Nymphalidae: Heliconiinae). Iheringia, Série Zoologia 94: 25–35

Pellmyr O, Segraves KA, Althoff DM, Balcázar-Lara M, Leebens-Mack J (2007) The phylogeny of yuccas. Molecular Phylogenetics and Evolution 43: 493-501

Penz CM (1999) Higher level phylogeny for the passion-vine butterflies (Nymphalidae, Heliconiinae) based on early stage and adult morphology. Zoological Journal of the Linnean Society 127: 277-344

Penz CM, Peggie D (2003) Phylogenetic relationships among Heliconiinae genera based on morphology (Lepidoptera: Nymphalidae). Systematic Entomology 28: 451-479

Rickard MA (1968) Life history of *Dryas julia delia* (Heliconiinae). Journal of the Lepidopterists' Society 22: 75-76

Rodrigues D, Moreira GRP (2004) Seasonal variation in larval host plants and consequences for *Heliconius erato* (Lepidoptera: Nymphalidae) adult body size. Austral Ecology 29: 437-445

Rodrigues D, Sanfelice D, Monteiro LR, Moreira GRP (2005) Ontogenetic trajectories and hind tibia geometric morphometrics of *Holymenia clavigera* (Herbst) and *Anisoscelis foliacea marginella* (Dallas) (Hemiptera: Coreidae). Neotropical Entomology 34: 769-776

Rosser N, Phillimore AB, Huertas B, Willmott KR, Mallet J (2012) Testing historical explanations for gradients in species richness in heliconiine butterflies of tropical America. Biological Journal of the Linnean Society 105: 479-497

Roth VL, Mercer JM (2000) Morphometrics in development and evolution. American Zoology 40: 801-810

Rout PK, Joshi MB, Mandal A, Laloe D, Singh L, Thangaraj K (2008) Microsatellite-based phylogeny of Indian domestic goats. BMC Genetics 9: 11

Sheppard PM, Turner JRG, Brown KS Jr, Benson WW, Singer MC (1985) Genetics and the evolution of muellerian mimicry in *Heliconius* butterflies. Philosophical Transactions of the Royal Society B 308: 433-613

Silva DS, Dell'Erba R, Kaminski LA, Moreira GRP (2006) Morfologia externa dos estágios imaturos de heliconíneos neotropicais: V. *Agraulis vanillae maculosa* (Lepidoptera, Nymphalidae, Heliconiinae). Iheringia, Série Zoologia 96: 219–228

Silva DS, Kaminski LA, Dell'Erba R, Moreira GRP (2008) Morfologia externa dos estágios imaturos de heliconíneos neotropicais: VII. *Dryadula phaetusa* (Linnaeus) (Lepidoptera, Nymphalidae, Heliconiinae). Revista Brasileira de Entomologia 52: 500-509

Stichel H (1906) Lepidoptera, fam. Nymphalidae, subfam.Heliconiinae. In: Wytsman P (ed). Genera Insectorum 37: 1–74

Tavares M, Kaminski LA, Moreira GRP (2002) Morfologia externa dos estágios imaturos de heliconíneos neotropicais: II. *Dione juno juno* (Cramer) (Lepidoptera: Nymphalidae: Heliconiinae). Revista Brasileira de Zoologia 19: 961–976

Turner JR (1976) Adaptive radiation and convergence in subdivisions of the butterfly genus *Heliconius* (Lepidoptera: Nymphalidae). Zoological Journal of the Linnean Society 58: 297-308

Turner JRG (1971) Two thousand generations of hybridization in a *Heliconius* butterfly. Evolution 25: 471-482

Vanderplank J (1991) Passion flowers and passion fruit. Cambridge, MIT

Villemant C, Simbolotti G, Kenis M (2007) Discrimination of *Eubazus* (Hymenoptera, Braconidae) sibling species using geometric morphometrics analysis of wing venation. Systematic Entomology 32: 625-634

Vinicius L, Lahr MM (2003) Morphometric heterochrony and the evolution of growth. Evolution 57: 2459-2468

Wahlberg N, Leneveu J, Kodandaramaiah U, Peña C, Nylin S, Freitas AVL, Brower AVZ (2009) Nymphalid butterflies diversify following near demise at the Cretaceous/Tertiary boundary. Proceedings of the Royal Society B 276: 4295-302

Webster M, Zelditch ML (2005) Evolutionary modifications of ontogeny: heterochrony and beyond. Paleobiology 31: 354-372

Wheeler QD (2005) Losing the plot: DNA "barcodes" and taxonomy. Cladistics 21: 405-407

Whinnett A, Brower AVZ, Lee M, Willmott KR, Mallet J (2005) Phylogenetic utility of Tektin, a novel region for inferring systematic relationships among Lepidoptera. Annals of the Entomological Society of America 98: 873-886

Wiens JJ (1999) Polymorphism in systematics and comparative biology. Annual Review of Ecology and Systematics 30: 327-362

Wiens JJ (2007) Species delimitation: new approaches for discovering diversity. Systematic Biology 56: 875-8

Will KW, Rubinoff D (2004) Myth of the molecule: DNA barcodes for species cannot replace morphology for identification and classification. Cladistics 20: 47-55

Zelditch ML, Sheets HD, Fink WL (2000) Spatiotemporal reorganization of growth rates in the evolution of ontogeny. Evolution 54: 1363-1371

Zelditch ML, Swiderski DL, Sheets HD, Fink WL (2004) Geometric Morphometrics for Biologists: a Primer. New York, Elsevier

2. CAPÍTULO I

External morphology of the immature stages of Neotropical heliconians: IX. *Dione glycera* (C. Felder & R. Felder, 1861) (Lepidoptera, Nymphalidae, Heliconiinae)*

* Este manuscrito foi submetido à **Revista Brasileira de Entomologia (setembro/2013)**

Running title: External morphology of *Dione glycera* immatures

External morphology of the immature stages of Neotropical heliconians: IX. *Dione glycera* (C. Felder & R. Felder, 1861) (Lepidoptera, Nymphalidae, Heliconiinae)

Héctor A. Vargas[1], Kim R. Barão[2], Darli Massardo[2] & Gilson R. P. Moreira[3*]

[1]Departamento de Recursos Ambientales, Facultad de Ciencias Agronómicas, Universidad de Tarapacá, Casilla 6-D. Arica, Chile. havargas@uta.cl

[2]PPG Biologia Animal, Departamento de Zoologia, Instituto de Biociências, Universidade Federal do Rio Grande do Sul, Avenida Bento Gonçalves, 9500, 91501-910 Porto Alegre-RS, Brazil. kbarao@gmail.com; darlimassardo@gmail.com;

[3]Departamento de Zoologia, Instituto de Biociências, Universidade Federal do Rio Grande do Sul, Avenida Bento Gonçalves, 9500, 91501-910 Porto Alegre-RS, Brazil.

*corresponding author: gilson.moreira@ufrgs.br

ABSTRACT. External morphology of the immature stages of Neotropical heliconians: IX. *Dione glycera* (C. Felder & R. Felder) (Lepidoptera, Nymphalidae, Heliconiinae). The biology of the Andean silverspot butterfly *Dione glycera* (C. Felder & R. Felder, 1861) is still poorly known. This species is restricted to high elevations in the Andes, where the immature stages are found in close association with species of *Passiflora* L. belonging to the section *Tacsonia* (Juss.) Harms, especially *P. tripartida* var. *mollissima* (Kunth), which is grown for subsistence by villagers. Herein we describe and illustrate the external features of the egg, larva and pupa of *D. glycera*, based on light and scanning electron microscopy.

KEYWORDS. Andean silverspot butterfly; egg; larva; pupa; banana passion-fruit.

RESUMO. Morfologia externa dos estágios imaturos de heliconíneos neotropicais: IX. *Dione glycera* (C. Felder & R. Felder, 1861) (Lepidoptera, Nymphalidae, Heliconiinae). A biologia da borboleta do maracujá, *Dione glycera* (C. Felder & R. Felder, 1861) é pouco conhecida. Tem distribuição restrita às altitudes elevadas da Cordilheira dos Andes, aonde os imaturos são encontrados em associação com espécies de *Passiflora* L. pertencentes à secção *Tacsonia* (Juss.) Harms, principalmente *Passiflora tripartida* (Juss.) Poir. var. *mollissima* (Kunth), em vilarejos, sob cultivo de subsistência. Neste estudo, descreve-se e ilustra-se as estruturas externas do ovo, larva e pupa, com base na microscopia óptica e eletrônica de varredura.

PALAVRAS-CHAVES. Borboletas do maracujá; ovo; larva; pupa; tumbo.

The passion-vine butterflies (Lepidoptera; Nymphalidae; Heliconiini) are well known for their aposematic wing patterns, extensive Müllerian mimicry, and co-speciation with their Passifloraceae host-plants (for reviews, see Benson *et al*. 1976; Brown 1981; Gilbert 1991). The genus *Dione* Hübner, [1819] is one of the most basal lineages of passion-vine butterflies, and comprises only three species (Lamas 2004): *Dione glycera* (C. Felder & R. Felder, 1861), *Dione juno* (Cramer, 1779) and *Dione moneta* Hübner, [1825]. Of these, only *D. glycera* shows no differentiation into subspecies throughout its geographic range (Emsley 1963; Lamas 2004), and is closely associated with mountainous landscapes of the Andes, from Venezuela to Argentina (Massardo *et al.* submitted).

The larvae of *D. glycera* feed on members of the section *Tacsonia* (Juss.) Harms of the genus *Passiflora* L., using preferentially as host plant the banana passion-fruit, *Passiflora tripartita* (Juss.) Poir. var. *mollissima* (Kunth). This plant is also native to the Andes (Schwerdtfeger 2004), and is grown from Venezuela to Bolivia, at altitudes above 1,800 m. Its fruits are aromatic, highly appreciated for their pleasant taste and juice (Simirgiotis *et al.* 2013). Other species of *Passiflora*, including *P. alnifolia*, *P. cyanea*, *P. ligularis*, *P. mixta*, *P. caerulea* and *P. edulis*, have also been listed as hosts of *D. glycera* (Beccaloni *et al.* 2008).

Although the southern limit of *D. glycera* on the eastern slopes of the Andes is in Argentina, its southern range on the western slopes of the Andes reaches only to northernmost Chile (Peña & Ugarte 1996; Massardo *et al.* submitted). Adjacent to the Atacama Desert, this area (Fig. 1) is dominated by arid landscapes (Luebert & Pliscof 2006), where the presence of *D. glycera* is generally associated with its main host-plant, *P. tripartita* var. *mollissima*. This plant is locally named "tumbo" and is cultivated by villagers for its fruit and fruit juice. The plants are usually grown outdoors on espaliers (Figs. 2, 3), in scattered locations in the valleys, for example at Socoroma, Belén, Codpa and Timar villages in Parinacota Province. Immatures and flying adults have been found in low numbers during the summer on these plants.

Detailed studies describing and illustrating the external morphology of immature stages have been published for *D. juno juno* (Tavares *et al.* 2002) and *D. moneta moneta* (Kaminski *et al.* 2008). However, knowledge of the immature stages of *D. glycera* remains restricted to brief descriptions (e.g. Brown 1981; Penz 1999). As part of a series of articles dealing with the morphology of Neotropical heliconians (Antunes *et al*. 2002; Kaminski *et al.* 2002, 2008; Tavares *et al.* 2002; Paim *et al.* 2004; Silva *et al.* 2006, 2008; Barão & Moreira 2010), here we describe and illustrate in detail the external

morphology of the immature stages of *D. glycera*, based on light and scanning electron microscopy. We also discuss the characteristics found for *D. glycera* in relation to congeneric species, and in addition, provide dichotomous keys to identify the species of *Dione* at the larval and pupal stages.

MATERIAL AND METHODS

Eggs and larvae were collected from leaves of tumbo in Socoroma Village, Parinacota Province on the western slopes of the northern Chilean Andes, at ca. 3,000 m elevation, from January 2009 to July 2013 (Fig. 1). They were brought to the entomology laboratory of the Facultad de Ciencias Agronómicas, Universidad de Tarapacá, Arica, and placed in plastic bottles, with leaves of the host plant added when necessary, and reared at room temperature. Some specimens of each stage and instar were fixed in Dietrich´s fluid and preserved in 70% ethanol for subsequent observation. Additional specimens were reared until the adult stage in order to confirm the taxonomic identification. The immature specimens were deposited in the collection of the Laboratório de Morfologia e Comportamento de Insetos (LMCI), Departamento de Zoologia, Universidade Federal do Rio Grande do Sul (UFRGS), Porto Alegre, Brazil, under accession number LMCI 79. Vouchers of adults were deposited in the Colección Entomológica de La Universidad de Tarapacá (IDEA), Arica, Chile.

Aspects of the general morphology of the immature stages were analyzed from material that was either fixed or embedded in glycerin jelly. Head capsules were hydrated, cleared in a 10% potassium hydroxide solution (KOH), and slide-mounted in glycerin jelly. Drawings were made from fixed specimens, using a reticulated ocular attached to a Leica® M125 stereomicroscope. The tegumentary ultrastructure was studied at the Centro de Microscopia Eletrônica of UFRGS. For the analyses, the

specimens were dehydrated in a Bal-tec® CPD030 critical-point dryer, mounted with double-sided tape on metal stubs, and coated with gold in a Bal-tec® SCD050 sputter coater. Specimens were examined and photographed in a JEOL® JSM5800 scanning electron microscope.

To distinguish larval instars, the greatest width of the head capsule in frontal view was measured with a micrometer scale mounted in the ocular of the stereomicroscope. By using the least-squares method, the resulting data were adjusted to the power function, y=ae^bx, and following the procedure described by Snedecor & Cochran (1980).

For the egg, we use the nomenclature employed by Dell'Erba *et al.* (2005). Larval body areas are labeled according to Peterson (1962). For the primary chaetotaxy and crochet of prolegs, we follow Stehr (1987) with the modification proposed by Duarte *et al*. (2005) for the CD group of the head. The setae of the paraproct and anal prolegs are labeled according to Kitching (1984). To describe the scoli, we follow Beebe *et al.* (1960), and for the nomenclature of the pupa, we follow Mosher (1916).

RESULTS AND DISCUSSION

Egg (Figs. 4, 8-12)

Sub-spherical; flat base abruptly narrowed near apex, with a slightly depressed area at apex. Dimensions (mean + standard error; n = 8): diameter = 1.06 $\pm$ 0.03 mm; height = 1.38 $\pm$ 0.01 mm. Light yellow when recently deposited, with brown and whitish spots subsequently (Fig. 4). Chorion ornamented (Figs. 8-12) with vertical (Vr) and horizontal (Hr) smooth carinae, their number varying from 14-16 and 18-23, respectively. Vertical carinae about three times as thick as horizontal carinae. All vertical carinae start at base, but some do not reach the apex. Intersections of vertical

and horizontal carinae delimit cells, with broadly rounded internal angles and smooth surface; the lower cells (Lc) (Fig. 12) are mostly rectangular, with the horizontal margin about 2.5 times as long as the vertical margin; the upper cells (Uc) (Fig. 11) are pentagonal. Micropylar region at chorion apex (Fig. 9) slightly rugose, ornamented with two strata of polygonal cells peripherally forming the annulus, and one stratum of oval cells centrally forming the rosette in the center of which are the micropyles. Aeropyles (Fig. 10) as small circular pores at intersections of vertical and horizontal carinae.

The gross morphology, color variation and ornamentation of the egg of *D. glycera* fit the pattern previously reported for the eggs of *D. juno juno* (Tavares *et al.* 2002; Dell'Erba *et al.* 2005) and *D. moneta moneta* (Dell'Erba *et al.* 2005; Kaminski *et al.* 2008). These aspects resemble the eggs of *Agraulis vanillae maculosa* (Stichel, [1908]) (Dell'Erba *et al.* 2005; Silva *et al.* 2006). However, in the lower cells of the chorion of the three species of *Dione* the length of the horizontal margin is more than twice that of the vertical margin, whereas in the lower cells of *A. vanillae maculosa* the length of the horizontal margin is less than twice that of the vertical one (Dell'Erba *et al.* 2005; Silva *et al.* 2006). Thus, the lower cells of *Dione* are comparatively broader, whereas in *A. vanillae maculosa* the lower cells are higher. Furthermore, some of the vertical carinae in the three species of *Dione* are well defined until near the micropylar region, slightly projected distally, encircling the micropylar region; whereas the vertical carinae of *A. vanillae maculosa* change slightly in orientation along the distal third, and are not projected distally (Dell'Erba *et al.* 2005; Silva *et al.* 2006).

Larva

First instar (Figs. 5, 13-15, 23-36)

Head (Figs. 5, 13-14, 23-29). Blackish, with setae smooth, variable in size, with apex widened in P2 and L1 (Figs. 13-14, 29) and pointed in the remaining cephalic setae (Figs. 13-14, 28); frontoclypeus triangular; frontoclypeal suture not differentiated; anteclypeus membranous, as a straight transverse stripe between frontoclypeus and labrum; antennal pocket lateral to mouthparts (Figs. 23, 25), membranous, with many round protuberances; a group of six stemmata (Figs. 13, 14, 24) dorsal to each antennal pocket; stemmata 1-5 in semicircle, stemma 6 slightly posterior to an imaginary line from stemmata 1 to 5. Antenna tri-segmented (Fig. 25); first segment ring-like, short, partially hidden by antennal pocket; second segment cylindrical, diameter about 2/3 that of first segment, four sensilla at apex; third segment cylindrical, short and narrow, about half length and diameter of second segment, also with four sensilla at apex.

Mouthparts of chewing type (Figs. 13, 14, 23). Labrum (Figs. 13, 23) bi-lobed, with distal margin broadly cleft at middle, six pairs of short, hair-like setae on external surface; mandible with five teeth on distal margin, two setae on external surface; maxilla (Fig. 27) with palpus and galea well differentiated; palpus with eight sensilla at apex and one on medial surface; galea with seven sensilla; labium (Fig. 26) with pair of bi-segmented palpi, each with one sensillum at apex, first segment about six times longer than second segment; spinneret postero-ventral to labial palpi, about 2.5 times the length of a labial palpus, with orifice opening at apex and a pair of small setae near the base.

Thorax and abdomen mostly reddish brown, with cream-white spots and a faint yellowish-brown dorsal stripe; prothoracic dorsal shield, anal shield, pinnacles, setae, thoracic legs and lateral plates of prolegs black; setae smooth, variable in size, with apex either acute or widened (Figs. 15, 30, 31). Prothoracic dorsal shield rectangular with rounded angles, anterior and posterior margins with slight cleft at middle. Anal

shield trapezoidal, with broadly rounded angles and posterior margin broadly convex. Spiracles (Figs. 15, 36) laterally on prothorax and A1-8, circular, with peritrema elevated; prothoracic spiracle posterior to pinnacle of lateral group of setae; abdominal spiracles between lateral and sub-dorsal groups of setae; diameter of prothoracic spiracle similar to that of A8 and slightly larger than the remaining A1-7. Two well-developed legs (Fig. 32), ventrally on each thoracic segment; coxa whitish brown, with a black transverse stripe interrupted laterally; trochanter a narrow transverse stripe between coxa and femur; femur, tibia, tarsus and tarsal claw black; tarsal claw slightly curved, with a plain, round enlargement at base and sharp apex. Two well-developed prolegs (Fig. 33) ventrally on A3-6 and A10, each with a blackish lateral plate, and provided with 13-14 crochets at apex; crochets of A3-6 in uniordinal, uniserial circle, those of A10 in semicircle. Integument mostly smooth, ventral area, prolegs and area surrounding the anus provided with conical microtrichia (Fig. 34), those surrounding the anus with longer apex (Fig. 35).

Chaetotaxy

Head (Figs. 13, 14). 17 pairs of setae, 4 pairs of microsetae and 11 pairs of pores.

Adfrontal (AF) group; bisetose; AF2 near dorsal angle of frontoclypeus; AF1 at about dorsal third of adfrontal suture; AFa pore closer to AF2 than to AF1. Anterior (A) group: trisetose; A1 dorsal to antennal pocket; A2 dorsomedial to A1; A3 dorsolateral to A2; Aa pore ventrolateral to A3. Cephalo-dorsal (CD) group: trisetose; CD1, CD2 and CD3 microsetae, almost in straight line posterior to P2; pore CDa posteroventral to CD1. Clypeal (C) group: bisetose; both setae near ventral margin of frontoclypeus; C1 closer to intersection of ventral margin of frontoclypeus and adfrontal suture; C2 medial

to C1. Frontal (F) group: unisetose; F1 slightly displaced toward ventral half of frontoclypeus. Lateral (L) group: unisetose; L1 about midway between P2 and S2; La pore posteroventral to L1. Microgenal (MG) group: unisetose, MG1 a microseta, posteroventral to S3; MGa pore anterodorsal to MG1. Posterodorsal (P) group: bisetose; P1 and P2 forming an imaginary line almost parallel to epicranial suture; P2 posterodorsal to P1; pore Pb anteroventral to P2; pore Pa ventral to P1. Stemmatal (S) group: trisetose; S1 at about midpoint between stemmata 1 and 5; S2 posterior to stemma 1; S3 posteroventral to S2; pore Sa ventral to S2; pore Sb between stemmata 3 and 4. Substemmatal (SS) group: trisetose; SS2 between stemmata 5 and 6; SS1 near antennal pocket; SS3 between SS1 and SS2; pore SSb between SS3 and SS2; pore SSa not found.

Thorax (Fig. 15). Prothorax: 10 pairs of setae (D1, D2, XD2, SD1, SD2, L1, L2, SV1, SV2, V1); D and XD groups on the prothoracic dorsal shield; D1 and XD2 near anterior margin, with XD2 displaced toward anterolateral angle of shield and D1 toward the middle; D2 near posterior margin of shield; pore XDc between XD2 and D2. SD group bisetose, with both setae on a pinnacle ventral to dorsal shield. L group bisetose, with both setae on a pinnacle anterior to spiracle. SV group bisetose, with both setae on a pinnacle posteroventral to L group. Ventral group unisetose, posteromedial to prothoracic coxa. Meso- and metathorax: eight pairs of setae (D1, D2, SD1, SD2, L1, SV1, SV2, V1); D1 and D2 on separate pinnacles, with D1 dorsal and slightly anterior to D2; SD group on a single pinnacle, ventral and slightly anterior to D2; L1 on a ventral pinnacle and slightly anterior to SD group; SV group on a single pinnacle ventral to L1; V1 posteromedial to mesothoracic coxa.

Abdomen (Fig. 15). A1: seven pairs of setae (D1, D2, SD1, L1, L2, SV1, V1); D1 and D2 on separate pinnacles, with D1 anterodorsal to D2; SD1 on a pinnacle

anteroventral to D2 and dorsal to spiracle; L group on separate pinnacles, with L1 posterodorsal to L2; SV1 on a small pinnacle between L group and V1. A2: eight pairs of setae (D1, D2, SD1, L1, L2, SV1, SV2, V1), with spatial distribution similar to preceding segment, but SV group on two small separate pinnacles. A3-6: eight pairs of setae (D1, D2, SD1, L1, L2, SV1, SV2, V1), with distribution similar to preceding segment, but SV group and V1 on the respective prolegs; SV group on a broad lateral plate, and V1 on the medial surface. A7, 8: six pairs of setae (D1, D2, SD1, L1, L2, SV1), with distribution of setae similar to A1, but V1 absent. A9: five pairs of setae (D1, D2, SD1, L1, SV1); pinnacles of right and left D1 medially fused; D1, D2, SD1 and L1 almost forming a straight line; SV1 posteroventral to L1. A10: 12 pairs of setae (D1, D2, SD1, SD2, PP1, SP1, PL1, PL2, PL3, PL4, PL5, V1); D and SD groups on anal shield; PP1 and SP1 on small pinnacles on posterior surface of proleg; PL1, PL2, PL3 and PL4 on lateral plate of proleg; PL5 and V1 on medial surface of proleg.

The gross morphology and chaetotaxy of the first instar of *D. glycera* fit the general pattern for Heliconiini (Antunes *et al.* 2002; Kaminski *et al.* 2002, 2008; Tavares *et al.* 2002; Paim *et al.* 2004; Silva *et al.* 2006, 2008; Barão & Moreira 2010). However, a conspicuous variation among the first instars is related to the shape of the apex of some primary setae of the head, thorax and abdomen, which is generally widened, as in *D. glycera* (this study), *D. moneta moneta* (Kaminski *et al.* 2008), *A. vanillae maculosa* (Silva *et al.* 2006), *Heliconius erato phyllis* (Fabricius, 1775) (Kaminski *et al.* 2002), *Dryadula phaetusa* (Linnaeus, 1758) (Silva *et al.* 2008), *Dryas iulia alcionea* (Cramer, 1779) (Paim *et al.* 2004), and *Philaethria wernickei* (Röber, 1906) (Barão & Moreira 2010), but it is acute in *Eueides isabella dianasa* (Hübner, 1806), and 3-4 tipped in *D. juno juno* (Tavares *et al.* 2002).

249 The distribution of the setae with widened apex on the head capsule enables us
250 to separate *D. glycera* from *D. moneta:* setae P2 and L1 have widened apices in *D.*
251 *glycera*, whereas in *D. moneta* setae P1 and P2 have this shape (Kaminski *et al.* 2008).
252
253 Subsequent instars
254 Color pattern is variable starting in the second instar. Three chromatic patterns
255 were observed in the fifth instar, with a large number of intermediate forms (Figs. 6, 17-
256 22). One of these patterns (Figs. 21, 22) is characterized by the head, thorax, prolegs,
257 scoli and verrucae mostly pinkish-yellowish brown; head with a blackish area
258 associated with the stemmata, mandibles dark orange; thorax and abdomen with a broad
259 whitish-cream lateral stripe, dorsal scoli on a longitudinal light-gray stripe with an
260 irregular yellowish-orange spot at the base of each scolus and some similar, scattered
261 spots; an irregular yellowish-orange spot at base of the remaining scoli, enclosed by an
262 irregular light-gray spot; some scattered small dark-gray spots; scoli darkening distally.
263 Another pattern (Figs. 17, 18) has the head, legs, prolegs, scoli and verrucae
264 black; thorax and abdomen with a broad whitish-cream lateral stripe; dorsal scoli on a
265 yellow longitudinal stripe with an irregular orange spot at the base of each scolus and
266 some similar, scattered spots; an irregular orange spot at the base of the remaining scoli,
267 enclosed by an irregular yellow spot; lateral plates of the prolegs black or dark
268 yellowish brown. In a third, intermediate pattern (Figs. 19, 20), two pairs of black
269 stripes present frontally on the orange head, and the body is bluish. There is substantial
270 variation in the corresponding tones of blue and also in the size of the black stripes on
271 the head.
272 The chaetotaxy also changes strikingly starting from the second instar (Fig. 16).
273 The primary setae are replaced by secondary setae (Figs. 37, 38, 41), scoli (Fig. 39) and

verrucae (Fig. 40). The head (Fig. 37) is smooth and covered by a large number of hair-like setae which vary in length; and bears two short stout scoli dorsally (Figs. 16-19), namely the cephalic scoli, which are provided with several short, hair-like setae. The thorax and abdomen have the integument covered by conical, striated microtrichia (Figs. 41, 42) and scattered hair-like setae (Fig. 41); prothoracic dorsal shield (Fig. 38) bears a number of short hair-like setae and two pairs of stout spine-like setae on small dorsal conical projections; elliptical spiracles (Fig. 43) with slightly elevated peritrema laterally on prothorax and abdominal segments A1-8, those of prothorax and A8 slightly larger than the remaining spiracles; prolegs (Fig. 44) with lateral plates covered by several hair-like setae, crochets (Fig. 45) in uniserial and multiordinal arrangement. Thirty pairs of thoracic and abdominal scoli, which are elongated conical tegumentary outgrowths, provided with some hair-like setae on the surface, one of which, typically the longest one, is placed at the apex; 11 dorsal pairs (T1-2 and A1-9); ten supraspiracular pairs (T1-2 and A1-8), with those of the meso- and metathorax anteriorly displaced; eight lateral pairs (A1-8), and one anal pair (A10). Thirteen pairs of thoracic and abdominal verrucae; three pairs on prothorax, one between dorsal shield and spiracle, which is provided with a spine-like seta, another greatly reduced pair anterior to spiracle, and another pair between spiracle and coxa; two pairs on meso and metathorax, one posterior to supraspiracular scolus and another dorsal to coxa; one pair on A1-2 and A7-8, which is ventral to lateral scolus; and two pairs on A9, one near the dorsal scolus, and another on the lateroventral face of the segment.

As in the first instar, the gross morphology of the subsequent instars of *D. glycera* fits the general pattern described for Heliconiini (Antunes *et al.* 2002; Kaminski *et al.* 2002, 2008; Tavares *et al.* 2002; Paim *et al.* 2004; Silva *et al.* 2006, 2008; Barão & Moreira 2010). However, the length of the cephalic scoli of *D. glycera* is less than

299 half the height of the head capsule, appearing as a short, stout projection. This pattern is
300 found with even greater reduction in *D. juno juno* (Tavares *et al.* 2002); meanwhile in
301 the other congener *D. moneta moneta* (Kaminski *et al.* 2008) these structures are
302 elongated, as in the remaining heliconians whose immature stages have been studied
303 (Antunes *et al.* 2002; Kaminski *et al.* 2002; Paim *et al.* 2004; Silva *et al.* 2006, 2008;
304 Barão & Moreira 2010).

305 The distribution pattern of the verrucae resembles that of *D. moneta moneta*
306 (Kaminski *et al.* 2008). However, the spine-like seta on the verruca between the
307 prothoracic dorsal plate and the prothoracic spiracle in *D. glycera* is absent in *D. moneta*
308 *moneta*. This seta has not been reported for any other heliconian for which the early
309 stages are described. Furthermore, the verruca anterior to the prothoracic spiracle and
310 that on the lateroventral face of A9 are less developed in *D. glycera* than in *D. moneta*
311 *moneta*.

312 Another interesting aspect of the larvae of *D. glycera* is the striking variation in
313 the color pattern among individuals (Figs. 17-22). Intraspecific variation in the color
314 pattern of heliconiines has been also recorded for the congeneric *D. moneta moneta*
315 (Kaminski *et al.* 2008) and for *A. vanillae maculosa* (Silva *et al.* 2006).

316

317 Instar identification

318 The first instar is strikingly different from the other stages in the absence of
319 scoli, and also in the color pattern. After the first molt, identification based on color
320 pattern or morphology is difficult, because the instars do not show stable differences in
321 these attributes. However, the successive instars can be accurately distinguished by the
322 width of the head capsule,, because the widths measured in successive instars did not
323 overlap (Table I). The following exponential growth equation was adjusted for the five

instars ($y=0.652e^{0.198x}$; n= 32; $r^2=0.975$; $p<0.05$). Thus, the growth pattern of the head capsule follows the Brooks-Dyar rule (Daly 1985). The mean growth ratio among instars was 1.56, similar to ratios previously reported for other Neotropical heliconians (Antunes *et al.* 2002; Kaminski *et al.* 2002, 2008; Tavares *et al.* 2002; Paim *et al.* 2004; Silva *et al.* 2006, 2008; Barão & Moreira 2010).

Pupa (Figs. 7, 46-65)

Variable in coloration throughout ontogeny, with mixture of light gray, dark brown, pinkish brown, cream white and black (Fig. 7). Abdominal segments A1 and A2 with pair of silvery blotches dorsally. Length (mean + standard error; n = 5) = 19.55 $\pm$ 0.34 mm.

Head with pair of short, angled cephalic projections (Figs. 46, 48, 51); epicranial suture absent; eyes (Fig. 49) with sculptured region near antenna, bearing few short hair-like setae (Fig. 50), and another smooth region near front; labrum as a slight, short longitudinal stripe between the mandibles; maxilla with well-developed galeae, along midline of ventral surface, anteriorly delimited by labrum and mandibles, slightly surpassing posterior margin of A4; antennae arising dorsally on head, projected ventrally to apex of maxilla, with many smooth, round tubercles on surface (Fig. 52).

Thorax with the three segments exposed. Prothorax as a small hexagonal plate in dorsal view, with anterior and posterior margins broadly excavated, with a pair of lateral tubercles (Figs. 47, 53). Mesothorax broadly expanded laterally along anterior half, with well-defined basilar tubercles (Fig. 57) and a longitudinal, meso-dorsal crest (Figs. 47, 54) that is greatly developed, broadly rounded, between a pair of round lateral tubercles; two parallel rows, termed submarginal and postmedian, with three tubercles each near apex of wing (Fig. 58, 59); mesothoracic spiracle (Fig. 61) opening laterally at anterior

margin of segment, as a simple cleft and with microtrichia. Metathorax as a narrow plate with anterior margin broadly excavated, with pair of lateral tubercles, hindwings as straight stripes between forewings and abdominal segments.

Abdomen with segments A1-4 partially hidden by wings; with pair of lateral tubercles on A1-8, which are little developed on A1-2 (Fig. 55), most developed on A3, and decreasing in size posteriorly; one meso-dorsal tubercle on A5-7 (Fig. 56); one supraspiracular tubercle (Fig. 60) on A3-4; pair of ventral tubercles (Fig. 63) on A5-6; spiracles of A1 and A2 hidden and partially hidden, respectively, by forewings, and spiracles of A3-7 elliptical (Fig. 62) with a well-developed filter apparatus; spiracles of A8 greatly reduced. Cremaster (Fig. 64) quadrate, with truncate apex, and a large number of short, curved hooks (Fig. 65).

The pupal morphology of *D. glycera* fits the pattern recognized by Mosher (1916) for Nymphalidae, characterized by the absence of an epicranial suture, and by the prothoracic and mesothoracic legs extended anteroventrally, reaching the posterior margin of the eye.

The cephalic projections of the pupa of *D. glycera* are short, slightly surpassing the anterior margin of the head. This pattern is also found in the pupae of the other two species of *Dione* (Tavares *et al.* 2002; Kaminski *et al.* 2008). The cephalic projections are more developed in *A. vanillae maculosa* (Silva *et al.* 2006); they substantially exceed the anterior margin of the head, and are as long as ca. half of the head.

Further remarks:

This is the first detailed study dealing with the external morphology of all the early stages of *D. glycera*. As similar studies are available for the other two species of the genus (Tavares *et al*. 2002; Kaminski *et al*. 2008), we compared the egg, first-instar

larva, fifth-instar larva, and pupa of the three species of *Dione* in order to test the diagnostic value of the morphology of the early stages.

The egg morphology easily separates *Dione* from the sister group *Agraulis* (Penz 1999; Massardo *et al.* submitted). However, as mentioned above, we could not find stable differences to distinguish among the species of *Dione* at this stage. On the other hand, field observations suggested that females of *D. glycera* generally lay eggs individually on the leaves of the host plant, usually members of *Tacsonia* (Juss.) Harms within the subgenus *Passiflora* L. Rarely more than one egg is deposited per leaf. This egg-laying behavior is strikingly different from that reported for the other two species of the genus. Clusters of 60-140 eggs have been mentioned for *D. juno* (Dell'Erba *et al.* 2005), and clusters of up to 20 eggs have been recorded for *D. moneta* (Dell'Erba *et al.* 2005; Kaminski *et al*. 2008). Occasionally the eggs can also be deposited individually in this species (Brown 1944; Brown 1981; DeVries 1987), which may make it difficult to distinguish them from eggs of *D. glycera* by means of this characteristic. *Dione moneta* and *D. glycera* are sister species, but the former occurs at much lower elevations, and the larvae are specialized feeders not on species of the subgenus *Passiflora* L., but on *Decaloba* (DC.) Rchb. (Massardo *et al*. submitted).

Nonetheless, we found clear differences for the first- and fifth-instar larvae and for the pupal stage, which allow their prompt identification, and which are summarized in the following dichotomous keys:

a) First-instar larva;

1 Dorsal setae of thorax and abdomen with widened apex …… 2

1' Dorsal setae of thorax and abdomen 3-4 tipped …… *D. juno*

2 Head seta P2 with widened apex and L1 with acute apex …… *D. moneta*

2' Head seta P2 with acute apex and L1 with widened apex …… *D. glycera*

399

400 b) Fifth-instar larva;

401 1 Prothoracic dorsal shield without scoli ……..…… 2

402 1’ Prothoracic dorsal shield with pair of scoli ……..…….…… *D. juno*

403 2 Cephalic scoli longer than half width of head …….…..… *D. moneta*

404 2’ Cephalic scoli shorter than half width of head ……..…….… *D. glycera*

405

406 c) Pupa;

407 1 One pair of golden spots dorsally on A1-2 ……..…… 2

408 1’ Dorsal surface of A1-2 without silver or golden spots ……...… *D. juno*

409 2 Cephalic projection broadly round and expanded laterally…… *D. moneta*

410 2’ Cephalic projection angled, not expanded laterally….……....…. *D. glycera*

411

412

413 ACKNOWLEDGEMENTS

414 We are grateful to the staff members of the Centro de Microscopia Eletrônica of
415 UFRGS for the use of facilities and for their assistance in scanning electron microscopy
416 analyses. Thanks are also due Janet W. Reid for editing the text. The financial support
417 for this study came in part from a CAPES Doctoral Fellowship granted to D. Massardo.
418 The work was also supported by CNPq, Brazil (Project 490124/2010-0, PROSUL –
419 08/2010, and project number 309676/2011-8, granted to G.R.P. Moreira.

420

421

422

423

424 REFERENCES

425 Antunes, F. A., A. O. Menezes Jr., M. Tavares & G. R. P. Moreira. 2002. Morfologia
426 externa dos estágios imaturos de heliconíneos neotropicais: I. *Eueides isabella*
427 *dianasa* (Hübner, 1816). **Revista Brasileira de Entomologia 46**: 601–610.

428 Barão, K. R. & G. R. P. Moreira. 2010. External morphology of the immature stages of
429 Neotropical heliconians: VIII. *Philaethria wernickei* (Röber) (Lepidoptera,
430 Nymphalidae, Heliconiinae). **Revista Brasileira de Entomologia 54**: 406-418. doi:
431 10.1590/S0085-56262010000300008.

432 Beccaloni, G. W., Á. L. Viloria, S. K. Hall & G. S. Robinson. 2008. **Catalogue of the**
433 **hostplants of the Neotropical butterflies**. Zaragoza, Sociedad Entomológica
434 Aragonesa, 403p. (Monografías Tercer Milenio, 8)

435 Beebe, W., J. Crane & H. Fleming. 1960. A comparison of eggs, larvae and pupae in
436 fourteen species of Heliconiine butterflies from Trinidad, W. I. **Zoologica 45**: 111-
437 154.

438 Benson, W. W., K. S. Brown Jr., & L. E. Gilbert. 1976. Coevolution of plants and
439 herbivores: passion vine butterflies. **Evolution 29**: 659-680.

440 Brown, F. M. 1944. The egg, larva and chrysalis of *Dione moneta* Hübner. **Bulletin of**
441 **the Brooklyn Entomological Society 39**: 132-134.

442 Brown, K. S. Jr. 1981. The biology of *Heliconius* and related genera. **Annual Review**
443 **of Entomology 26**: 427-456. doi: 10.1146/annurev.en.26.010181.002235.

444 Daly, H. V. 1985. Insect morphometrics. **Annual Review of Entomology 30**: 415–438.

445 Dell'Erba, R., L. A. Kaminski & G. R. P. Moreira. 2005. O estágio de ovo dos
446 Heliconiini (Lepidoptera, Nymphalidae) do Rio Grande do Sul, Brasil. **Iheringia,**
447 **Série Zoologia 95**: 29–46.

448 DeVries, P. J. 1987. **The butterflies of Costa Rica and their natural history.**
449 **Papilionidae, Pieridae, Nymphalidae**. Princeton, Princeton University, 327 p.
450 Duarte, M., R. K. Robbins & O. H. H. Mielke. 2005. Immature stages of *Calicopis*
451 *caulonia* (Hewitson, 1877) (Lepidoptera, Lycaenidae, Techlinae, Eumaeini), with
452 notes on rearing detritivorous hairstreaks on artificial diet. **Zootaxa 1063**: 1-31.
453 Emsley, M. 1963. A morphological study of imagine Heliconiinae (Lepidoptera,
454 Nymphalidae) with a consideration of the evolutionary relationships within the
455 group. **Zoologica 48**: 85-129.
456 Gilbert, L. E. 1991. Biodiversity of a Central American *Heliconius* community: Pattern,
457 process, and problems. p. 403-427. *In*: Price, P.W., T. M. Lewinsohn, G. W.
458 Fernandes & W. W. Benson (eds.) **Plant-animal interactions: Evolutionary**
459 **ecology in tropical and temperate regions**. New York: John Wiley & Sons.
460 Kaminski, L. A., R. Dell'Erba & G. R. P. Moreira. 2008. Morfologia externa dos
461 estágios imaturos de heliconíneos neotropicais: VI. *Dione moneta moneta* Hübner
462 (Lepidoptera, Nymphalidae, Heliconiinae). **Revista Brasileira de Entomologia 52**:
463 13–23.
464 Kaminski, L. A., M. Tavares, V. G. Ferro & G. R. P. Moreira. 2002. Morfologia externa
465 dos estágios imaturos de heliconíneos neotropicais: III. *Heliconius erato phyllis*
466 (Fabricius) (Lepidoptera: Nymphalidae: Heliconiinae). **Revista Brasileira de**
467 **Zoologia 19**: 977–993.
468 Kitching, I. J. 1984. The use of larval chaetotaxy in butterfly systematics, with special
469 reference to the Danaini (Lepidoptera: Nymphalidae). **Systematic Entomology 9**:
470 49–61.

Lamas, G. 2004. Checklist: Part 4A. Hesperioidea - Papilionoidea. p. 261-274, *In*: Heppner, J. B. (ed.). **Atlas of Neotropical Lepidoptera**. Volume 5A. Gainesville, Association for Tropical Lepidoptera, Scientific Publishers.

Luebert, F. & P. Pliscoff. 2006. **Sinopsis bioclimática y vegetacional de Chile.** Editorial Universitaria, Santiago, Chile, 316p.

Massardo, D., G. L. Gonçalves, R. Fornel, M. R. Kronforst & G. R. P. Moreira. submitted. Multilocus DNA sequences and geometric morphometrics analysis reveal evolutionary history of the passion vine butterfly genus *Dione*. **BMC Evolutionary Biology** [September, 2013]

Mosher, E. 1916. A classification of the Lepidoptera based on characters of the pupa. **Bulletin of the Illinois State Laboratory of Natural History 12**: 1–165.

Paim, A. C., L. A. Kaminski & G. R. P. Moreira. 2004. Morfologia externa dos estágios imaturos de heliconíneos neotropicais. IV. *Dryas iulia alcionea* (Lepidoptera: Nymphalidae: Heliconiinae). **Iheringia, Série Zoologia 94**: 25–35.

Penz, C. M. 1999. Higher level phylogeny for passion-vine butterflies (Nymphalidae, Heliconiinae) based on early stage and adult morphology. **Zoological Journal of the Linnean Society 127**: 277-344.

Peña-G., L. E. & A. J. Ugarte-P. 1996. Las mariposas de Chile. The butterflies of Chile. Santiago, Editorial Universitaria, 359 p.

Peterson, A. 1962. **Larvae of insects. An introduction to Nearctic species. Part Lepidoptera and plant infesting Hymenoptera**. Ann Arbor, Edwards Brothers Inc., 315 p.

Schwerdtfeger, M. 2004. Passiflowers of the Andes, p.75-77. *In*: Ulmer, T. & J. M. MacDougal (eds.) ***Passiflora*: Passionflowers of the World**. Portland, Timber Press, 432 p.

496 Silva, D. S., R. Dell'Erba, L. A. Kaminski & G. R. P. Moreira. 2006. Morfologia
497 externa dos estágios imaturos de heliconíneos neotropicais: V. *Agraulis vanillae*
498 *maculosa* (Lepidoptera, Nymphalidae, Heliconiinae). **Iheringia, Série Zoologia**
499 **96**: 219–228.
500 Silva, D. S., L. A. Kaminski, R. Dell'Erba & G. R. P. Moreira. 2008. Morfologia
501 externa dos estágios imaturos de heliconíneos neotropicais: VII. *Dryadula phaetusa*
502 (Linnaeus) (Lepidoptera, Nymphalidae, Heliconiinae). **Revista Brasileira de**
503 **Entomologia 52**: 500-509.
504 Simirgiotis, M. J., G. Schmeda-Hirschmann, J. Bórquez & E. J. Kennelly. 2013. The
505 *Passiflora tripartita* (Banana Passion) Fruit: A Source of bioactive flavonoid C-
506 glycosides isolated by HSCCC and characterized by HPLC–DAD–ESI/MS/MS.
507 **Molecules 18**: 1672-1692.
508 Snedecor, G. W. & W. G. Cochran. 1980. **Statistical methods**. Ames, Iowa State
509 University, 507 p.
510 Stehr, F. W. 1987. Order Lepidoptera, p. 288–305. *In*: F. W. Stehr (Ed.). **Immature**
511 **insects**. Vol. I. Dubuque, Kendall/ Hunt Publishing Company, 975 p.
512 Tavares, M., L. A. Kaminski & G. R. P. Moreira. 2002. Morfologia externa dos estágios
513 imaturos de heliconíneos neotropicais: II. *Dione juno juno* (Cramer) (Lepidoptera:
514 Nymphalidae: Heliconiinae). **Revista Brasileira de Zoologia 19**: 961–976.
515
516 Legends:
517 Figs. 1-7. Life-history of *Dione glycera* (C. Felder & R. Felder). 1, Habitat (Socoroma
518 Valley, Parinacota Province, Atacama Desert, Chile, 3,000 m); 2, Larval host plant
519 [*Passiflora tripartita* (Juss.) Poir.] under cultivation*;* 3,corresponding leaves and

520 flowers in detail; 4) egg on leaf upper surface; 5, first instar; 6, fifth instar; 7, pupa. Bars
521 = 1, 1, 5 and 2.5 mm, respectively.
522
523 Figs. 8–12. Scanning electron micrographs of *Dione glycera* (C. Felder & R. Felder)
524 egg. 8, lateral view; 9, micropylar region; 10, aeropyle; 11, upper cells; 12, lower cells.
525 Ac, aeropyle; Ap, anterior pole; Hr, horizontal carina; Lc, lower cell; Mp, micropyles;
526 Uc, upper cell; Vr, vertical carina. Bars = 500, 100, 20, 100 and 100 μm, respectively.
527
528 Figs. 13–16. Chaetotaxy of *Dione glycera* (C. Felder & R. Felder). 13, frontal view of
529 head capsule; 14, lateral view of head capsule; 15, first instar, lateral view; 16, fifth
530 instar, lateral view. A, anterior seta; AF, adfrontal seta; C, clypeal seta; D, dorsal seta;
531 F, frontal seta; L, lateral seta; P, postero-dorsal seta; S, stemmatal seta; SS,
532 substemmatal seta; PL, seta of proleg cylindrical section of tenth abdominal segment;
533 PP, paraproctal seta; Sc, cephalic scolus; SD, subdorsal seta; Sl, subspiracular scolus;
534 Sn, anal scolus; So, dorsal scolus; Sp, supraspiracular scolus; SV, subventral seta; XD,
535 prothoracic seta. Bars = 1 and 5 mm, respectively.
536
537 Figs. 17-22. Variation in coloration patterns among fifth-instar larvae of *Dione glycera*
538 (C. Felder & R. Felder), shown schematically for the head capsule and fourth abdominal
539 segment, respectively in frontal and lateral views. 17, 20, blackish; 18, 21 bluish; 19,
540 22, brownish.
541
542 Figs. 23–29. Scanning electron micrographs of *Dione glycera* (C. Felder & R. Felder)
543 first-instar head. 23, antero-ventral view of head; 24, stemmatal region, lateral; 25,

544 antenna, antero-lateral; 26, spinneret, lateral; 27, maxilla, anterior; 28 and 29, setae of
545 head, lateral. Bars = 200, 100, 40, 40, 40, 50 and 50 μm, respectively.
546
547 Figs. 30-36. Scanning electron micrographs of *Dione glycera* (C. Felder & R. Felder)
548 first-instar thorax and abdomen. 30, chalazae, lateral view; 31, corresponding apex of
549 setae in detail; 32, mesothoracic leg; 33, proleg with exposed crochets; 34, microtrichia
550 of ventral region; 35, microtrichia of anal plate; 36, spiracle of eighth abdominal
551 segment; Bars = 100, 40, 50, 50, 10, 10 and 50 μm, respectively.
552
553 Figs. 37-45. Scanning electron micrographs of *Dione glycera* (C. Felder & R. Felder)
554 fifth instar. 37, stemmatal region, dorso-frontal view; 38, prothoracic plate, postero-
555 dorsal; 39, dorsal scolum; 40, verruca, lateral; 41, microseta and microtrichia of dorsal
556 region; 42, microtrichia of scoli basis; 43, spiracle of eighth abdominal segment; 44,
557 proleg of fifth abdominal segment; 45, corresponding crochets in detail. Bars = 200,
558 500, 200, 100, 20, 20, 100, 200 and 100 μm, respectively.
559
560 Figs. 46-47. *Dione glycera* (C. Felder & R. Felder) pupa, ventral (46) and dorsal (47)
561 views. A, abdominal segment; T, thoracic segment. Bar = 5 mm.
562
563 Figs. 48-53. Scanning electron micrographs of *Dione glycera* (C. Felder & R. Felder)
564 pupal head and thorax. 48, head, ventral view; 49, eye, lateral; 50, seta from eye
565 sculptured region; 51, cephalic projection, dorsal; 52, tubercles of antennal median
566 portion; 53, prothoracic tubercle, dorsal. Bars = 1000, 300, 200, 500, 150, and 50 μm,
567 respectively.
568

Figs. 54-65. Scanning electron micrographs of *Dione glycera* (C. Felder & R. Felder) pupal thorax and abdomen. 54, mesothoracic meso-dorsal crest, lateral view; 55, latero-dorsal tubercle of third abdominal segment, lateral; 56, median-dorsal tubercle, lateral; 57, basilar tubercle, lateral; 58, distal tubercles of forewing; 59, distal tubercle of forewing in detail; 60, supra-spiracular tubercle (seta) of seventh abdominal segment; 61, mesothoracic spiracle; 62, spiracle of seventh abdominal segment; 63, ventral tubercle; 64, cremaster, ventral; 65, cremaster hooks in detail. Bars = 1000, 1000, 200, 500, 500, 100, 300, 200, 200, 400, 1000 and 40 μm, respectively.

Table I. Mean and standard error (SE), interval of variation (IV), and growth rates (GR) of head capsule width in larval instars of *Dione glycera* (C. Felder & R. Felder) reared on *Passiflora tripartita* (Juss.) Poir. var. *mollissima* (Kunth).

		Head capsule width (mm)		
Instar	**N**	**Mean ± SE**	**IV**	**GR**
I	5	0.58±0.02	0.52 - 0.66	---
II	7	0.92±0.04	0.90 - 1.10	1.58
III	8	1.54±0.03	1.41 - 1.71	1.67
IV	5	2.55±0.07	2.44 - 2.79	1.65
V	7	3.46±0.05	3.30 - 3.73	1.35

Figs. 1-7_Vargas et al.
(adjust to page width)

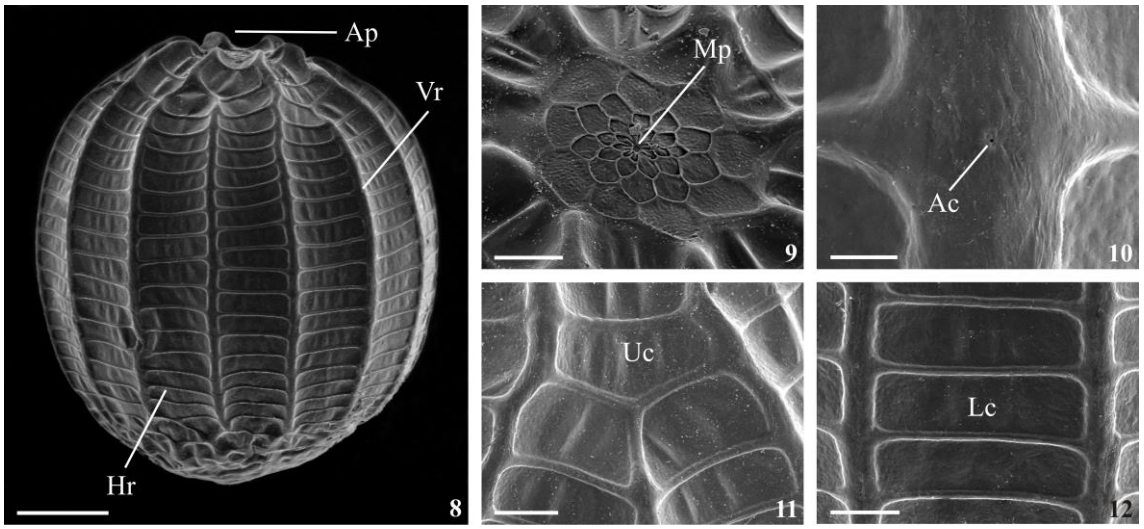

Figs. 8-12_Vargas et al.
(adjust to page width)

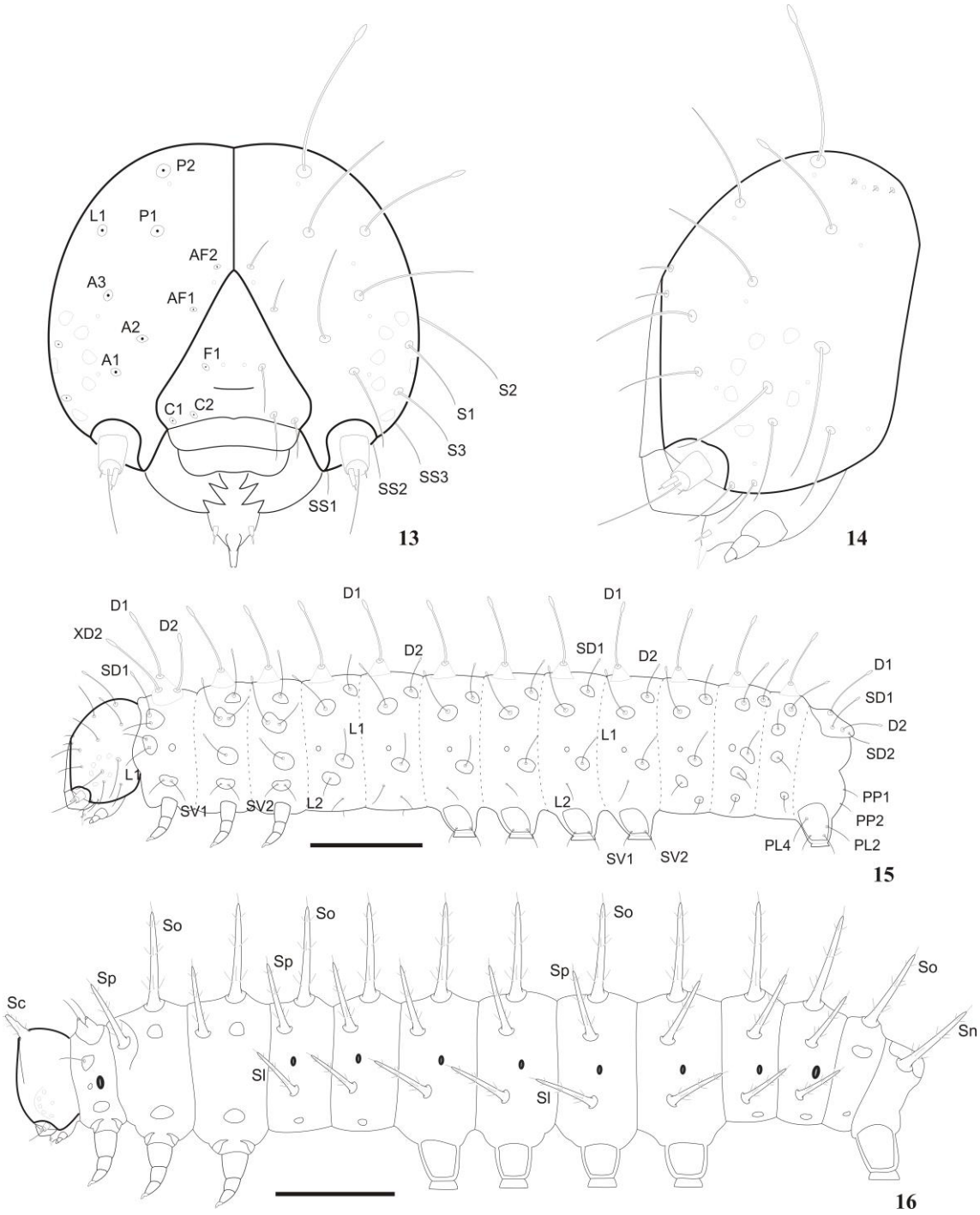

Figs. 13-16_Vargas et al.
(adjust to page width)

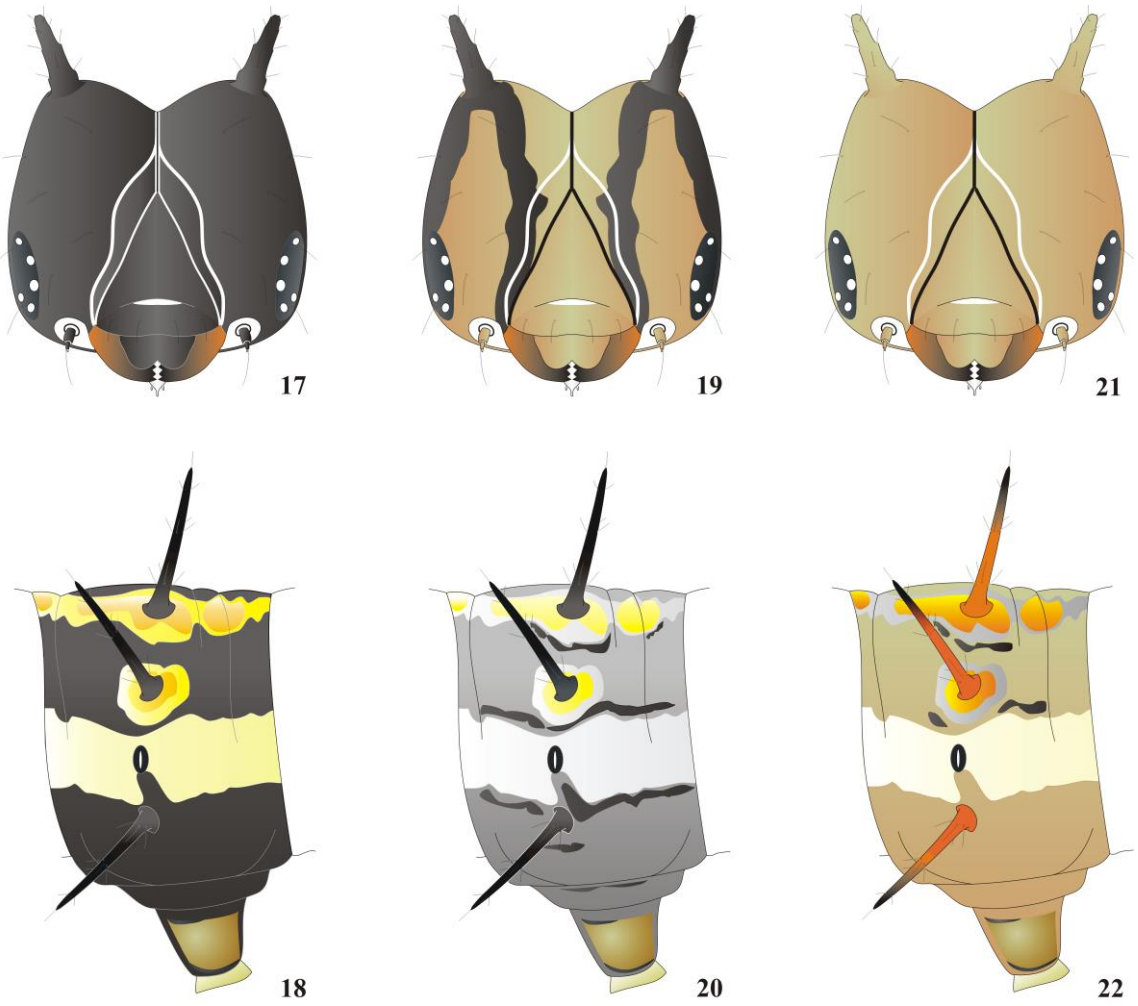

Figs. 17-22_Vargas et al.
(adjust to page width)

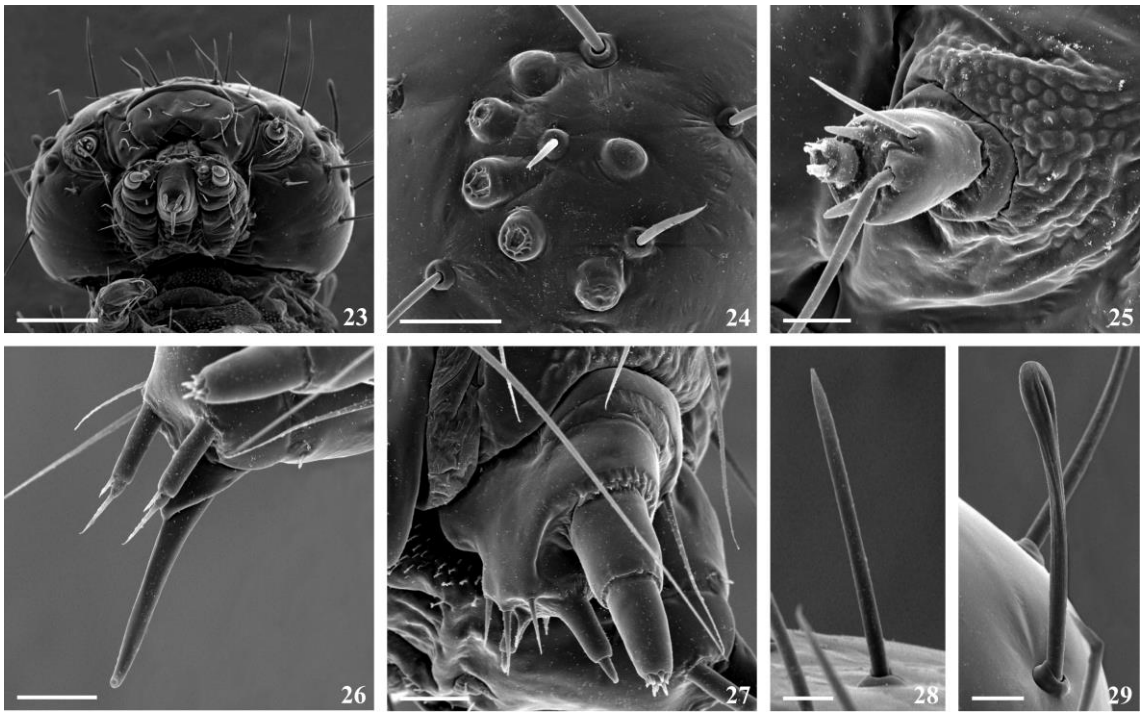

Figs. 23-29_Vargas et al.
(adjust to page width)

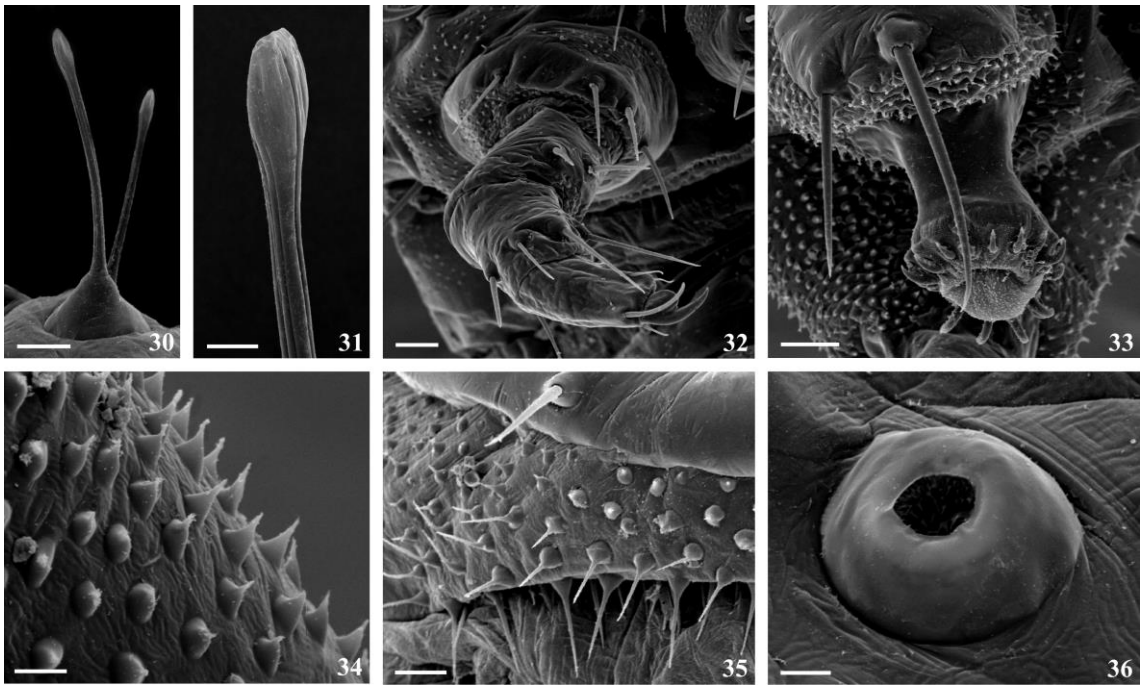

Figs. 30-36_Vargas et al.
(adjust to page width)

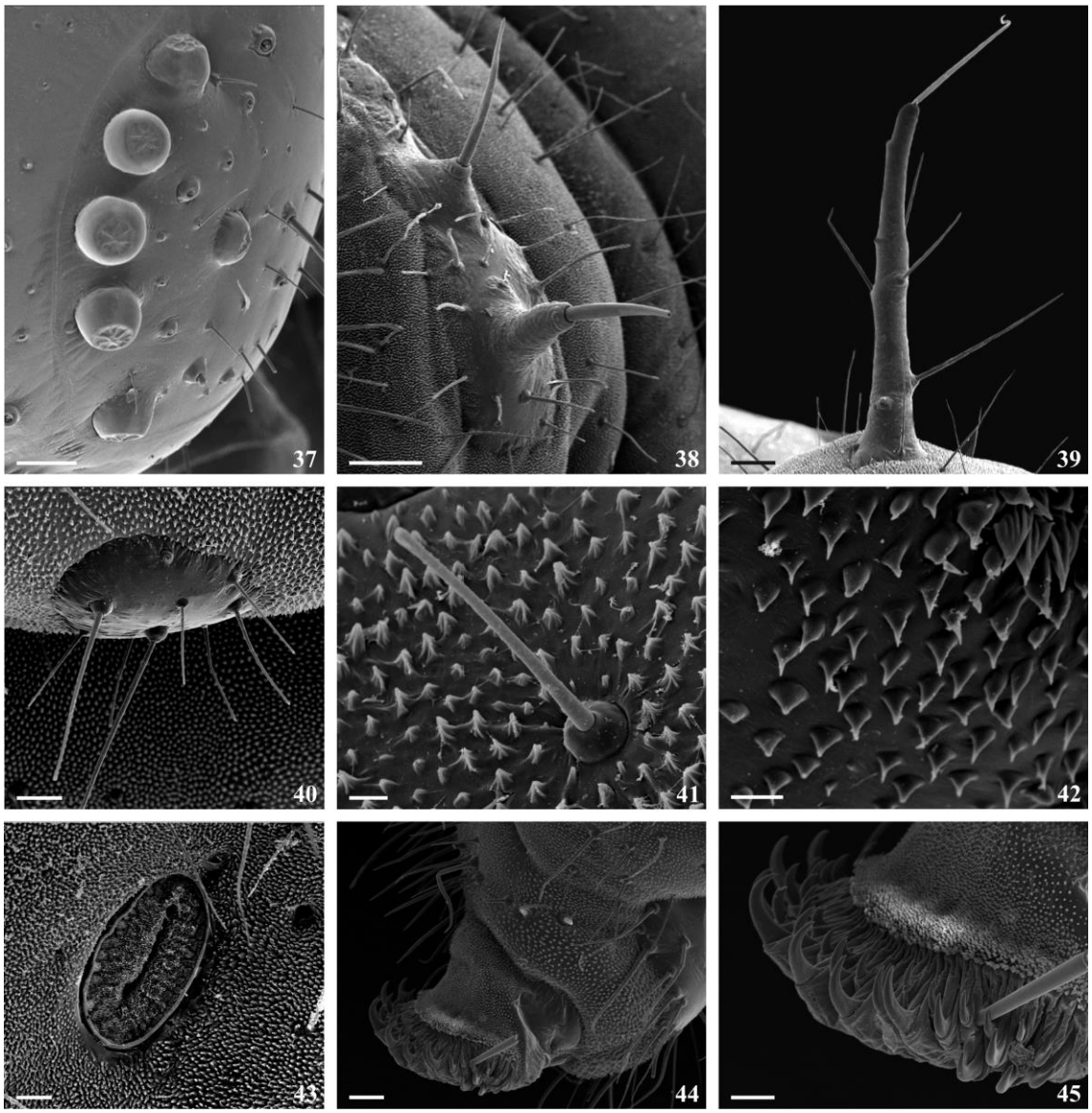

Figs. 37-45_Vargas et al.
(adjust to page width)

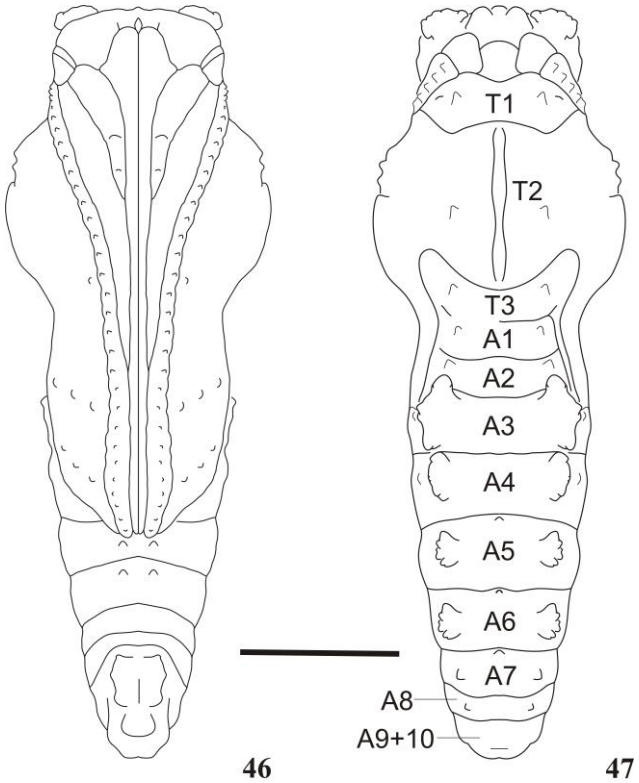

Figs. 46-47_Vargas et al.
(adjust to half page)

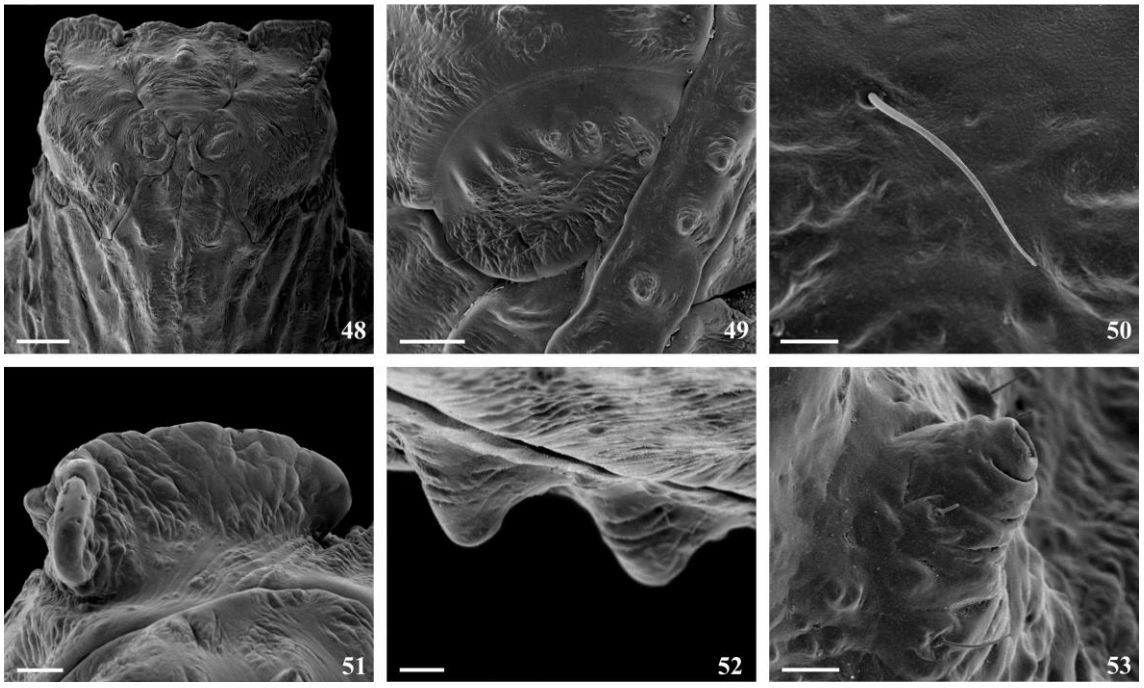

Figs. 48-53_Vargas et al.
(adjust to page width)

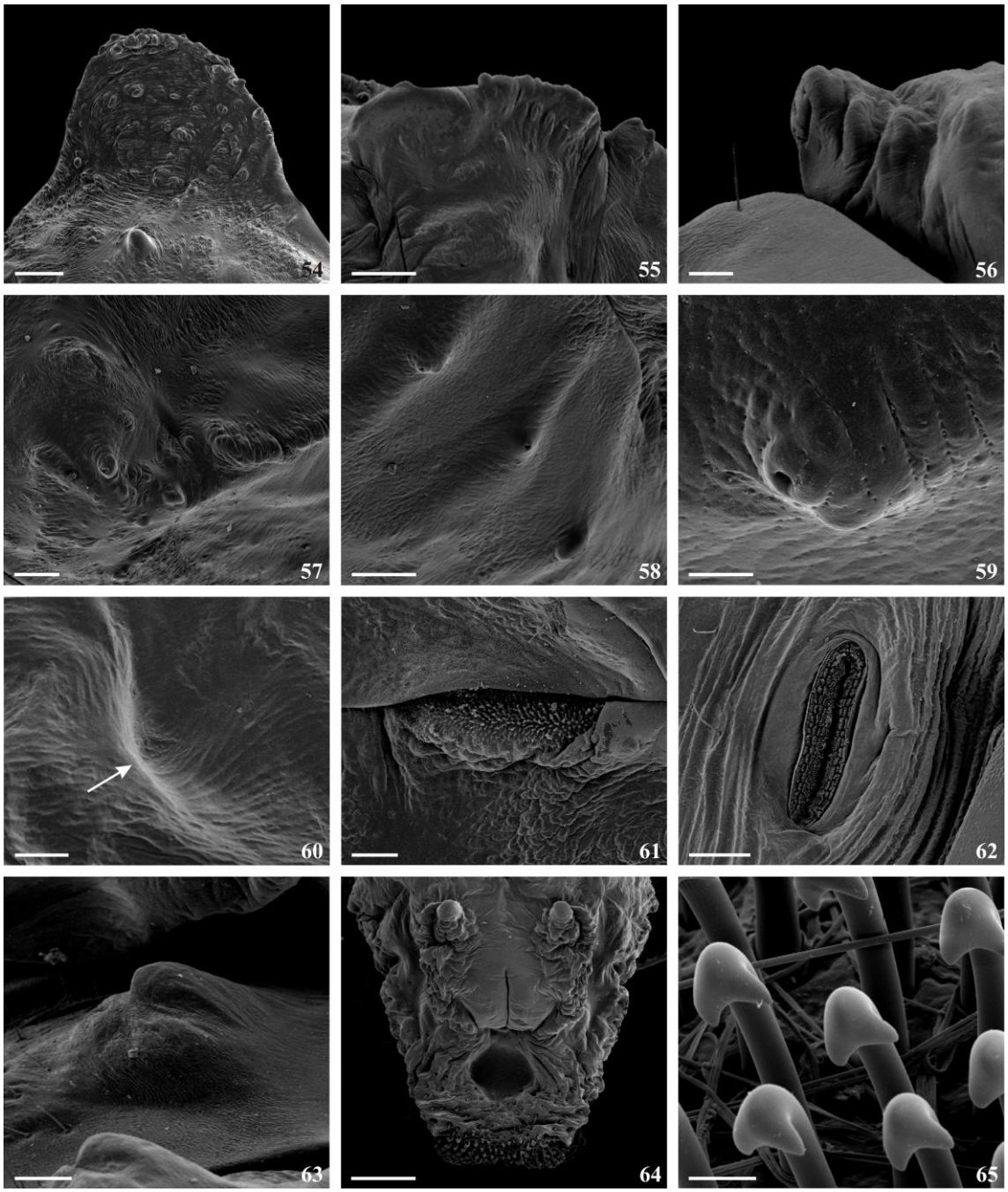

Figs. 54-65_Vargas et al.
(adjust to page width)

3. CAPÍTULO II

Development of a microsatellite library for the passion flower butterfly *Dione moneta* Hübner (Lepidoptera: Nymphalidae: Heliconiinae)*

* Este manuscrito está publicado na **Conservation Genetics Resources, Volume 4, Issue 3, pp 719-724.**

Development of a microsatellite library for the passion flower butterfly *Dione moneta* Hübner (Lepidoptera: Nymphalidae: Heliconiinae)

Darli Massardo[1,*], Paula A. Roratto[2], Héctor A. Vargas[3], Marcus R. Kronforst[4] , Gilson R. P. Moreira[1]

1. Departamento de Zoologia, Universidade Federal do Rio Grande do Sul, Porto Alegre, RS, Brazil

2. Departamento de Genética, Universidade Federal do Rio Grande do Sul, Porto Alegre, RS, Brazil

3. Facultad de Ciencias Agronómicas, Universidad de Tarapaca, Arica, Chile

4. FAS Center for Systems Biology, Harvard University, Cambridge, MA, USA

* Corresponding author: Darli Massardo

Email addresses: darlimassardo@gmail.com (D. Massardo), p.angelica21@gmail.com (P. A. Roratto), havargas@uta.cl (H. A. Vargas), mkronforst@cgr.harvard.edu (M. R. Kronforst), gilson.moreira@ufrgs.br (G. R. P. Moreira).

Abstract

We characterized 19 polymorphic microsatellite loci in the Neotropical butterfly *Dione moneta*. Based on the genotypes of 20 individuals from one population, we detected one to 13 alleles per locus, observed heterozygosities ranging from 0.00 to 0.80, and expected heterozygosities ranging from 0.23 to 0.88. Levels of variation were high, although heterozygosity deficiencies were found at most loci. The loci showed broad amplification success in a second population of *D. m. moneta*, in *D. m. butleri*, other species of the genus (*D. juno juno* and *D. glycera*) and the related species, *Agraulis vanillae maculosa*. These polymorphic markers should provide efficient tools to study population genetic structure of *D. moneta* and other closely related butterflies.

Keywords: Mexican Silverspot butterfly; Genetic markers; Short tandem repeats; Genetic diversity.

Introduction

Microsatellites are important molecular markers for studies of population genetics and evolution (Néve and Meglécz 2000), but the development of these markers in Lepidoptera has been difficult (Zhang 2004; Sinama et al. 2011) because they are rare within genomes and difficult to amplify (Meglécz and Solignac 1998). Microsatellites in Lepidoptera are associated with the flanking regions characterized by repetitive sequences (Meglécz et al. 2004) and mobile elements leading to multiple copies of loci (Zhang 2004). These properties can result in a deficit of heterozygotes due to the presence of null alleles (Meglécz et al. 2004).

Heliconiini (*sensus* Penz and Peggie 2003) is a well-studied lineage of nymphalid butterflies, yet microsatellites have only been developed for two species, both belonging to the derived genus *Heliconius* (Flanagan et al. 2002; Mavárez and González 2006). Here, we developed novel microsatellite loci for the primitive genus *Dione*. Using these microsatellites, we then measured genetic variation in two separate populations of *Dione moneta moneta* and examined cross amplification in *D. moneta butleri*, in the congeneric *D. glycera* and *D. juno juno*, and in a sister lineage, *Agraulis vanillae maculosa*. These microsatellites will be useful for a variety of purposes, including examining potential migratory behavior in *D. moneta* (Gilbert 1969) and in developing management strategies for *D. glycera*, *D. juno*, and *A. vanillae*, which are pests of cultivated *Passiflora* (Aguiar-Menezes et al. 2002; Beccaloni et al. 2008).

Genomic DNA was isolated from one individual of *D. m. moneta* using the cetyltrimethyl ammonium bromide (CTAB) method (Doyle and Doyle 1990). A genomic-enriched library was constructed following the protocol described by Billotte et al. (1999). Genomic DNA (20 lg) was digested with the RsaI restriction enzyme (Invitrogen, Carlsbad, CA) and the resulting fragments were linked to RsaI adapters. Dinucleotide $(CT)_8$ and $(GT)_8$

biotinylated probes were used in a selective hybridization to retrieve RsaI digested fragments that contained microsatellites. This process utilized Streptavidin magnetic particles (Promega, Fitchburg, WI). Selected fragments were PCR amplified using primer sequences complementary to the RsaI adapters with the amplification conditions: 95 LC for 1 min followed by 25 cycles of 40 s at 94 LC, 1 min at 60 LC, 2 min at 72 LC, and a 5-min final extension at 72 LC. The PCR products were ligated into the pGEM-T vector (Promega) and transferred into Escherichia coli XL-1 Blue strain cells by Calcium chloride ($CaCl_2$) transformation (Sambrook and Russell 2002).

A total of 239 clones were sequenced, of which 73 contained microsatellites. Of these, 43 microsatellites were unique and 30 of these had flanking sequences suitable for primer design. These loci all contained repetitions of CA, GT or ACAT. Primers were designed using the software PRIMER 3 (Rozen and Skaletsky 2000) and each forward primer contained a M13 tail for fluorescent labeling. The sequences were deposited in GenBank (accession numbers HQ848307–HQ848322 and JQ522937–JQ522945). PCR amplifications were performed in a 10 µl final volume containing 50 ng of DNA, 0.25 µM forward and M13 fluorescently labeled (FAM) primer and 0.5 µM reverse primer, 0.2 µM dNTPs, and 2.3 mM $MgCl_2$, 19 buffer (AdvII), 1 U Taq DNA polymerase and ultrapure water. PCRs were performed using the following conditions: 95 LC for 2 min followed by 35 cycles of 30 s of 94 LC, specific annealing temperature for 30 s (see Table 1), 1 min of 72 LC, and a final extension of 72 LC for 4 min. The final analysis was based on the 19 microsatellites that yielded reliable amplification across multiple samples.

PCR products were separated on an ABI 3700 DNA sequencer using GS500-ROX size standard (Applied Bio-systems, Foster City, CA). Alleles were sized and scored using Peak Scanner Software v1.0 (Applied Biosystems). The genotyping results were checked with Micro Checker 2.2.3 (van Oosterhout et al. 2004) and then Arlequin 3.5.1.3 (Excoffier

and Schneiser 2005) was used to estimate the number of alleles, observed and expected heterozygosity, and linkage disequilibrium among loci. Significance thresholds were adjusted by Bonferroni's correction (Rice 1989).

The number of alleles per locus ranged from 1 to 13 in *D. m. moneta* (population 1). Observed and expected heterozygosities ranged from 0.00 to 0.80 and 0.23 to 0.88, respectively (Table 1). Only two loci were monomorphic in population 1 (Dmon9, Dmon26). However, Dmon9 exhibited two alleles in population 2 and in *A. v. maculosa*, and Dmon26 was polymorphic in population 2, *D. m. butleri* and *A. v. maculosa*. Most loci amplified successfully across species and subspecies (Table 1).

After applying the Bonferroni's correction, there was evidence of linkage disequilibrium in four pairs of loci in population 1 (Dmon2–Dmon10, Dmon11–Dmon13, Dmon13–Dmon15, Dmon10–Dmon18). A majority of loci exhibited low observed heterozygosities, with significant deviations from Hardy–Weinberg equilibrium (after Bonferroni's correction) at 12 loci in population 1 (Table 1). Although analysis with MicroChecker did not reveal evidence of large allele drop out in our dataset, the reduced heterozygosity could be explained by the presence of null alleles, a common issue with microsatellites in the Lepidoptera. In addition, the observed deviations from linkage and HW equilibrium may also be compounded by the interesting biology of *D. moneta*. This species may be migratory, and recent mixing of distinct sub-populations could produce the observed results due to the Wahlund effect, as has been demonstrated in other studies (Carvalho-Costa et al. 2006; Lumley et al. 2009; Sinama et al. 2011). Future population studies applying these loci in a broader sampling area will help to clarify this question.

Acknowledgments We thank CBMEG/UNICAMP and LCE/ UFRGS staff, Brazil, for their support on the first phase of study. Thanks are also due to Sabrina Thiele (UFRGS, Brazil) and Julian Adolfo Salazar (Centro de Museos de La Universidad de Caldas, Colombia) for providing specimens used in the study. Financial support for this work came in part from National Counsel of Technological and Scientific Development (CNPq)/Brazil (project numbers 200695/2011-8 and 309676/2011-8, granted to DM and GRPM, respectively) and NIH NIGMS Grant GM068763 and NSF grant DEB-1020355 to MRK.

Table 1. Characteristics and summary statistics of microsatellite loci genotyped in *Dione moneta*, and cross-species amplified in *Dione glycera*, *Dione juno* and sister species, *Agraulis vanillae*

Locus	Primer sequence (5′-3′)	Repeat motif	T_a (C)	*Dione moneta moneta*					
				Population 1 (n = 20)				Population 2 (n = 8)	
				N_a	Size Range (bp)	H_O	H_E	N_a	Size Range (bp)
Dmon1	F-CGAACCACAAGTTCCTGAGTT R-ACGCGTGGATGTAGACACAA	$(CA)_{15}$	52	4	171–183	0.10000	0.23333	5	173–183
Dmon2	F-TTCACATCAAGATCAATGACCAG R-CCGTATTGCACGATGTTCAC	$(CA)_9$	52	7	182–206	0.35000*	0.75385	6	182–194
Dmon3	F-GCTCAACAACGACGAGCTG R-CGTGAGATATTGCGTGTTGC	$(AC)_{13}$	55	3	182–190	0.05000*	0.52179	4	182–198
Dmon4	F-CGTAGTTACTTAATTTGGACGAATC R-ATGCTTCTCTCGCTTCATCG	$(TG)_{16}$	52	9	173–193	0.70000*	0.82179	6	173–199
Dmon7	F-CTCTGCAAGAGCGAGGAAAT R-TCTTGCTTACGCGTGGACTA	$(GT)_{13}$	52	6	175–191	0.15000*	0.64103	3	183–191
Dmon8	F-ACCTCGACTGCCACTACCC R-TCGCACCTAGCCATGGTATT	$(CA)_8$	52	9	180–226	0.05263*	0.75818	6	174–222
Dmon9	F-CAATTCACAATCTATTGTTTTTGTTTA R-CAGTGAACGACGAGTGATCG	$(GT)_{20}$	52	1	219	Monomorphic		2	189–219
Dmon10	F-CAGGCTACGCAAGGAGAATC R-CTAGCAGTGGCAACGATTGA	$(TG)_{12}$	52	4	166–188	0.70000	0.51538	7	160–190
Dmon13	F-ACAATAAAGGGCAGCACTGG R-GTGAAGGACGGGGTGAGTTA	$(GT)_{15}$	55	13	192–226	0.50000*	0.88205	7	190–218
Dmon15	F-AAGCCATTATCGCGGTTAAA R-TAACATACCGCTCCCGCTGT	$(TG)_{10}$	55	5	169–177	0.80000*	0.64359	–	–
Dmon18	F-GGCTTCTTCAAGCTGACCAC R-TGACAGTCAACATGTGTGTGC	$(CA)_{10}$	52	2	218–220	0.00000*	0.46667	4	184–220
Dmon19	F-TCTCATGTAACATCATCCCACA R-TGATAAAAGGCGAAGGTTTACA	$(AC)_9T(AC)_4G\ (CA)_6$	55	2	243–249	0.10000*	0.46667	–	–
Dmon20	F-CAGGTAGTGATGACGGAACCT R-CATACCCACGGGATTCTCTG	$(CA)_9\ldots\ (CA)_7$	52	5	291–341	0.60000	0.48462	4	183–291
Dmon22	F-CACGCACCTTCTTTGTTTCA R-TCAATGACAGTGGACGAGGA	$(ACAT)_8\ldots\ (ACAT)_6$	55	5	217–241	0.05000*	0.63462	5	175–283
Dmon23	F-GAACCTAATGTCCGTGTCAATG R-GCGTGGTCTAACCAGTCCAT	$(TG)_{11}$	55	3	239–241	0.20000	0.27308	4	207–251
Dmon24	F-TGTATCTCACGGTCGGTTTTT R-AGTGCCGTGTTCACATTCAA	$(CA)_9$	55	4	187–195	0.05000*	0.69103	5	179–195

Table 1. continued

Locus	Primer sequence (5′-3′)	Repeat motif	T_a (C)	*Dione moneta moneta*					
				Population 1 (n = 20)				Population 2 (n = 8)	
				N_a	Size Range (bp)	H_O	H_E	N_a	Size Range (bp)
Dmon25	F-ATTGAGCGATAATCCCGATG R-TCTTGCTTACGCGTGGTCTA	$(GT)_{10}$	52	5	341–383	0. 35000	0.31795	5	237–267
Dmon26	F-TAGGTCGGGCTCGTCTATTG R-TCGATGGGAATCGTGTTGTA	$(GT)_{10}$	52	1	298	Monomorphic		6	212–300
Dmon27	F-GTGTATCCGTGTGCGCTCTA R-TCTTGCTTACGCGTGGACTA	$(AC)_{14}$	52	9	165–199	0.00000*	0.87619	–	–

Locus	Primer sequence (5′–3′)	Repeat motif	T_a (C)	*Dione moneta butleri* (n = 8)		*Dione glycera* (n = 4)		*Dione juno juno* (n = 4)		*Agraulis vanillae maculosa* (n = 4)	
				N_a	Size Range (bp)	N_a	Size Range (bp)	N_a	Size Range (bp)	N_a	Size Range (bp)
Dmon1	F-CGAACCACAAGTTCCTGAGTT R-ACGCGTGGATGTAGACACAA	$(CA)_{15}$	52	6	175–189	4	171–181	–	–	3	191–193
Dmon2	F-TTCACATCAAGATCAATGACCAG R-CCGTATTGCACGATGTTCAC	$(CA)_9$	52	2	190–192	3	174–194	2	202–204	3	192–206
Dmon3	F-GCTCAACAACGACGAGCTG R-CGTGAGATATTGCGTGTTGC	$(AC)_{13}$	52	2	190–192	–	–	–	–	2	164–168
Dmon4	F-CGTAGTTACTTAATTTGGACGAATC R-ATGCTTCTCTCGCTTCATCG	$(TG)_{16}$	52	8	175–209	3	165–177	2	171–217	3	173–181
Dmon7	F-CTCTGCAAGAGCGAGGAAAT R-TCTTGCTTACGCGTGGACTA	$(GT)_{13}$	52	4	189–203	2	173–175	3	193–227	1	203
Dmon8	F-ACCTCGACTGCCACTACCC R-TCGCACCTAGCCATGGTATT	$(CA)_8$	52	2	182–226	–	–	4	184–230	4	186–218
Dmon9	F-CAATTCACAATCTATTGTTTTTGTTTA R-CAGTGAACGACGAGTGATCG	$(GT)_{20}$	52	1	219	1	219	1	195	2	187–189
Dmon10	F-CAGGCTACGCAAGGAGAATC R-CTAGCAGTGGCAACGATTGA	$(TG)_{12}$	52	2	166–168	5	174–226	3	172–200	4	166–200
Dmon13	F-ACAATAAAGGGCAGCACTGG R-GTGAAGGACGGGGTGAGTTA	$(GT)_{15}$	52	5	194–214	–	–	2	232–238	3	196–218
Dmon15	F-AAGCCATTATCGCGGTTAAA R-TAACATACCGCTCCCGCTGT	$(TG)_{10}$	52	2	169–171	–	–	–	–	–	–

Table 1. continued

Locus	Primer sequence (5′–3′)	Repeat motif	T_a (C)	*Dione moneta butleri* (n = 8)		*Dione glycera* (n = 4)		*Dione juno juno* (n = 4)		*Agraulis vanillae maculosa* (n = 4)	
				N_a	Size Range (bp)	N_a	Size Range (bp)	N_a	Size Range (bp)	N_a	Size Range (bp)
Dmon18	F-GGCTTCTTCAAGCTGACCAC R-TGACAGTCAACATGTGTGTGC	$(CA)_{10}$	52	3	218–220	1	180	3	184–218	2	182–222
Dmon19	F-TCTCATGTAACATCATCCCACA R-TGATAAAAGGCGAAGGTTTACA	$(AC)_9T(AC)_4G\ (CA)_6$	55	2	243–249	2	237–239	–	–	–	–
Dmon20	F-CAGGTAGTGATGACGGAACCT R-CATACCCACGGGATTCTCTG	$(CA)_9…(CA)_7$	52	1	291	–	–	1	179	–	–
Dmon22	F-CACGCACCTTCTTTGTTTCA R-TCAATGACAGTGGACGAGGA	$(ACAT)_8…(ACAT)_6$	55	1	225	4	191–301	1	263	2	177–181
Dmon23	F-GAACCTAATGTCCGTGTCAATG R-GCGTGGTCTAACCAGTCCAT	$(TG)_{11}$	55	2	241–259	2	239–255	2	239–241	3	239–263
Dmon24	F-TGTATCTCACGGTCGGTTTTT R-AGTGCCGTGTTCACATTCAA	$(CA)_9$	55	2	187–189	–	191	2	161–191	1	191
Dmon25	F-ATTGAGCGATAATCCCGATG R-TCTTGCTTACGCGTGGTCTA	$(GT)_{10}$	52	2	327–341	2	299–311	1	265	2	319–325
Dmon26	F-TAGGTCGGGCTCGTCTATTG R-TCGATGGGAATCGTGTTGTA	$(GT)_{10}$	52	2	216–298	–	–	–	–	3	194–268
Dmon27	F-GTGTATCCGTGTGCGCTCTA R-TCTTGCTTACGCGTGGACTA	$(AC)_{14}$	52	–	–	3	175–203	2	189–191	2	175–177

Forward primer sequence (F), reverse primer sequence (R), annealing temperature (T_a), number of individuals for which loci successfully amplified (n), number of alleles (N_a), observed and expected heterozygosity (H_O and H_E, respectively). * Deviation from HWE (p = 0.0026) after Bonferroni's correction. *D. m. moneta* populations 1 and 2 were located respectively in Porto Alegre (30°4'23"S; 51°7'33"W) and Augusto Pestana (28º31'01" S; 53º59'32" W) municipalities, Rio Grande do Sul State, Brazil. *D. m. butleri* specimens were collected in Caldas Department, Manizales (75°33'10"W; 05°06'15"N), Colombia. *D. glycera* specimens were collected in Parinacota Province, Socoroma (18°15′49″S; 69°36′60″W), Chile. *A. v. maculosa* specimens came from a population also located in the Porto Alegre area, and those of *D. j. juno* from São Bento do Sul (26º15'01"S; 49º22'43"W) municipality, Santa Catarina State, Brazil. Corresponding vouchers were deposited in the tissue collection of Laboratório de Morfologia e Comportamento de Insetos (LMCI), Departamento de Zoologia/UFRGS, Porto Alegre city, RS, Brazil, under access numbers: LMCI 158, 31, 93, 112, 158, and 110, respectively

References

Aguiar-Menezes EL, Menezes EB, Cassino PC et al (2002) Passion fruit. In: Pena JE, Sharp JL, Wysoki M (eds) Tropical fruit pests and pollinators. CAB International, New York, pp 361–390

Beccaloni GW, Viloria AL, Hall SK et al (2008) Catalogue of the hostplants of the neotropical butterflies. The Natural History Museum, London, pp 223–256

Billotte N, da Lago PJL, Risterucci AM, Baurens FC (1999) Microsatellite-enriched libraries: applied methodology for the development of SSR markers in tropical crops. Fruits 54: 277–288

Carvalho-Costa LF, Hatanaka T, Galetti PM Jr (2006) Isolation and characterization of polymorphic microsatellite markers in the migratory freshwater fish *Prochilo duscostatus*. Mol Ecol Notes 6:818–819

Doyle JJ, Doyle JL (1990) Isolation of plant DNA from fresh tissue. Focus 12:13–15

Excoffier L, Schneiser S (2005) Arlequin version 3.0: an integrated software package for population genetics data analysis. Evol Bioinform Online 1:47–50

Flanagan NS, Blum MJ, Davison A, Alamo M, Albarrán R, Faulhaber K, Peterson E, McMillan WO (2002) Characterization of microsatellite loci in neotropical Heliconius butterflies. Mol Ecol Notes 2:398–401

Gilbert LE (1969) On the ecology of natural dispersal: *Dione moneta poeyii* in Texas (Nymphalidae). J Lepid Soc 23:177–185

Lumley LM, Davis CS, Sperling FAH (2009) Isolation and charac-terization of eight microsatellite loci in the spruce budworm species *Choristoneura fumiferana* and *Choristoneura occiden-talis*, and cross-species amplification in related tortricid moths. Conserv Genet Resour 1:501–504

Mavárez J, González M (2006) A set of microsatellite markers for *Heliconius melpomene* and

closely related species. Mol Ecol Notes 6:20–23

Meglécz E, Solignac M (1998) Microsatellite loci for Parnassius mnemosyne (Lepidoptera). Hereditas 128:179–180

Meglécz E, Petenian F, Danchin E et al (2004) High similarity between flanking regions of different microsatellites detected within each of two species of Lepidoptera: *Parnassius apollo* and *Euphydryas aurinia*. Mol Ecol 13:1693–1700

Néve G, Meglécz E (2000) Microsatellite frequencies in different taxa. Trends Ecol Evol 15:376–377

Penz CM, Peggie D (2003) Phylogenetic relationships among Heliconiinae genera based on morphology (Lepidoptera: Nymp-halidae). Syst Entomol 28:451–479

Rice WR (1989) Analyzing tables of statistical tests. Evolution 43: 223–225

Rozen S, Skaletsky HJ (2000) Primer3 on the www for general users and for biologist programmers. In: Krawetz S, Misener S (eds) Bioinformatics methods and protocols: methods in molecular biology. Humana Press, Totowa, pp 365–386

Sambrook J, Russell DW (2002) Molecular cloning: a laboratory manual, 3rd edn. Science Press of China, Beijing, pp 1723–1726 Sinama M, Dubut V, Costedoat C, Gilles A, Junker M et al (2011) Challenges of microsatellite development in Lepidoptera: Eu-phydryas aurinia (Nymphalidae) as a case study. Eur J Entomol 108:261–266

van Oosterhout C, Hutchinson WF, Wills DPM et al (2004) Micro-Checker: software for identifying and correcting genotyping errors in microsatellite data. Mol Ecol Notes 4:535–538

Zhang DX (2004) Lepidopteran microsatellite DNA: redundant but promising. Trends Ecol Evol 19:507–509

Multilocus DNA sequences and geometric morphometric analysis reveal evolutionary history of the passion-vine butterfly genus *Dione*

Darli Massardo[1], Gislene L Gonçalves[2, 3], Rodrigo Fornel[4], Marcus R Kronforst[5], Gilson R P Moreira[6*]

[1] PPG Biologia Animal, Departamento de Zoologia, Universidade Federal do Rio Grande do Sul. Av. Bento Gonçalves, 9500, Bloco IV, Prédio 43435, Av. Bento Gonçalves 9500, Porto Alegre, RS 91501-970, Brazil

[2] PPG Genética e Biologia Molecular, Departamento de Genética, Universidade Federal do Rio Grande do Sul, Av Bento Gonçalves 9500, Porto Alegre, RS 91501-970, Brazil

[3] Instituto de Alta Investigación, Universidad de Tarapacá, Antofagasta 1520, Arica, Chile

[4] Programa de Pós-Graduação em Ecologia, Departamento de Ciências Biológicas, Universidade Regional Integrada do Alto Uruguai e das Missões—Campus de Erechim, Erechim, RS 99700-000, Brazil

[5] Department of Ecology & Evolution, University of Chicago,1101 E. 57th St., Chicago, IL 60637, USA

[6] Departamento de Zoologia, Universidade Federal do Rio Grande do Sul. Av. Bento Gonçalves, 9500, Bloco IV, prédio 43435, 91501-970, Porto Alegre, RS 91501-970, Brazil

* Corresponding author

Email addresses:

DM: darlimassardo@gmail.com

GLP: gislene.ufrgs@gmail.com

RF: rodrigofornel@hotmail.com

MRK: mkronforst@uchicago.edu

GRPM: gilson.moreira@ufrgs.br

Abstract:

Background: The heliconiines (Lepidoptera: Nymphalidae: Heliconiini) form a diverse group of butterflies distributed in the Neotropics, which have been repeatedly explored in genetic and ecological studies. This is particularly true for species of the most derived genus *Heliconius,* Klug, which have been extensively investigated in relation to speciation, mimicry and hybridization processes. However, most of the other heliconiine lineages, such as *Dione,* Hübner, which are less diversified from a phenotypic perspective, have not received much attention, where even the most basic information such as species limits and geographical distributions remains uncertain. We used an integrative approach based on multilocus DNA sequences, variation of wing pattern geometric morphometrics, and geographical distribution, across the entire range of *Dione* in the Neotropical region, in order to make inferences on taxonomic boundaries, geographical distributions and evolutionary history of this poorly known heliconiine lineage, at both specific and subspecific levels.

Results Our data showed that *Dione* forms a monophyletic clade, sister of *Agraulis* Boisduval & Le Conte. We demonstrated that *Dione* species [*D. juno* (Cramer), *D. glycera* (C. Felder & R. Felder) and *D. moneta* Hübner] are reciprocally monophyletic, form genetic clusters, and are phenotypically diagnosable. However, we found an extensive overlap in the wing-color patterns used to distinguish their subspecies, most of which are not allopatrically distributed, and thus supposedly hybridize throughout their distribution ranges. The estimated time divergences strongly supported the contention that speciation in *Dione* coincided with both the rise of Passifloraceae and the uplift of the Andes.

Conclusion: By using large sample sizes and an integrative taxonomic approach, including molecular markers and geometric morphometrics, this study deals with the evolutionary history of *Dione*. The corresponding species are herein confirmed from a taxonomic perspective. Especially for *D. juno*, the presently assigned subspecies were not fully

diagnosable, and we thus questioned their validity and usefulness either as taxonomic entities or evolutionary units from a conservation biology perspective. Since the sister species *D. glycera* and *D. moneta* are specialized feeders on passion-vine lineages that are endemic to areas located either within or adjacent to the Andes, we hypothesized that they co-speciated there and at that time.

Keywords: Insect and plant co-speciation, Neotropics, Andes uplift, Passifloraceae, Heliconian butterflies

Background

Passion-vine butterflies (Lepidoptera: Nymphalidae: Heliconiini) are a diverse group distributed in the Neotropics, which have been repeatedly surveyed in genetic and ecological studies. For example, the genus *Heliconius*, Klug, known as the most diverse within the tribe (including hundreds of geographical races recognized based on wing coloration pattern) has been extensively investigated in relation to speciation and hybridization processes [1-7], as evidenced by a recent annotation of its complete genome [8]. However, most of the other heliconiine lineages, such as *Agraulis* Boisduval & Le Conte, *Dione* Hübner, *Dryas* Hübner , *Dryadula* Michener, *Philaethria* Michener and *Podotricha* Michener, which are less diversified from a phenotypic perspective, have not yet received much attention. Despite the several phylogenies proposed in the last 50 years, using both morphological data [9-11] and molecular markers [12-14], the phylogenetic relationships, age of lineages and even species-level relationships [15] are not resolved in most genera of passion-vine butterflies.

Particularly, the genus *Dione* is a conspicuous example of a poorly known heliconiine lineage. Overall, these are characterized by orange coloration on the dorsal side of the wing and reflexive silverspots on the ventral side [9, 16], and are thus commonly known as

silverspot butterflies. Three species are currently assigned to the genus: *Dione juno* (Cramer, 1779), *Dione moneta* Hübner, [1825] and *Dione glycera* (C. Felder & R. Felder, 1861). The first two have been further classified into subspecies [17]: *Dione juno juno* (Cramer, 1779) *D. juno suffumata* Brown & Mielke, 1972, *D. juno huascuma* (Reakirt, 1866), *D. juno miraculosa* (Hering, 1926), *D. juno andicola* (Bates, 1864), *D. moneta moneta* Hübner, [1825], *D. moneta poeyii* Butler, 1873 and *D. moneta butleri* Stichel, [1908] (Figure 1).

An original phylogeny proposed by Emsley [9] using adult morphological characters considered *Dion*e as the sister group of *Agraulis*, with the corresponding clade occupying a "basal" position in the tribe Heliconiini (Additional file 1a). Subsequently, Brown [10], using morphological and ecological characters to reconstruct relationships among heliconiines, also placed *Dione* as the sister of *Agraulis* (Additional file 1b). In the age of mitochondrial DNA sequences, Brower [12] used this type of data to reconstruct relationships within heliconiine and found evidence for *Dryas* being the most basal lineage within the family, rather than *Dione* as previously proposed (Additional file 1c). However, Brower and Egan [13] revised the phylogeny of Brower [12], and using a combination of mitochondrial and nuclear DNA markers, proposed *Agraulis* as the most basal to the tribe, and *Dione* as the sister lineage to all remaining heliconiines (Additional file 1d). Penz [11], based on morphological characters of immature stages, including egg, larval (first and fifth instar), pupal and adult stages, analyzed the phylogenetic relationships among 24 species of heliconiines, representatives of the 10 genera included in the tribe. Accordingly, *Dione* was considered a sister group of *Agraulis*, and also placed as a basal lineage (Additional file 1e). More recently, Beltrán et al. [14] reassessed the phylogenetic relationships of 60 species of heliconiines through multilocus DNA sequences. *Dione* and *Agraulis* also clustered as sister lineages occupying the most basal position, although not strongly supported. Considering species-level results for *Dione* in this previous analysis, the internal branches indicated that *D. moneta* did fall outside a clade formed by *D. juno* + *D. glycera* (Additional file 1f), although this topology had low

support. This results conflict with the phylogeny proposed by Penz [11] based on morphological characters, in which *D. juno* emerged as the clade formed by *D. moneta* + *D. glycera.* Thus, previous studies have suggested, based on branch position, that *Dione* is an ancestral heliconiine, although the corresponding divergence time has not been estimated. Moreover, the internal relationships of this group have not yet been resolved; the position depends on the methods of reconstruction and the data used to build trees. Also, the taxonomic status of subspecies proposed for *Dione* is controversial and remains to be evaluated.

The present study used an integrative approach based on multilocus DNA sequences, wing geometric morphometric data, and spatial distribution across the entire range of *Dione* in the Neotropical region, in order to make inferences on the evolutionary history of this poorly known heliconiine lineage. Additionally, variations in linear morphometrics and wing color patterns of subspecies of *Dione* were determined, and their taxonomic implications are discussed.

Results and Discussion

Molecular phylogeny and time of divergence estimates

Nucleotide data analyzed included a total of 4,594 positions (2,116 mitochondrial and 2,477 nuclear). Patterns of genetic variability for each individual marker and models of sequence evolution were characterized at the tribe (Heliconiini) and generic levels (*Dione*) (Table 1). Congruence ILD tests between mitochondrial data (*CO-I* + tRNAleu + *CO-II* + *16S*) versus nuclear data (*Ap* + *Th* + *Ef-1α* + *Wg* + *dpp*) provided no evidence for incongruence ($P = 0.08$).

The relationships among heliconiines were well resolved and supported; a consensus time-calibrated tree based on combined markers is presented (Figure 2). The cladogenesis leading to the heliconiine lineages occurred in the Middle Oligocene, around 30.3 (95% Confidence Internal [CI]: 33.3-26.2) mya (Figure 2). It suggests that this group was in part diversified before the end of the Miocene Epoch. The estimated origin of the tribe Heliconiini is concurrent with the rise of passion vines (Passifloraceae), its host plant, which ranges from 38 to 33 mya [18]. It also coincides with the uplift of the Andes, which is estimated as from ca. 60 to ca. 5 mya [19]. These aspects would be presumably related to the rise of *D. glycera* and *D. moneta*, since their host plants and their own distribution ranges are confined to that region. As discussed below, the former feeds primarily on passion-vine lineages that have geographical distributions closely related to the Andes. Thus, we hypothesize that these *Dione* species derived from their ancestral-like *D. juno*, which is presently distributed in the Neotropics, feeding upon different hosts with which they dispersed and co-speciated during the Andes uplift. This hypothesis should be tested, for example from a phylogeographical perspective, in association with studies related to the use of and preference for the corresponding host plants.

Contrary to earlier studies based on molecular data [12, 13], we found evidence that *Dione* is an independent and well-supported sister lineage of *Agraulis*, a result congruent with more recent morphological studies [11]. These clades diverged from each other ca. 10.9 mya, and accounted for 6.9 % of genetic divergence, compared to the largest proportion (3.8%) obtained here among the *Dione* species. Thus, our data do not support the contention of Lamas that *Agraulis* Boisduval & Le Conte is synonymous with *Dione* Hübner [17].

The results also suggested that *Agraulis* + *Dione* (Node B; Table 2) formed a group that emerged around 20.5 (27.5 -13.5) mya. The clade formed by *Heliconius/Laparus/Neruda* and *Eueides* (which has been suggested as the most derived clade) originated around 19.4 (CI: 25.2-13.6) mya. Based on the age of these two diversification events, an unclear pattern

of ancient/derived lineages is evident, particularly because the confidence intervals of nodes overlap, and therefore mean differences could be neglected (Table 2). Additionally, we found that the genus *Dione* started the speciation process around 10.9 (CI: 15.9-6.1) mya. Similarly, Walhberg et al. [20] estimated the emergence of *Dione* as around 15 mya. These findings suggest a different evolutionary scenario than that constructed for Heliconiini in the past 20 years. Based on the time-divergent tree estimated here, we propose that *Dione* and *Agraulis* do not represent the most basal lineages within heliconiines, nor the most derived. We suggest that a burst of speciation might have occurred in Heliconiini around 25 mya, leading to diversification in a short period of time. Accordingly, previous definitions of ancestral and derived lineages should be cautiously re-evaluated.

The species-level phylogeny of *Dione* also showed some discrepancies in internal relationships, based on the markers used and/or the methods of reconstruction (distance and Bayesian/ML), despite the mode of heritance (mtDNA *vs.* nuclear loci) (Figure 3). However, a general pattern emerged in all the topologies, in which *Dione* was conspicuously supported as monophyletic. Also, each species (*D. glycera*, *D. moneta* and *D. juno*) was strongly supported as an independent lineage. Trees reconstructed based on *16S*, *Ef1-α*, *Wg* and *dpp* showed a consistent pattern with previously suggested topology for *Dione* (Additional file 1e; [11]) and were supported by our results based on morphology, i.e., that *D. moneta* and *D. glycera* form an ingroup clade, sister to *D. juno*. Contrary to our expectation, *CO*, *Th* and *Ap* showed a different pattern, grouping *D. juno* with *D. glycera* and separating *D. moneta* as a sister lineage (Fig. 3). Beltrán et al. [14] also observed a polytomy within *Dione* using several markers (mtDNA and nuclear loci) to reconstruct the phylogenetic relationships. These results indicated that the resolution at this level remains unclear, depending on the data used.

Soft polytomies, such as in this case, might result from conflicting data and lack of information about the true bifurcating pattern of speciation [21], also known either as unrecognized phylogenies [22] or as gene trees. *Dione* species possibly diverged at short (but

distinct) different times from each other. Thus, we suggest that this polytomy might result from a short coalescence time of some markers used in this study (e.g. *CO*, *Th* and *Ap*), which has pushed the consensus topology in a different direction than would be expected based on morphology, instead of an incomplete lineage-sorting process. DNA sequences usually evolve faster than complex phenotypic traits. Consequently, conspicuous differences in morphology among species of *Dione* were found, as well as in most of the DNA variants, but the resolutions of specific markers used in this study were not strong enough to resolve internal relationships of the genus, in contrast to those findings based on wing shape patterns using geometric morphometrics.

Geometric morphometrics: wing shape and size variation in *Dione*

Species level

For interspecific wing log-centroid size variation, we found significant differences among the three species of *Dione* (ANOVA: $F_{(2, 726)} = 78.68$, $P < 0.001$). Corresponding pairwise comparisons performed by using Tukey's tests for wing size were all significant ($P < 0.05$). *D. moneta* was the largest species, followed by *D. juno* of intermediate size, and *D. glycera* with the smallest wings (Figure 4a).

The MANOVA results for shape showed significant differences among the three species for both forewing (FW: $\lambda_{Wilks} = 0.009$, $F_{(2, 726)} = 187.66$, $P < 0.001$) and hindwing (HW: $\lambda_{Wilks} = 0.019$, $F_{(2,726)} = 154.34$, $P < 0.001$). The pairwise MANOVAs showed significant differences in all species comparisons for both wings (Additional file 2). For interspecific wing shape, the PCA showed structured data and suggested three different species also, for both forewing (Figure 4b) and hindwing (Figure 4c). However, the first two PCs scores for both wings showed a partial superimposition between *D. glycera* and *D. moneta* (Figure 4b and 4c). For FW the PC 1 (50.2% of variance) showed a proportionally

narrower wing at the base and wider at the top of the FW for *D. juno* than for the other species (Figure 4b). The PC 2 (17.6% of variance) showed a wing with proportionally more open angles for *D. glycera* than for *D. moneta* (Figure 4b). For HW, the PC 1 (51.8% of variance) showed a wing proportionally extended laterally (wider and shorter) for *D. juno* than for the other two species (Figure 4c). The PC 2 (12.1% of variance) showed a wing with differences at the top of wing (Figure 4c). Cross-validation based on wing shape correctly assigned species with percentages above 95% for FW (*D. glycera* 96.92%, *D. juno* 100%, and *D. moneta* 99.59%) and for HW (*D. glycera* 97.69%, *D. juno* 99.71%, and *D. moneta* 99.19%).

Subspecies level

We found significant variation in wing size among most subspecies of *Dione* (ANOVA: $F_{(8, 720)} = 30.9$, $P < 0.001$; Tukey's multiple comparison tests alpha = 0.05; Figure 5a). In *D. juno*, the subspecies *D. juno huascuma* and *D. juno juno* are larger than *D. juno suffumata* and *D. juno miraculosa* ($P < 0.05$). *D. juno andicola* is intermediate in size and did not differ from the other four subspecies (Figure 5a). In *D. moneta*, the subspecies *D. moneta poeyii* is larger than *D. moneta moneta* and *D. moneta butleri* ($P < 0.001$) (Figure 5a).

For the intraspecific level, we found significant differences in wing shape among subspecies within *D. juno* for FW (MANOVA: $\lambda_{Wilks} = 0.189$, $F_{(4, 346)} = 4.769$, $P < 0.001$) and HW (MANOVA: $\lambda_{Wilks} = 0.144$, $F_{(4, 346)} = 7.121$, $P < 0.001$). Regarding MANOVA pairwise comparisons for FW, only two comparisons were not significant; for HW, all comparisons were significant (Additional file 3). For the cross-validation percentage of correct classification, only three subspecies of *D. juno* were equal or above 70% for both wings: *D. juno juno*, *D. juno huascuma*, and *D. juno miraculosa* (Additional file 4).

Subspecies of *D. moneta* showed significant shape differences for FW (MANOVA: $\lambda_{Wilks} = 0.137$, $F_{(2, 245)} = 10.609$, $P < 0.001$) and HW (MANOVA: $\lambda_{Wilks} = 0.239$, $F_{(2, 245)} = 8.114$, $P < 0.001$). Corresponding MANOVA pairwise comparisons showed significant

differences for all subspecies (Additional file 5). The percentages of correct classification for *D. moneta* subspecies based on FW were higher than 80%; however, for the HW of *D. moneta moneta* specimens, these scores were lower than 80% (Additional file 6).

Phenograms based on Mahalanobis distances show the morphological relationship among subspecies for wing shape in the genus *Dione* (Figure 5b and 5c). The configuration of trees for each wing (FW and HW) is very similar, but *D. glycera* is arranged in different ways in each phenogram (Figure 5b and 5c).

Linear Measurements

When we analyzed the size of the wing (AB) among the five subspecies of *Dione juno* (n=531), we observed that *D. juno huascuma* differed from *D. juno juno* and *D. juno miraculosa* ($P<0.05$), and do not differ from the other subspecies ($P>0.05$) (Figure 6a).

With respect to the width of the black bar (CF), *D. juno andicola* differed from the other subspecies, and *D. juno juno* from *D. juno huascuma* ($P<0.05$). The other subspecies did not differ among each other in this parameter (Figure 6b).

Comparing the proportion of the wing size in relation to the width of the black bar (AB/CF), we found that *D. juno andicola* and *D. juno huascuma* overlapped with each other and with the other subspecies (Figure 6c).

Regarding the subspecies that have eyespots on the black bar (DE), *D. juno huascuma* was significantly different from *D. juno andicola* and *D. juno miraculosa*; although *D. juno miraculosa* and *D. juno andicola* were not different from each other (Figure 6d). This difference may be attributed to the fact that *D. juno huascuma* shows sexual dichromatism, where the male do not display some eyespots on the black bar, whereas females always have all eyespots on black bar. When we excluded the males from the analysis, *D. juno huascuma* was not significantly different from the other subspecies.

To reduce the subjectivity of taxonomic conclusions in cases of difficult resolution, morphometric statistics has been mainly applied to linear measurements. These measurements mainly involve variations in the size of particular structures [23, 24]. Although metric overlapping characters are common among different species, it was expected that the data set would allow us to identify them properly. The statistical approach adopted herein was based on a large sample, covering most of the geographical distribution, in order to include a representative variation in the analysis. In *Dione*, previous subspecific-level comparisons regarding wing color patterns have been based on only a few specimens [9, 16, 25, 26].

Geographical distribution

We compiled a total of 2,610 geographical records, with information from 1,109 localities for *Dione*. This database was made available online via the website (https://www.google.com/fusiontables/DataSource?docid=18Y6cmJt4IVFr8IREMpAMuaO8Xv75wknYSrmqr1k), enabling users to download data, add additional records, and plot subspecies distributions. Maps of our sampling effort are shown in Figure 7, and the complete data together with material compiled from Rosser et al. [27] are given in Additional file 7-9.

Our data showed a larger number of records for the three species of *Dione* in the Neotropical region, principally on the eastern slopes of the Andes (Figure 7a), as previously noted by Rosser et al. [27]. This pattern is common in other Neotropical groups including beetles [28], birds [29] and mammals [30], and also concords with patterns seen in other butterfly groups [31-33].

D. juno occurs in almost all of Central America and South America, and is the most common *Dione* species in the Neotropical region. The next most common species is *D. moneta*, with a distribution in Central America, the Andes, and South America. *D. glycera* is restricted to the Andes (Figure 7a). This species is closely associated with mountainous

landscapes of the Andes, occurring from Venezuela to Argentina (Figure 7b), generally in association with *Passiflora tripartite* (Juss.) Poir. var. *mollissima* (Kunth). This passion-vine species belongs to the section *Tacsonia* (Juss.) Harms of the genus *Passiflora*, which is also native to the Andes, where it is known as the banana passion-fruit, grown by villagers for the production of fruit juice, at altitudes above 1,800 m [34]. *D. glycera* is the only species in the genus that shows no differentiation into subspecies throughout its geographical range [17].

The regions of Mexico and Central America are mainly represented by *D. moneta poeyii* and *D. juno huascuma* (Figure 7c and 7d), in concordance with Rosser et al. [27]. In South America, there is the widespread occurrence of *D. juno juno* and a broad representation of the three species of *Dione* close to the Andes (Figure 7d), especially *D. juno andicola*, *D. juno miraculosa*, *D. juno juno* (Figure 7d) and *D. moneta butleri* (Figure 7c).

Mexico and Central America showed a good representation of *D. juno huascuma* and *D. moneta poeyii* (Figure 7c and 7d), also in agreement with Rosser et al. [27]. In Brazil, we observed a significant representation of *D. moneta moneta*, *D. juno juno* and *D. juno suffumata* (Figure 7c and 7d). Principally in central and southern Brazil, we had significant representation of *D. moneta moneta*, *D. juno juno* and *D. juno suffumata* (Figure 7c and 7d; Additional files 8 and 9) which were not as well represented in Rosser et al. [27]; this difference may be due to the fact that we visited additional entomological collections in South America that have larger holdings of these subspecies.

D. moneta showed a disjunct geographical distribution, where *D. moneta poeyii* occurs in Central America and Mexico, *D. moneta butleri* close to the Andes and *D. moneta moneta* in relatively arid zones of southern Brazil, part of Argentina, Paraguay and Bolivia (Figure 7c), as previously shown by Rosser et al. [27]. The distribution of *D. moneta moneta* is determined preponderantly by *Passiflora morifolia*, the preferred host plant and effectively used in the southern limit of its distribution in the Neotropics (S. Thiele, UFRGS, unpublished data).

The eastern parts of Colombia and Venezuela (Llanos) have been little sampled for *Dione*, which may the reason why specimens from those regions are poorly represented in insect collections [27]. This may not be the case for central Brazil, where the scarcity of records presented herein is supposedly related to their comparatively lower natural occurrence in the Amazon Basin and Cerrado, which should be further explored.

Taken together, these results demonstrated that *Dione* species represent independent lineages, as judged on three criteria (for a discussion, see Barão et al. [15]): 1) they are diagnosable, by having fixed morphological differences; 2) monophyletic; and 3) show discrete genetic clustering. This is not the case at the subspecific level, especially in *D. juno* for the first criterion, where there is substantial overlap regarding the morphometric parameters associated with the variations in wing color pattern that are used to identify their subspecies. Thus, we questioned their taxonomic validity and usefulness, since most of them (e.g., *D. juno andicola*, *D. juno juno*, *D. juno miraculosa*, and *D. juno suffumata*) are neither fully diagnosable nor isolated in spatial distribution. As pointed out by Braby et al. [35], the use of subspecific taxonomic units would be recommended only for geographically restricted, evolving populations of isolated lineages in the case of allopatric species, showing at least one diagnosable difference that is evolutionarily independent, to be maintained as evolutionary units from a conservation biology perspective. Unfortunately, the molecular markers used herein are not appropriate to examine this aspect and the other two criteria listed above, due to the low variation that they show in the genome at the subspecific level in Heliconiini [12, 13]. Further studies in this regard should instead use other more appropriate, less conserved molecular markers, such as microsatellites, as specifically developed for *Dione* by Massardo et al. [36].

Conclusion

By using large sample sizes and an integrative taxonomic approach, including molecular markers and geometric morphometrics, this study deals with the evolutionary history of *Dione* Hubner, a tropical genus of heliconiine butterfly (Lepidoptera: Nymphalidae) to which three species are assigned: *Dione juno* (Cramer, 1779), *Dione moneta* Hübner, [1825] and *Dione glycera* (C. Felder & R. Felder, 1861). Our data showed that *Dione* forms a monophyletic clade, sister of *Agraulis* Boisduval & Le Conte, thus also a valid genus. We demonstrated that *Dione* species are reciprocally monophyletic, form genetic clusters and are phenotypically diagnosable, and thus are all validated herein from a taxonomic perspective. However, we found a strong overlap in the wing-color patterns used to distinguish the subspecies of *D. juno* and *D. moneta*, most of which are not allopatric in distribution, and thus supposedly hybridize throughout their distribution ranges. As a consequence, since they are not fully diagnosable, we questioned their validity and usefulness either as taxonomic entities or evolutionary units from a conservation biology perspective. The time divergences estimated herein strongly support the contention that speciation in *Dione* coincided with both the rise of Passifloraceae and the uplift of the Andes. Since the sister species *D. glycera* and *D. moneta* are specialized feeders on passion-vine lineages that are endemic to areas located either within or adjacent to this region, we hypothesize that they co-speciated there and at that time. Our findings thus add to other studies that have demonstrated the utility of large sample sizes and an integrative taxonomic approach when investigating species and subspecies boundaries. Such practices are relevant not only for specific investigations concerning nymphalid butterflies but within the wider scenario of taxonomic and biogeographical studies.

Methods

Molecular phylogeny

Genomic DNA was extracted from tissue samples obtained from either field-collected samples or laboratory-reared adults using the Qiagen Blood and Tissue Kit (Qiagen, Valencia, CA). Representative specimens of *D. glycera* (n=7), *D. moneta* (n=7) and *D. juno* (n=8) were used to reconstruct the phylogeny at species level (Table 3). In addition, 24 specimens of Heliconiini from the genera *Agraulis*, *Dryas*, *Dryadula*, *Eueides*, *Heliconius*, *Laparus*, *Neruda*, *Philaethria* and *Podotricha* were included in order to investigate the phylogenetic position of *Dione* within Heliconiini (Table 3). To evaluate the evolutionary relationships among heliconiine lineages, we included *Cethosia cyane* (Acraeinii) and *Actionote anteas* (Acraeinii) as the outgroup (Table 3). A total of 4,594 base pairs of gene regions, including the standard loci employed for molecular systematics of Lepidoptera (*CO-I*/tRNA-*leu*/*CO-II*, *16S* and *wingless*; [37]), plus novel introns (*Th*, *Ap* and *dpp*; [38]) were amplified through polymerase chain reaction (PCR). Primer sequences are described in electronic supplementary material (Additional file 10). PCR conditions varied for the markers used. For CO-I and CO-II, we used 95°C for 2 min, 95°C for 30 s, 65°C for 30 s, 72°C for 1 min for 15 cycles, 95°C for 30 s, 50°C for 30 s, 72°C for 1 min for 25 cycles and 72°C for 6 min. All other loci followed conditions proposed by Beltrán et al. [14]: 94°C for 5 min, 94°C for 30 s, 55°C for 30 s, and 72°C for 1 min for 34 cycles. Primer sequences are described in electronic supplementary material (Additional file 10). PCR products were purified using the enzymatic method of Exonuclease I (GE Healthcare) and Shrimp alkaline phosphatase, and sequenced in the Northwest Labs-FAS (Faculty of Art and Sciences) at Harvard University (Cambridge, Massachusetts, USA) using BigDye chemistry. All sequences were deposited in GenBank and the accession numbers are given in Table 3. Contigs were constructed using SeqMan software. Sequences were aligned and visually inspected in MUSCLE (Multiple

Sequence Alignment - www.ebi.ac.uk/tools/msa/muscle) and manually adjusted through BioEdit (Sequence Alignment Editor). Patterns of genetic variability for each marker individually and models of sequence evolution at the tribe (Heliconiini) and genus level (*Dione*) were estimated. The Incongruence for Length Difference test (ILD; [39]) implemented by PAUP* was used to evaluate incongruence between mtDNA (CO-I/tRNA-leu/CO-II vs. 16S) and nuclear (*Ap, Th, Ef-1α, Wg, dpp*) data partitions.

Coalescent species trees of *Dione* were inferred using the Bayesian method through BEAST v2.01 [40] based on multilocus data, which is more accurate than similar methods when applied to rapid radiations [41]. Concatenated sequenced loci were unlinked to allow for variation in substitution models, and the clock models for the mtDNA were linked to account for their presumed single hierarchical history. A separate analysis based on mtDNA and nuclear loci was also performed. The analysis was run using a Yule species tree prior and the GTR+Γ model of nucleotide substitution with four rate categories. The Markov chains were run for 50 million generations and repeated 10 times to test for Markov chain - Monte Carlo chain convergence, and priors exceeded 200 to ensure effective sample sizes (ESS). Burn-in was determined in Tracer v1.5 [42] based on ESS and parameter trajectories, and was then removed in TreeAnnotator. Phylogenetic trees were also reconstructed using maximum likelihood (ML) in the software PHYML 3.0 [43] and Neighbor joining (p-distance) to resolve relationships of *Dione* at species level. Monophyly confidence limits were assessed with the bootstrap method [44] at 60% cutoff after 1,000 bootstrap iterations.

Time of divergences and topology of heliconiine lineages were estimated simultaneously using the program BEAST v. 2.01. The data set included mitochondrial + nuclear loci, but was split into mitochondrial gene regions (*CO* and *16S*) and nuclear genes (*Th, Ef1-α, Ap, Wg* and *dpp*) due to the high proportion of A-T nucleotides in the mitochondrial gene compared with the approximately equal base ratios of the nuclear genes. The tree prior was set to the Yule calibrated process; the independent models for the two

partitions were set to GTR (mitochondrial data set) and HKY (nuclear data set), while all other priors were left to defaults. The branch lengths were allowed to vary under a relaxed clock model with an uncorrelated lognormal distribution [45]. The analyses were run for 40 million generations with every 4000th generation sampled. One prior was specified in the form of a calibration point as the time of the most recent common ancestor (tMRCA) for Heliconiini (47.2 mya; [20]). Convergence, effective sample sizes, and divergence times with upper and lower 95% highest posterior density (HPD) bounds were assessed in Tracer 1.5. TreeAnnotator was used for all analyses, with 20% of the samples removed for burn-in to generate a tree that was then visualized and edited in FigTree v1.3.1 [46].

Geometric Morphometrics Analyses

The material examined consisted of 729 individuals of genus *Dione* (Table 4). They came from museum collections (Additional file 11; https://www.google.com/fusiontables/DataSource?docid=18Y6cmJt4IVFr8IREMpAMuaO8Xv75wknYSrmqr1k), and had a wide geographical range, totaling 310 localities (Figure 7a-d).

Images of ventral forewings (FW) and hindwings (HW) were captured for the left side of all specimens having undamaged wings, by using a Sony DSC-H20 digital camera with 10.1 megapixels of resolution, macro function on, and no flash. We used 17 landmarks for the FW and 14 landmarks for the HW (Figure 8b and Additional file 12). The anatomical landmarks were digitized by the same person (D.M.) for each specimen using TPSDig2, version 2.16 [47]. Cartesian coordinates (x and y) of the landmarks were superimposed using a generalized Procrustes analysis (GPA) algorithm [48]. This was used to remove differences unrelated to shape such as scale, position, and orientation [49-51]. The size of a wing was estimated using its centroid size, namely the square root of the sum of the squares of the distance of each landmark from the centroid (mean of all coordinates) of the configuration

[52]. We used a single value for wing size coupling FW and HW landmark configurations together to calculate the log-transformed centroid size. Because we used different distances in the wing photographs, a size correction was made by IMP CoordGen6f [53] using a scale factor.

Variations in centroid size were represented by their median and corresponding quartiles. Corresponding differences were compared among species and subspecies through analysis of variance (ANOVA), followed by Tukey's multiple comparison tests. For wing shape, the principal components analysis (PCA) was calculated on the variance-covariance matrix of generalized least-square superimposition residuals, as an exploratory analysis. The PCs were used as new shape variables, to reduce the dimensionality of the data set as well as to analyze independent variables. We performed a linear discriminant analysis (LDA), calculated on a subset of PCs, to compute leave-one-out cross-validation to determine the percentages of correct classification among species and among subspecies defined a priori [54].

For the statistical test of wing shape differences, we used multivariate analysis of variance (MANOVA) on shape variables. Differences in the shape of the wings inferred from statistical analyses were visualized through multivariate regression of shape variables on principal components.

Mahalanobis distances were used to compute Neighbor-joining trees (phenograms) to visualize the shape relationship among *Dione* subspecies. To visualize wing shape differences in the phenograms, we adopted the consensus (all) shape configurations of landmarks for all samples versus the mean shape for each subspecies in terminal branches.

For all statistical analyses and to generate graphs, we used the "R" language and environment for statistical computing, version 2.14.1 (R development Core Team; http://www.r-project.org) and the libraries "ape" [55], "ade4" [56], "MASS" [57], and "stats"

[58]. Geometric morphometrics procedures were carried out using the "Rmorph" library for R [59].

Linear Morphometrics

As discussed above, subspecies of *D. moneta* were allopatric in distribution, and thus we saw no need to evaluate their wing variation at the subspecific level.

Characterization of Dione juno subspecies

Criteria that are commonly used to identify *Dione* species and subspecies are scattered in the literature. DeVries [16] characterized *Dione juno* by having the anterior margin of the forewing excavated, a dark bar that crosses the discal cell, and a broad black hindwing margin. According to Brown [25], *D. juno suffumata* is readily distinguished from the *D. juno juno* form by the extensive invasion of the red-orange areas on the upper surface by the black borders, producing a very dark forewing apex and broad black hindwing margin. According to Brown [26], *D. juno miraculosa* shows morphology identical to that of *D. juno juno*, of which *miraculosa* should be considered a reddened southern subspecies. Emsley [9] characterized *D. juno huascuma* as larger, usually paler, with the dark border to the posterior margin of the hindwing spotted with ground color, and is more variable. Sexual dichromatism is pronounced; females are lighter in color, and with the dark markings less precise. Also, according to Emsley, *D. juno andicola* differs from *D. juno huascuma* principally in its smaller size, and in that the dark markings of both sexes are paler.

Thus, to evaluate variation in hindwing characteristics among subspecies of *D. juno,* we performed linear measurements (length and width of the marginal bar and eyespots) for 600 specimens: 351 related to *D. juno juno*, 22 to *D. juno suffumata*, 51 to *D. juno andicola*, 133 to *D. juno huascuma* and 17 to *D. juno miraculosa*

(https://www.google.com/fusiontables/DataSource?docid=18Y6cmJt4IVFr8IREMpAMuaO8Xv75wknYSrmqr1k). For these measurements, we used specimens that had at least one of the hindwings intact. As shown in Fig. 8a, the length of the hindwing (vector A-B) corresponded to the line segment formed between the common origin of the Subcostal vein (Sc) and Sector-radial (Rs), and the distal end of the Rs. The ratio for the hindwing length in relation to the width of the marginal black band (=A-B/C-F) was determined. In this case, the mean C-F = [(C1-F1)+(C2-F2)+(C3-F3)]/3, each C-F vector was taken in the middle for cells M1, M2 and M3. Using the same line vectors, the mean width of the corresponding eyespots was determined as the mean D-E = [(D1-F1)+(D2-F2)+(D3-F3)]/3.

All linear measurements were performed on the digitalized images with the AxioVision software (Carl Zeiss, Release 4.8.2, June 2010). The corresponding data were evaluated for normality using the Kolmogorov-Smirnov test. They did not fit into a normal distribution and were then compared using the Kruskal-Wallis nonparametric test, followed by Dunn's multiple comparison tests. Data are presented as the median and corresponding quartiles. Statistical analyses were performed in GraphPad Prism 5 software [60].

Geographical Distribution

Our main sources of geographical distribution data were museum collections (Additional file 11). We added to them the more recent geographical distribution database (total of 1,200 records) for *Dione juno* published by Rosser et al. [27]. A complete list of the material analyzed and compiled, with their respective collection information, locality and geographical coordinates are available on the World Wide Web site at https://www.google.com/fusiontables/DataSource?docid=18Y6cmJt4IVFr8IREMpAMuaO8Xv75wknYSrmqr1k.

Locality records in our database refer to individual specimens. Older museum specimens were often labeled with generalized localities, and when it was not possible to determine the correct locality from the labels, these specimens were excluded from the samples. They were georeferenced from geospatial databases Global Gazetter [61]. Maps were generated in ArcMap version 9.3 (ESRI).

Polygons were drawn for the delimitation of geographical distributions of the species and subspecies. We clipped the polygons around the point of occurrence and coastlines [27]. We also clipped polygons to exclude sampled areas where we were confident that the absence of records was not an artifact, and filled the polygons where we were sure of the occurrence of the species.

Authors' contributions

DM gathered and organized the museum data, photographed the specimens and marked the wing landmarks; carried out the DNA extraction, amplification, sequencing and the sequence alignment; and drafted the manuscript. GLP performed the molecular analyses and helped to draft the manuscript. RF performed the geometric morphometric analyses and helped to draft the manuscript. MRK participated in the design and coordination of the molecular analyses, and helped to draft the manuscript; GRPM conceived of the study, participated in its design and coordination, and helped to draft the manuscript.

Acknowledgements

We are grateful to the following curators of insect collections for making specimens available for this study: O. H. H. Mielke (DZUP), J. Y. Miller (FSMC), H. A. Vargas (IDEA), M. V. Colomo (IFML), A. R. Alsina (MACN), G. Carvalho (MCTP), N. Pierce (MCZ), A. Lanteri

(MLPA), M. Monné (MNRJ), O. Silveira (MPEG), G. Lamas (MUSM), M. Duarte (MZSP) and R. K. Robbins (USNM). Thanks are also due to H. A. Vargas (Universidad de Tarapacá, Chile), C. Millan and J. A. Salazar (Universidad de Caldas, Colombia), and S. Thiele (UFRGS) for providing some of the specimens used in the molecular analyses. K. R. Barão and R. Brito (UFRGS) provided photographs of some specimens in museum collections. D. Massardo is particularly grateful to A. Tenger-Trolander and N. Chamberlain (FAS Center for Systems Biology, Harvard University) for their help with laboratory work, and to J. Y. Miller (FSMC), R. K. Robbins (USNM), B. Harris and G. Lamas (MUSM) for their kind assistance during the museum visits. Thanks are also due Janet W. Reid for editing the text. Molecular work was supported by NSF grant DEB-1316037 to M. R. Kronforst. D. Massardo was supported by a CAPES Ph.D. fellowship and CNPq SWE grant number 200695/2011-8. G. L. Gonçalves and G. R. P. Moreira were supported by CNPq grants (156153/2011-4 and 309676/2011-8, respectively).

References

1. Mallet J: **Hybridization, ecological races and the nature of species: empirical evidence for the ease of speciation.** *Philosophical Transactions of the Royal Society B* 2008, **63:** 2971-2986
2. Mallet J: **Rapid speciation, hybridization and adaptive radiation in the *Heliconius melpomene* group.** In: *Speciation and patterns of diversity.* Edited by Butlin RK, Bridle JR, Schluter D. Cambridge: Cambridge University Press; 2009:177-194
3. Chamberlain NL, Hill RI, Kapan DD, Gilbert LE, Kronforst MR: **Polymorphic butterfly reveals the missing link in ecological speciation.** *Science* 2009, **326:** 847-850

4. Kronforst MR, Salazar CA, Linares M, Gilbert LE: **No genomic mosaicism in a putative hybrid butterfly species.** *Proceedings of the Royal Society of London Series B, Biological Sciences* 2009, **274:** 1255-1264.

5. Kronforst MR: **Mimetic butterflies introgress to impress.** *PLoS Genetics* 2012, **8:** e1002802

6. Rosser N, Phillimore AB, Mallet J: **Extensive range overlap between *Heliconius* sister species: evidence for sympatric speciation in butterflies?** *Submitted.*

7. Brower AVZ: **Introgression of wing pattern alleles and speciation via homoploid hybridization in Heliconius butterflies: a review of evidence from the genome.** *Proceedings of the Royal Society of London Series B, Biological Sciences* 2013, **280** (1752), 20122302

8. Heliconius Genome Consortium: **Butterfly genome reveals promiscuous exchange of mimicry adaptations among species**. *Nature* 2012, **487:** 94-98

9. Emsley M: **A morphological study of imagine Heliconiinae (Lepidoptera, Nymphalidae) with a consideration of the evolutionary relationships within the group**. *Zoologica* 1963, **48:** 85-129

10. Brown KSJr: **The biology of *Heliconius* and related genera.** *Annual Review of Entomology* 1981, **26:** 427-456

11. Penz CM: **Higher level phylogeny for the passion-vine butterflies (Nymphalidae, Heliconiinae) based on early stage and adult morphology.** *Zoological Journal of the Linnean Society* 1999, **127:** 277-344

12. Brower AVZ: **Rapid morphological radiation and convergence among races of the butterfly *Heliconius erato* inferred from patterns of mitochondrial DNA evolution.** *Proceedings of the National Academy of Sciences of the USA 1994*, **91:** 6491-6495

13. Brower AVZ, Egan MG: **Cladistic analysis of *Heliconius* butterflies and relatives (Nymphalidae: Heliconiiti): a revised phylogenetic position for *Eueides* based on**

sequences from mtDNA and a nuclear gene. *Proceedings of the Royal Society of London Series B, Biological Sciences* 1997, **264:** 969-977

14. Beltrán M, Jiggins CD, Brower AVZ, Bermingham E, Mallet J: **Do pollen feeding, pupal-mating and larval gregariousness have a single origin in *Heliconius* butterflies? Inferences from multilocus DNA sequence data.** *Biological Journal of the Linnean Society* 2007, **92:** 221-239
15. Barão KR, Gonçalves GL, Mielke OHH, Kronforst MR, Moreira GRP: **Species boundaries in *Philaethria* butterflies: an integrative taxonomic analysis based on genitalia ultrastructure, wing geometric morphometrics, DNA sequences and AFLPs.** *Zoological Journal of the Linnean Society,* in press.
16. DeVries PJ: *The butterflies of Costa Rica and their natural history. Papilionidae, Pieridae, Nymphalidae.* Princeton: Princeton University; 1987.
17. Lamas G: **Checklist: Part 4A. Hesperioidea - Papilionoidea.** In: *Atlas of Neotropical Lepidoptera.* Edited by Heppner JB. Gainesville: Association for Tropical Lepidoptera, Scientific Publishers; 2004: 1-274
18. Muschner VC, Zamberlan PM, Bonatto SL, Freitas, LB: **Phylogeny, biogeography and divergence times in *Passiflora* (Passifloraceae).** *Genetics and Molecular Biology* 2012, **35:** 1036–1043
19. Horton B, Parra M, Saylor J, Nie J, Mora A, Torres V, Stockli D, Strecker M: **Resolving uplift of the northern Andes using detrital zircon age signatures.** *GSA Today* 2010, **20**: 7
20. Wahlberg N, Leneveu J, Kodandaramaiah U, Peña C, Nylin S, Freitas AVL, Brower AVZ: **Nymphalid butterflies diversify following near demise at the Cretaceous/Tertiary boundary.** *Proceedings of the Royal Society of London Series B, Biological Sciences* 2009, **276:** 4295–4302

21. Maddison WP: **Reconstructing character evolution on polytomous cladograms.** *Cladistics* 1989, **5:** 365–377

22. Grafen A: **The phylogenetic regression.** *Philosophical Transactions of the Royal Society of London B* 1989, **326:** 119–157

23. Rohlf FJ: **An overview of image processing and analysis techniques for morphometrics.** *In Morphometrics Workshop.* Special Publication no. 2. Edited by Rohlf FJ, Bookstein FL. Proc. Mich. Univ. of Michigan: Museum of Zoology; 1990: 37-60

24. Mutanen M, Pretorius E: **Subjective visual evaluation vs. traditional and geometric morphometrics in species delimitation: a comparison of moth genitalia.** *Systematic Entomology* 2007, **32:** 371–386

25. Brown KS: **The heliconians of Brazil (Lepidoptera: Nymphalidae). Part V. Three new subspecies from Mato Grosso and Rondônia.** *Bulletin of the Allyn Museum* 1973, **13:** 1–19

26. Brown KS, Benson WW: **The heliconians of Brazil (Lepidoptera: Nymphalidae) Part VI. Aspects of the biology and ecology of Heliconius demeter with description of four new subspecies.** *Bulletin of the Allyn Museum* 1975, **26:** 1–19

27. Rosser N, Phillimore AB, Huertas B, Willmott KR, Mallet J: **Testing historical explanations for gradients in species richness in heliconiine butterflies of tropical America.** *Biological Journal of the Linnean Society* 2012, **105:** 479-497

28. Pearson DL, Carroll SS: **Predicting patterns of tiger beetle (Coleoptera: Cicindelidae) species richness in Northwestern South America**. *Studies on Neotropical Fauna and Environment* 2001, **36:** 125-136

29. Orme CDL, Davies RG, Burgess M, Eigenbrod F, Pickup N, Olson VA, Webster AJ, Ding T-S, Rasmussen PC, Ridgely RS, Stattersfield AJ, Bennett PM, Blackburn TM,

Gaston KJ, Owens IPF: **Global hotspots of species richness are not congruent with endemism or threat.** *Nature* 2005, **436:** 1016–1019

30. Willig MR, Kaufman DM, Stevens RD: **Latitudinal gradients of biodiversity: pattern, process, scale, and synthesis.** *Annual Review of Ecology, Evolution, and Systematics* 2003, **34:** 273–309

31. Brown KS: **Historical and ecological factors in the biogeography of aposematic Neotropical butterflies.** *American Zoologist* 1982, **22:** 453–471

32. Willmott KR: **The genus Adelpha: its systematics, biology and biogeography (Lepidoptera: Nymphalidae: Limenitidini)**. *Gainesville, FL: Scientific Publishers* 2003

33. Mullen SP, Savage WK, Wahlberg N, Willmott KR: **Rapid diversification and not clade age explains high diversity in neotropical *Adelpha* butterflies.** *Proceedings of the Royal Society of London Series B, Biological Sciences* 2011, **278:** 1777–1785

34. Vargas HA, Barão KR, Massardo D, Moreira GRP: **External morphology of the immature stages of Neotropical heliconians: IX. *Dione glycera* (C. Felder & R. Felder, 1861) (Lepidoptera, Nymphalidae, Heliconiinae).** *Submitted*

35. Braby MF, Eastwood R, Murray N: **The subspecies concept in butterflies: has its application in taxonomy and conservation biology outlived its usefulness?** *Biological Journal of the Linnean Society* 2012, **106:** 699–716

36. Massardo DP, Roratto A, Vargas HA, Kronforst MR, Moreira GRP: **Development of a microsatellite library for the passion flower butterfly *Dione moneta* Hübner (Lepidoptera: Nymphalidae: Heliconiinae).** *Conservation Genetics Resources* 2012, **4:** 719-724

37. Sperling FAH: **Butterfly molecular systematics: from species definitions to higher-level phylogenies.** In: *Butterflies: ecology and evolution taking flight*. Edited by Boggs CL, Watt WB, Ehrlich PR. Chicago: University of Chicago Press; 2003:431–458

38. Kronforst MR: **Primers for the amplification of nuclear introns in *Heliconius* butterflies**. *Molecular Ecology Notes* 2005, **5:** 158-162

39. Farris JS, Källersjö M, Kluge AG, Bult C: **Testing significance of congruence.** *Cladistics* 1994, **10:** 315-319

40. Drummond AJ, Suchard MA, Xie D, Rambaut A: **Bayesian phylogenetics with BEAUti and the BEAST 1.7.** *Molecular Biology and Evolution* 2012, **29 (8)**: 1969–1973

41. Heled J, Drummond AJ: **Bayesian inference of population size history from multiple loci.** *BMC Evolutionary Biology* 2008, **8:** 289

42. Drummond AJ, Rambaut A: **Beast: Bayesian evolutionary analysis by sampling trees**. *BMC Evolutionary Biology* 2007, **7:** 214

43. Guindon S, Dufayard J-F, Lefort V, Anisimova M, Hordijk W, Gascuel O: **New algorithms and methods to estimate maximum-likelihood phylogenies: assessing the performance of PhyML 3.0.** *Systematic Biology* 2010, **59:** 307–321

44. Felsenstein J: **Confidence limits on phylogenies: an approach using the bootstrap**. *Evolution* 1985, **39:** 783–791

45. Drummond A J, Ho SYW, Phillips MJ, Rambaut A: **Relaxed phylogenetics and dating with confidence.** *PLoS Biology* 2006, **4**(5): e88

46. Rambaut A: *FigTree v1.3.1 2006–2009*. 2009. Available with the program package at http://tree.bio.ed.ac.uk/software/figtree

47. Rohlf FJ: *TPSdig v.2.10.* 2010. Stony Brook: State University of New York. Available at: http://life.bio.sunysb.edu/morph

48. Dryden IL, Mardia KV: *Statistical shape analysis*. New York, NY: John Wiley & Sons, Inc; 1998.

49. Rohlf FJ, Slice D: **Extensions of Procrustes method for the Optimal Superimposition of Landmarks.** *Systematic Biology* 1990, **39:** 40–59

50. Rohlf FJ, Marcus LF: **A revolution in morphometrics.** *Trends in Ecology and Evolution* 1993, **8:** 129–132

51. Adams DC, Rohlf FJ, Slice DE: **Geometric Morphometrics: ten years of progress following the 'revolution'**. *Italian Journal of Zoology* 2004, **71:** 5–16

52. Bookstein FL: *Morphometric tools for landmark data: geometry and biology*. London: Cambridge University Press; 1991.

53. Sheets HD: *IMP: CoordGen6f - Coordinate Generation Utility software***.** New York: Department of Physics, Canisius College; 2001.

54. Baylac M, Friess M: **Fourier descriptors, procrustes superimposition, and data dimensionality: an example of cranial shape analysis in modern human populations**. In: Slice DE, ed. *Modern morphometrics in physical anthropology, part 1 theory and methods*. New York, NY: Kluwer Academic/Plenum Publishers; 2005: 142–165

55. Paradis E, Claude J, Strimmer K: **APE: analyses of phylogenetics and evolution in R language.** *Bioinformatics* 2004, **20:** 289-290

56. Dray S, Dufour AB: The ade4 package: implementing the duality diagram for ecologists. *Journal of Statistical Software* 2007, **22**(4): 1-20

57. Venables WN, Ripley BD: *Modern Applied Statistics with S* (MASS). Springer: New York; 2002.

58. R Development Core Team: R: A language and environment for statistical computing. Version 2.15.0. Vienna: R Foundation for Statistical Computing; 2011. http://www.R-project.org.

59. Baylac M: *Rmorph: a R geometric and multivariate morphometrics library*. 2007. Available from the author: baylac@mnhn.fr

60 Motulsky HM, Christopoulos A: *Fitting models to biological data using linear and nonlinear regression: a practical guide to curve fitting.* San Diego: GraphPad Software Inc.; 2003.

61 Falling Rain Genomics: *Global Gazetteer ver. 2.1, 1996-2006*. 2007. Available at: http://www.fallingrain.com/world/

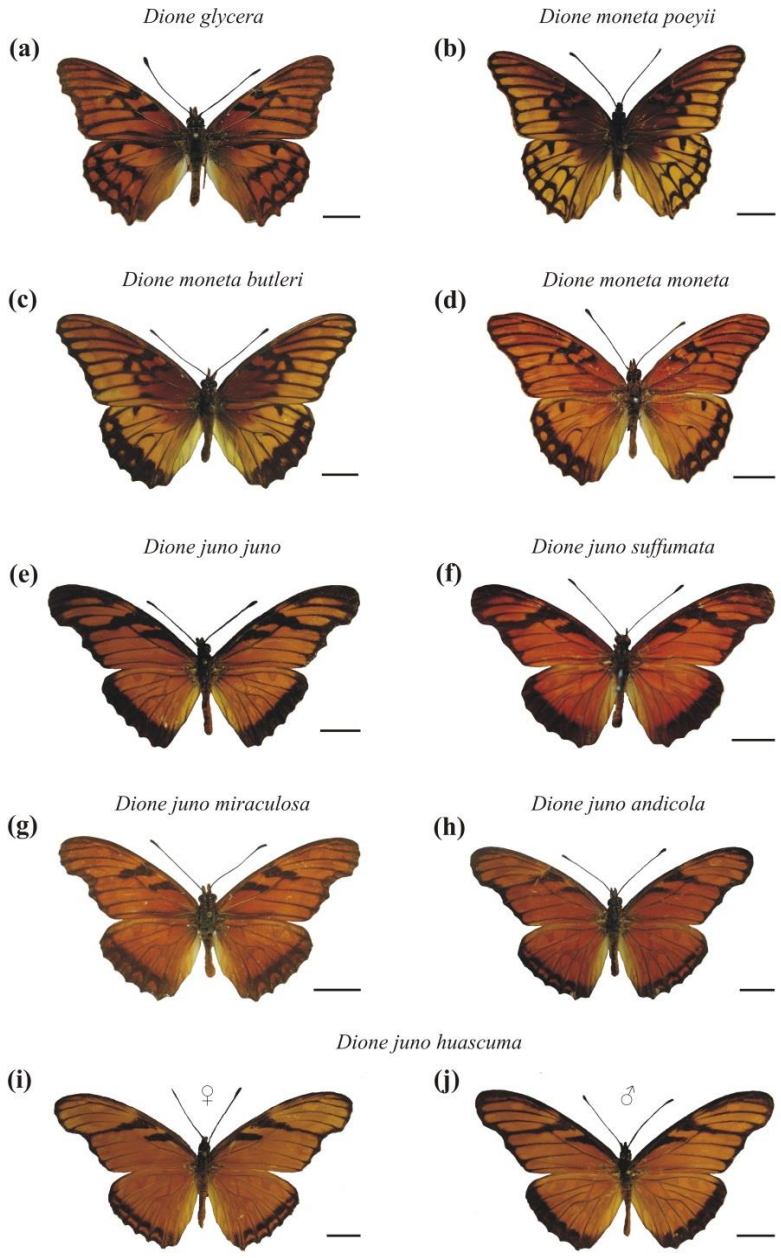

Figure 1 Putative specimens of *Dione* species and subspecies. Scales=10 mm.

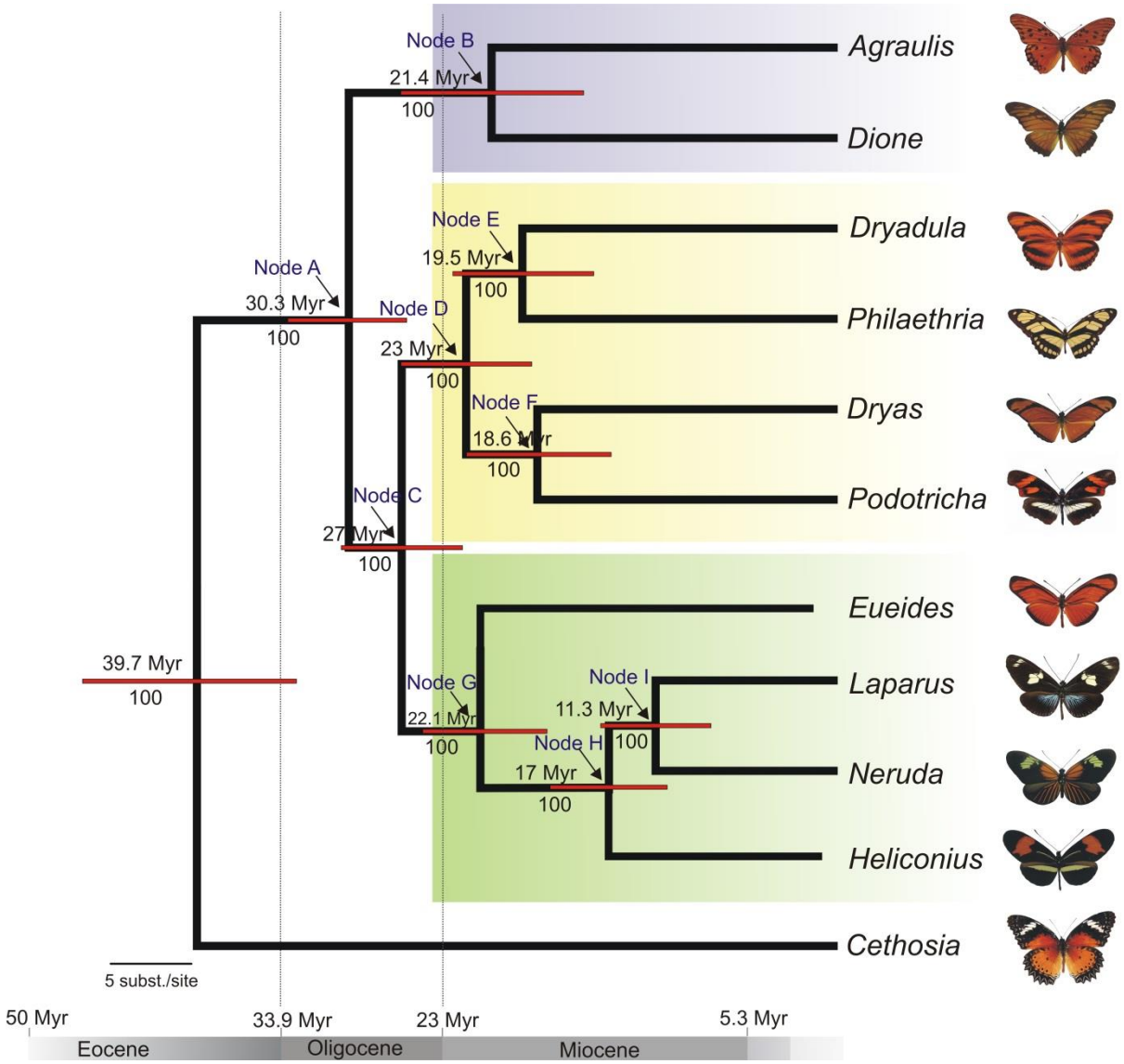

Figure 2 Molecular phylogeny of Heliconiini. Bayesian time-calibrated consensus tree based on 4.5 Kb of combined mitochondrial (*CO* and *16S*) and nuclear data (*AP*, *TH*, *EF-1α, WG* and *DPP*). *Cethosia* was used to root the tree. Values below branches represent posterior probability support for the equivalent node. Node letters (A-I) indicate major lineages (for age details see Table 2).

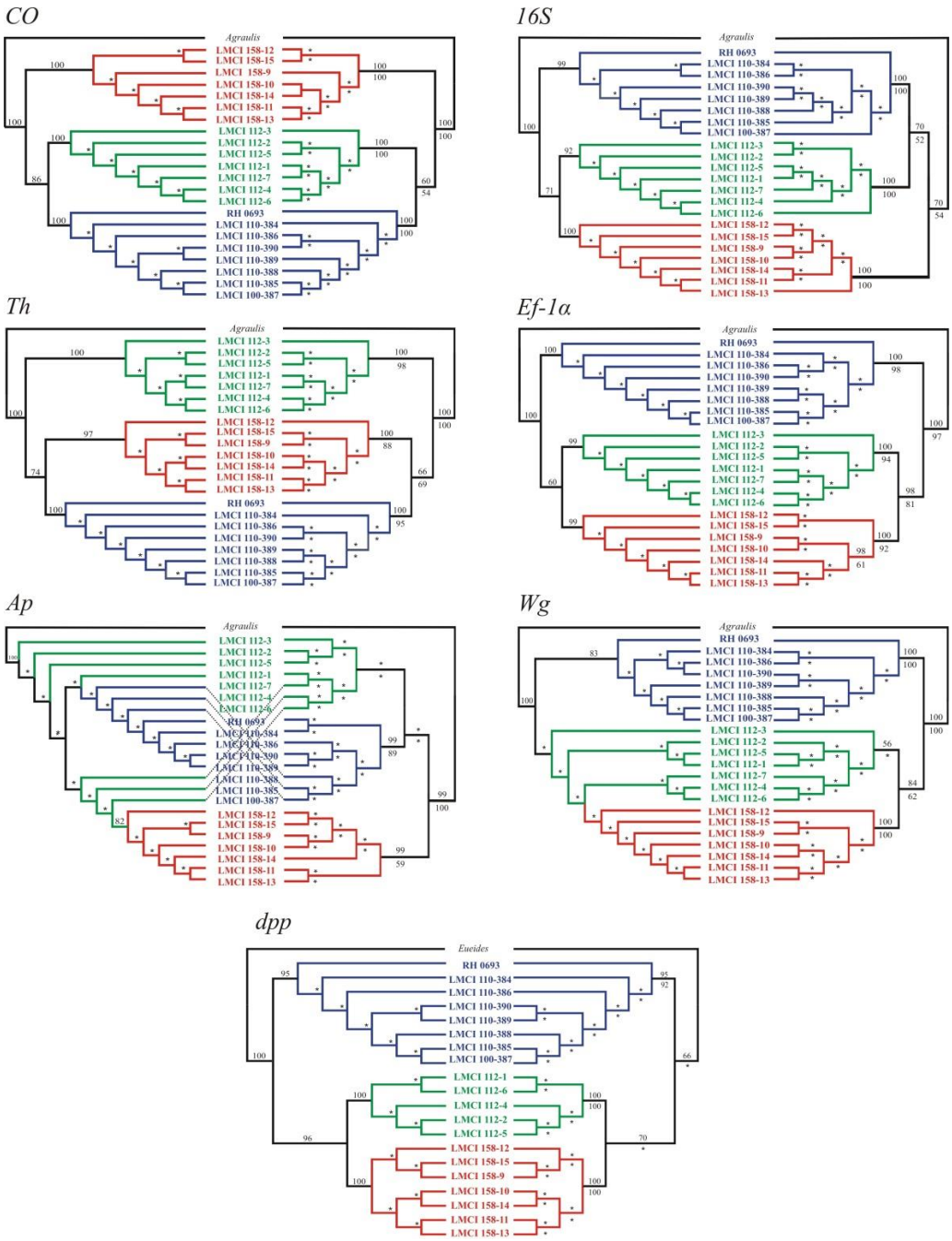

Figure 3 Reconstruction of *Dione* species molecular phylogenies based on seven markers (*CO, 16S, Ap, Th, Ef-1α, W*g and *dpp*). Trees on the left were reconstructed based on the distance method, and on the right side, on Bayesian Inference (BI) and Maximum likelihood (only BI is depicted, as topologies were equal). *D. glycera*, *D. moneta* and *D. juno* are represented in green, red and blue respectively. Values above branches on the left-hand trees represent bootstrap support. On the right-hand trees, numbers above branches indicate posterior probability support; numbers below branches represent bootstrap values higher than 50%. Branches with an asterisk have node support < 49%.

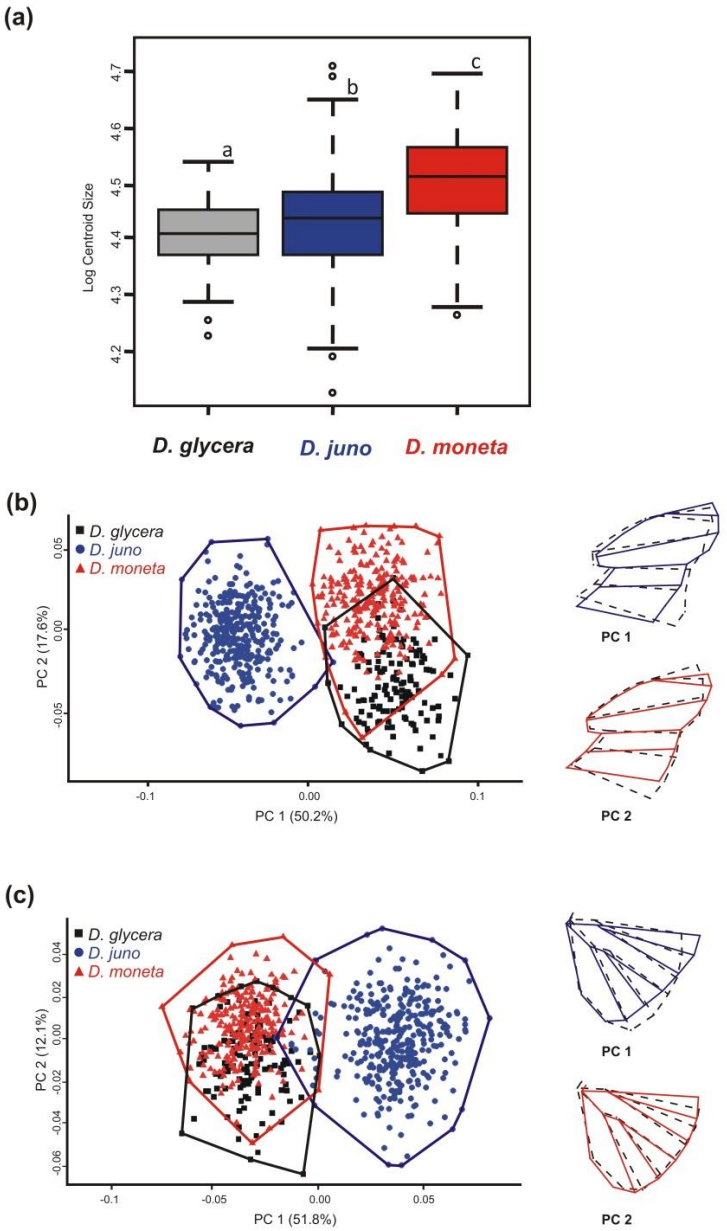

Figure 4 Wing size and shape variation among *Dione* species. (**a**) Centroid size. Boxes show the median and respective quartiles; dots indicate outliers. Different letters above boxes represent significant differences among species (One-way ANOVA, followed by Tukey's multiple comparison tests; alpha = 0.05). (**b**) and (**c**) Scatterplots of first two Principal Components (PCs), respectively, for the forewing and hindwing shape variation; PC 1 and PC 2, indicate the variation on the first and second axes, respectively; the solid blue line indicates negative scores and the dotted black line indicates positive scores. Percentage of variance is given in parentheses.

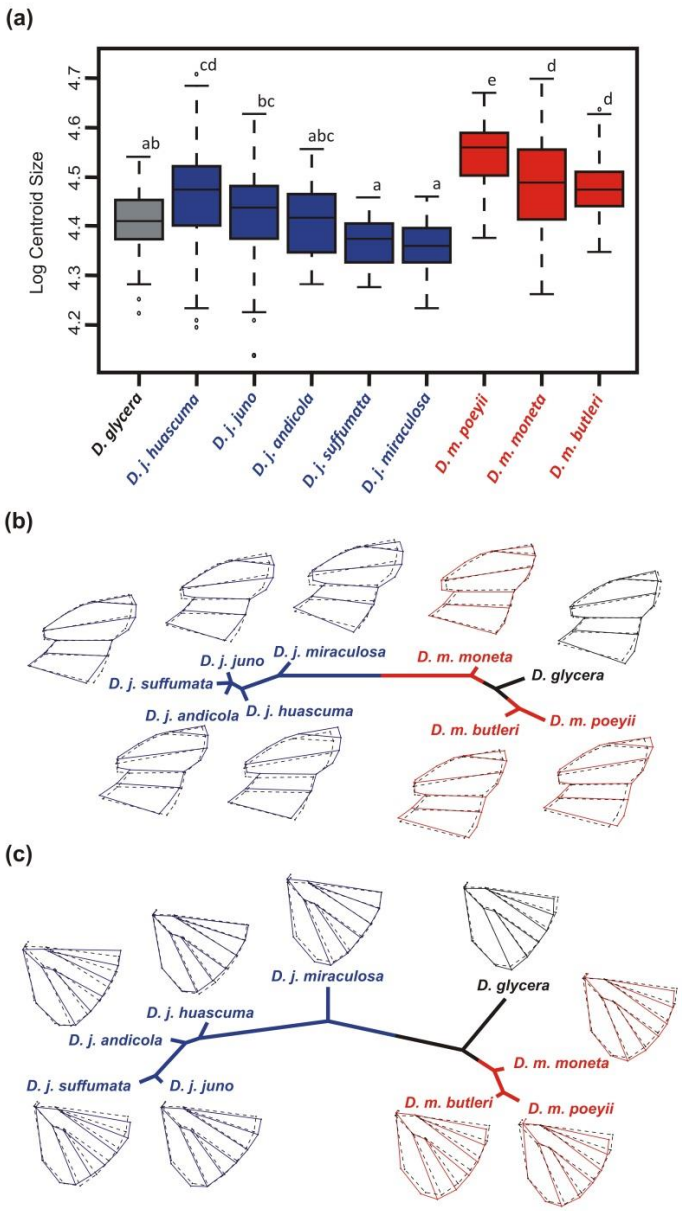

Figure 5 Wing size and shape variation among *Dione* subspecies. (**a**) Centroid size. Boxes show the median and respective quartiles; dots indicate outliers. Different letters above boxes represent significant differences among subspecies (One-way ANOVA, followed by Tukey's multiple comparison tests; alpha = 0.05). (**b**) and (**c**) Neighbor-joining trees based on Mahalanobis distances for forewing and hindwing shape, respectively. In both trees, branches are associated with the consensus landmarks in dotted lines, and the mean shape configuration of landmarks for each subspecies, in solid lines.

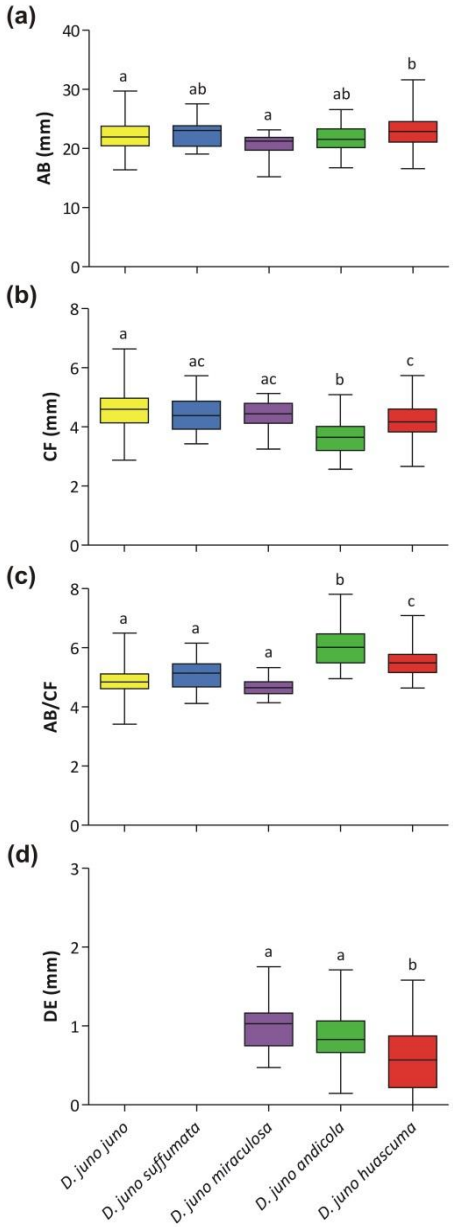

Figure 6 Measurements of the hindwing of *Dione juno* subspecies. (**a**) AB, length of the wing, (**b**) CF, width of the black bar, (**c**) AB / CF, ratio of the wing length in relation to the width of the black bar, and (**d**) DE, width of the eyespots in the black bar. Different letters represent significant differences between subspecies (Kruskal-Wallis test, followed by Dunn's multiple comparison tests, $P < 0.05$). See Figure 8 for details of measurements.

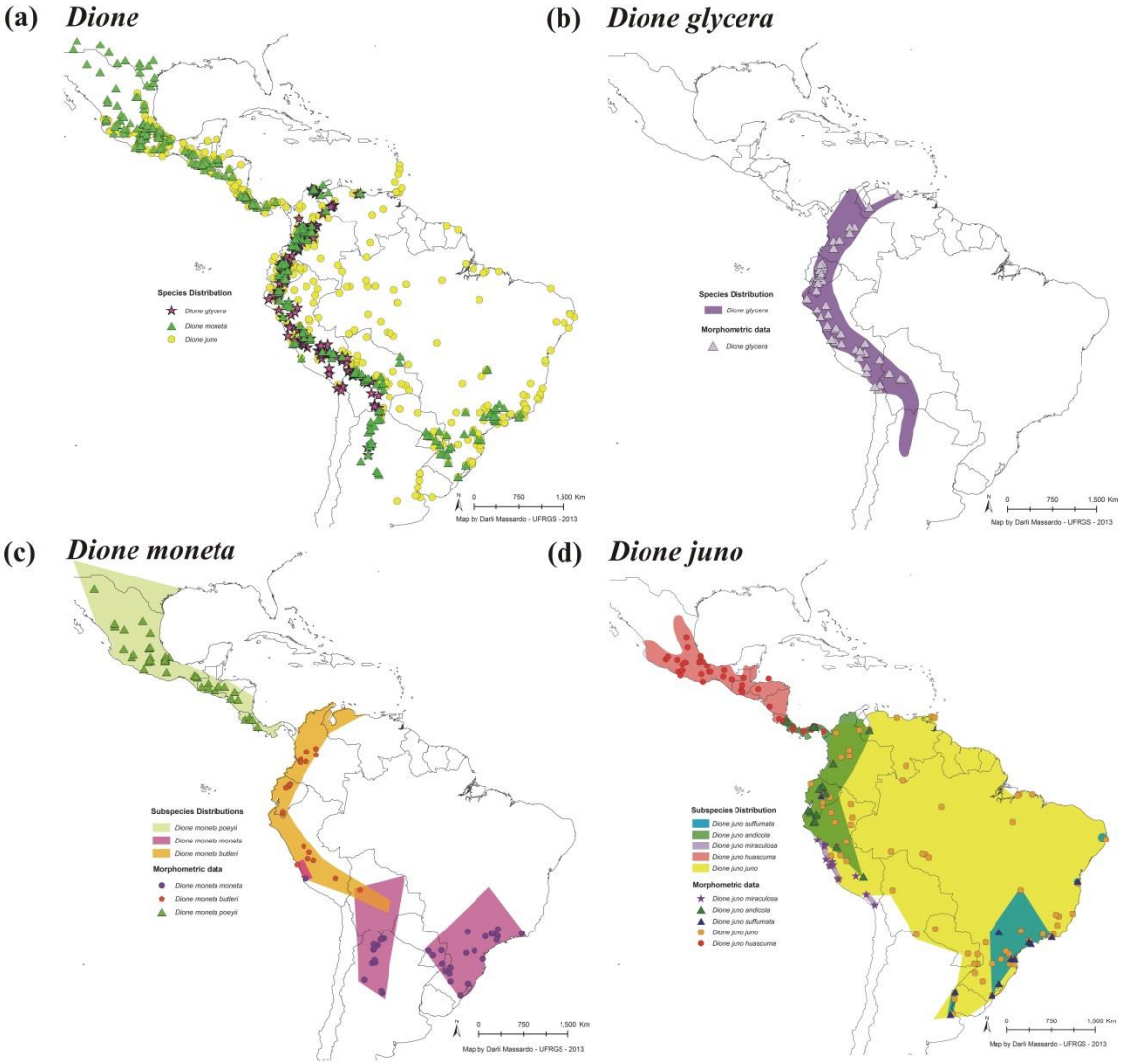

Figure 7 Geographical distributions of *Dione* species and subspecies. Polygons represent the geographical distribution for total specimens recovered from museum collections, and dots indicate only those used in the geometric morphometric analyses.

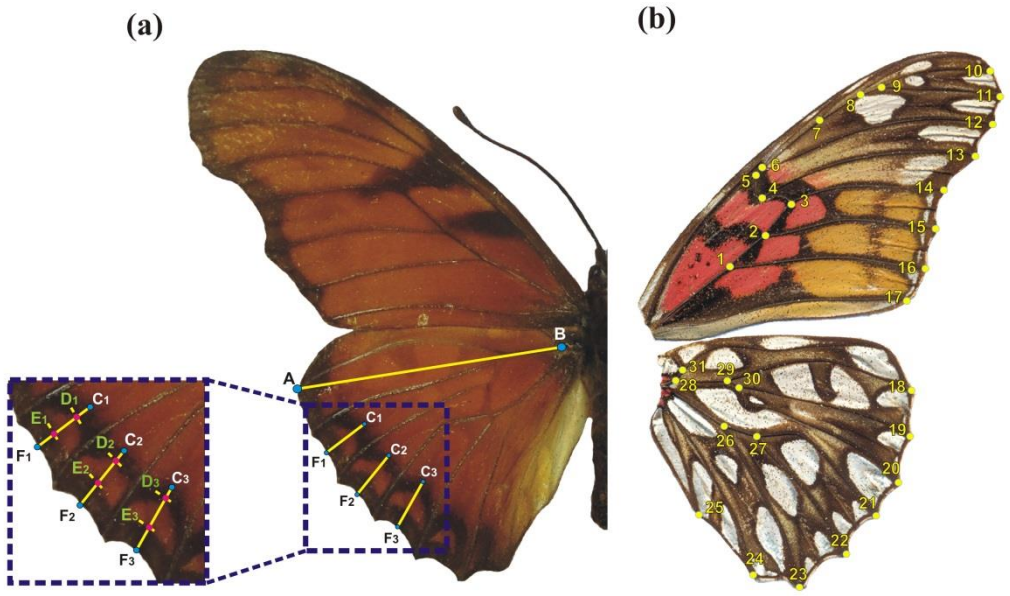

Figure 8 Linear measurements and landmarks used in geometric morphometric analyses of *Dione* wing. (**a**) Vectors measured on the hindwing, dorsal view. A-B, the wing length, from the joint of the Subcostal vein (Sc) and Sector-radial (Rs) to the distal end of the Rs. Detail (dotted squares): widths of the marginal black bar (C-F) and corresponding eyespots (D-E). (**b**) Landmarks (yellow dots), ventral view. Landmark descriptions are detailed in Additional file 12.

Table 1 Best-supported models of molecular evolution and estimated parameter values at family (Heliconiini) and genus (*Dione*) levels for each marker surveyed.

Level	Data set	*CO*	*16S*	*EF1-A*	*TH*	*WG*	*AP*	*DPP*
Heliconiini								
	Variable sites	398 (25%)	116 (22%)	144 (18%)	196 (27%)	122 (27%)	45 (24%)	85 (29%)
	Model	GTR+G+I	GTR+G+I	GTR+G+I	GTR+G	K2+G+I	GTR+G	GTR+G
	Base Frequencies							
	A	0.33	0.42	0.26	0.27	0.25	0.25	0.24
	T	0.41	0.37	0.23	0.23	0.25	0.21	0.21
	C	0.14	0.08	0.26	0.3	0.25	0.26	0.28
	G	0.12	0.13	0.25	0.2	0.25	0.27	0.27
	Substitution model							
	Tr/Tv ratio	2.18	0.36	3.08	2.87	4.37	4.12	2.63
	Invariable sites	0.57	0.34	0.6	N/A	0.65	N/A	N/A
	Gamma parameter	0.53	0.21	0.71	0.21	4.09	0.2	0.33
Dione								
	Variable sites	255 (16%)	45 (8%)	36 (4%)	81 (11%)	44 (9%)	19 (10%)	58 (20%)
	Model	GTR+G	GTR+G+I	TN93+G	TN93+I	K2+G	K2+G	T92
	Base Frequencies							
	A	0.34	0.42	0.26	0.27	0.25	0.25	0.23
	T	0.4	0.37	0.23	0.24	0.25	0.25	0.23
	C	0.14	0.08	0.26	0.29	0.25	0.25	0.27
	G	0.12	0.13	0.25	0.2	0.25	0.25	0.27
	Substitution model							
	Tr/Tv ratio	3.1	0.9	7.64	3.26	3	3.53	1.15
	Invariable sites	N/A	0.74	N/A	N/A	N/A	N/A	N/A
	Gamma parameter	0.13	0.81	0.05	0.46	0.15	0.05	N/A

Table 2 Divergence time estimates. Mean time ($\bar{x}$) to the most recent common ancestor (tMRCA), standard deviation (SD), and 95% credibility intervals (95% CI) in millions of years, calculated using a relaxed molecular clock on multilocus DNA sequences of Heliconiini lineages. Node letters correspond to those in Figure 2.

		Divergence time (tMRCA)		
Node	**Lineage**		**SD**	**95% CI**
A	All Heliconiini	30.1	0.01	26.2-33.9
B	*Agraulis* + *Dione*	20.55	0.02	13.5-27.5
C	Heliconiini except *Agraulis* + *Dione*	25.4	0.02	20.2-30.6
D	*Dryadula* + *Philaethria* + *Dryas* + *Podotricha*	21.1	0.01	14.8-26.9
E	*Dryadula* + *Philaethria*	15.7	0.01	10.3-21.3
F	*Dryas* + *Podotricha*	14.8	0.02	8.1-21.5
G	*Eueides* + *Laparus* + *Neruda* + *Heliconius*	19.4	0.02	13.6-25.2
H	*Laparus* + *Neruda* + *Heliconius*	14.2	0.02	8.8-19.6
I	*Laparus* + *Neruda*	11.3	0.01	6.1-15.1

Table 3 Heliconiini species included in the study, including sample locality and GenBank accession numbers for each marker sequenced.

Taxa	Locality	ID No.	GenBank accession number						
			CO	***16S***	***TH***	***EF1 alpha***	***AP***	***WG***	***DPP***
INGROUP									
Agraulis vanillae	Honduras	MRK-RH09-62	KF234580	KF277253	KF277301	KF277349	KF277476	KF277395	-
Agraulis vanillae vanillae	Colombia: Zarzal	LMCI103-01	KF234581	KF277254	KF277302	KF277350	KF277477	KF277396	-
		LMCI103-02	KF234582	KF277255	KF277303	KF277351	KF277478	KF277397	-
		LMCI103-03	KF234583	KF277256	KF277304	KF277352	KF277479	KF277398	-
Agraulis vanillae maculosa	Brazil: RS, Porto Alegre	LMCI158-60	KF234584	KF277257	KF277305	KF277353	KF277480	KF277399	-
		LMCI158-61	KF234585	KF277258	KF277306	KF277354	KF277481	KF277400	-
		LMCI158-62	KF234586	KF277259	KF277307	KF277355	KF277482	KF277401	-
Dione glycera	Chile: Socoroma	LMCI112-1	KF234587	KF277260	KF277308	KF277356	KF277483	KF277402	-
		LMCI112-2	KF234588	KF277261	KF277309	KF277357	KF277484	KF277403	KF277443
		LMCI112-3	KF234589	KF277262	KF277310	KF277358	KF277485	KF277404	KF277444
		LMCI112-4	KF234590	KF277263	KF277311	KF277359	KF277486	KF277405	KF277445
		LMCI112-5	KF234591	KF277264	KF277312	KF277360	KF277487	KF277406	KF277446
		LMCI112-6	KF234592	KF277265	KF277313	KF277361	KF277488	KF277407	KF277447
		LMCI112-7	KF234593	KF277266	KF277314	KF277362	KF277489	KF277408	-
Dione juno	Honduras	MRK-RH0962	KF234594	KF277267	KF277315	KF277363	KF277490	KF277409	KF277448
Dione juno juno	Brazil: SC, São Bento	LMCI110-384	KF234595	KF277268	KF277316	KF277364	KF277491	KF277410	KF277449
		LMCI110-385	KF234596	KF277269	KF277317	KF277365	KF277492	KF277411	KF277450
		LMCI110-386	KF234597	KF277270	KF277318	KF277366	KF277493	KF277412	KF277451
		LMCI110-387	KF234598	KF277271	KF277319	KF277367	KF277494	KF277413	KF277452
		LMCI110-388	KF234599	KF277272	KF277320	KF277368	KF277495	KF277414	KF277453
		LMCI110-389	KF234600	KF277273	KF277321	KF277369	KF277496	KF277415	KF277454
		LMCI110-390	KF234601	KF277274	KF277322	KF277370	KF277497	KF277416	KF277455
Dione moneta moneta	Brazil: RS, Porto Alegre	LMCI158-10	KF234602	KF277275	KF277323	KF277371	KF277498	KF277417	KF277456
		LMCI158-11	KF234603	KF277276	KF277324	KF277372	KF277499	KF277418	KF277457
		LMCI158-12	KF234604	KF277277	KF277325	KF277373	KF277500	KF277419	KF277458

		LMCI158-13	KF234605	KF277278	KF277326	KF277374	KF277501	KF277420	KF277459
		LMCI158-14	KF234606	KF277279	KF277327	KF277375	KF277502	KF277421	KF277460
		LMCI158-15	KF234607	KF277280	KF277328	KF277376	KF277503	KF277422	KF277461
		LMCI158-9	KF234608	KF277281	KF277329	KF277377	KF277504	KF277423	KF277462
Dryadula phaetusa	Brazil: Pará	LMCI100-34	KF234609	KF277282	KF277330	KF277378	KF277505	KF277424	KF277463
	Brazil: Paraná	LMCI84-5	-	KF277283	KF277331	KF277379	KF277506	KF277425	KF277464
	Honduras	MRK-RH0976	KF234610	KF277284	KF277332	KF277380	KF277507	KF277426	KF277465
Dryas iulia alcionea	Brazil: RS, Porto Alegre	LMCI159-41	KF234611	KF277285	KF277333	KF277381	KF277508	KF277427	-
		LMCI159-42	KF234612	KF277286	KF277334	KF277382	KF277509	KF277428	-
Dryas iulia	Honduras	MRK-RH09293	KF234613	KF277287	KF277335	KF277383	KF277510	KF277429	-
Eueides aliphera	Honduras	MRK-RH09411	KF234614	KF277288	KF277336	KF277384	KF277511	KF277430	KF277466
Eueides isabella dianasa	Brazil: SC, São Bento	LMCI110-230	KF234615	KF277289	KF277337	KF277385	KF277512	KF277431	KF277467
Euiedes isabela	Honduras	MRK-RH09166	KF234616	KF277290	KF277338	KF277386	KF277513	KF277432	-
Laparus doris	Honduras	MRK-RH09789	KF234617	KF277291	KF277339	KF277387	KF277514	KF277433	KF277468
Heliconius erato phyllis	Brazil: RS, Porto Alegre	LMCI159-1	KF234618	KF277292	KF277340	KF277388	KF277515	KF277434	KF277469
Heliconius melpomene nanna	Brazil: Espírito Santo	LMCI105-62	KF234619	KF277293	KF277341	KF277389	KF277516	KF277435	KF277470
Neruda aoede	Ecuador	MRK-RIH1509	KF234620	KF277294	KF277342	KF277390	KF277517	KF277436	KF277471
Philaethria wernickei	Brazil: SC, São Bento	LMCI110-5	KF234621	KF277295	KF277343	KF277391	KF277518	KF277437	KF277472
		LMCI110-4	-	KF277297	KF277345	KF277393	KF277520	KF277439	KF277474
Philaethria sp	Honduras	MRK-RH09359	KF234622	KF277296	KF277344	KF277392	KF277519	KF277438	KF277473
Podotricha telesiphe	Ecuador	MRK-RH10116	KF234623	KF277298	KF277346	KF277394	KF277521	KF277440	KF277475
OUTGROUP									
Actinote anteas	Honduras	MRK-RH0982	KF234624	KF277299	KF277347	-	KF277522	KF277441	-
Cethosia cyane	Thailand	MRK-10-1	KF234625	KF277300	KF277348	-	KF277523	KF277442	-

Table 4 Sample size of *Dione* specimens

Species	**Subspecies**	***N***
Dione juno	*D. juno juno*	200
	D. juno andicola	25
	D. juno huascuma	90
	D. juno miraculosa	15
	D. juno suffumata	21
Dione moneta	*D. moneta moneta*	98
	D. moneta butleri	65
	D. moneta poeyii	85
Dione glycera	-	130
Total:		729

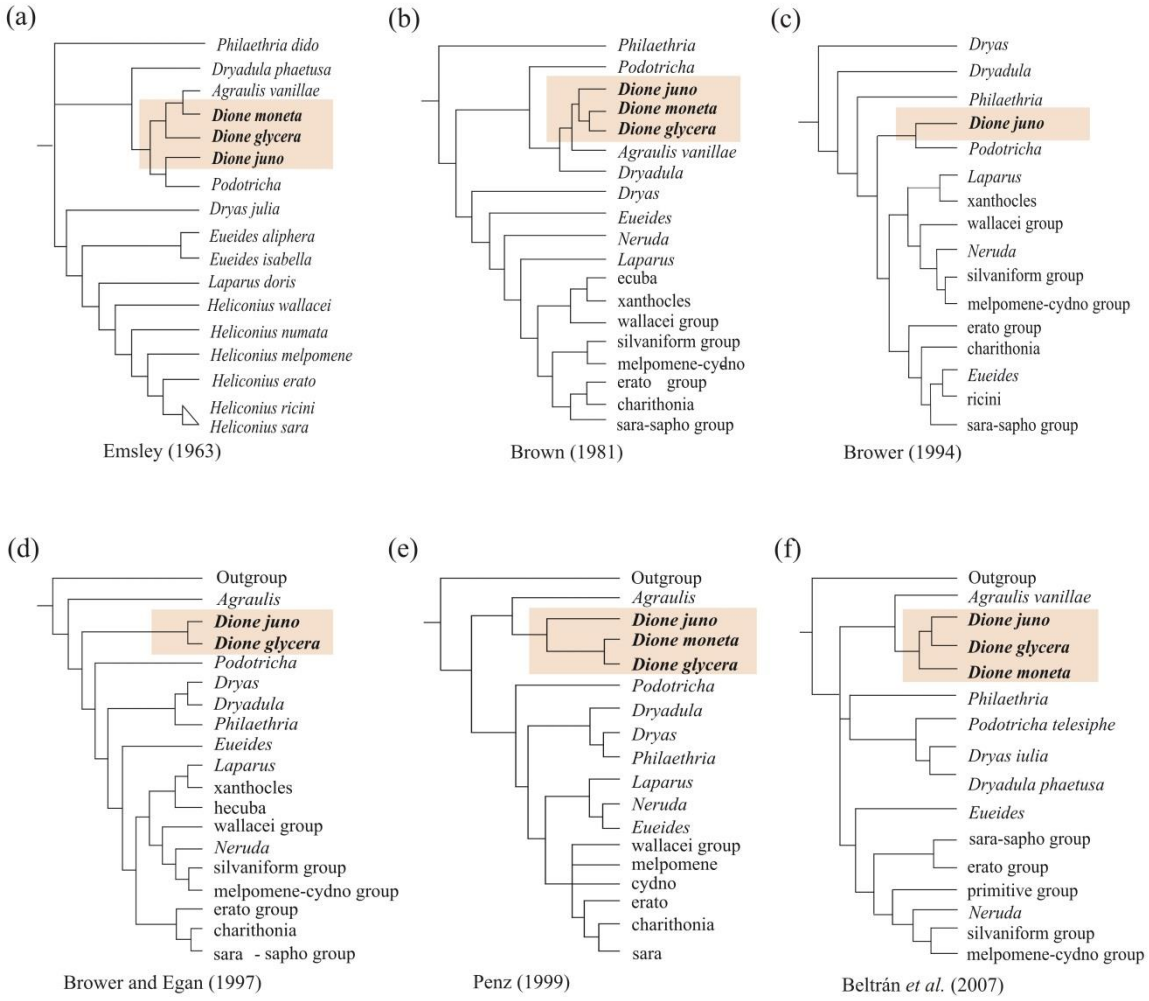

Additional file 1: Summary of major phylogenetic hypotheses for Heliconiini butterflies published in the last 50 years. (**a**) Emsley [3], based on morphological characters; (**b**) Brown [6], based on morphological and ecological characters; (c) Brower [7], based on the mitochondrial markers COI and COII; (d) Brower & Egan [8], based on mitochondrial (COI, COII) and nuclear (*Wg*) markers; (e) Penz [9], based on morphological characters; and (f) Beltrán *et al.* [32], based on mtDNA and nuDNA markers. Boxes in pale brown indicate the position of *Dione*.

Additional file 2: Table S1. Wing shape pairwise MANOVA comparison among the three species of genus *Dione*.

	Dione juno	***Dione glycera***
Dione glycera	290.860*; 187.270*	-
Dione moneta	396.990*; 275.640*	70.233*; 63.761*

First and second records are the *F* values for the fore- (FW) and hindwing (HW), respectively. * $p < 0.001$.

Additional file 3: Table S2. Wing shape pairwise MANOVA comparison among the subspecies of *Dione juno*.

	D. juno andicola	***D. juno huascuma***	***D. juno juno***	***D. juno miraculosa***
D. juno huascuma	2.256*; 3.025*	-		
D. juno juno	2.731*; 5.433*	8.603*; 11.267*	-	
D. juno miraculosa	3.150; 18.780*	6.129*; 12.949*	9.256*; 17.050*	-
D. juno suffumata	5.059*; 7.526*	6.557*; 7.699*	2.406*; 2.720*	6.748; 15.580*

First and second records are the *F* values for fore- (FW) and hindwing (HW), respectively. * $p < 0.001$.

Additional file 4: Table S3. Cross-validation percentages of correct classification based on wing shape for the subspecies of *Dione juno*, based on fore- (FW) and hindwing (HW).

Subspecies	**FW**	**HW**
D. juno andicola	32	32
D. juno huascuma	70	74.44
D. juno juno	91.5	89
D. juno miraculosa	80	100
D. juno suffumata	33.33	19.5

Additional file 5: Table S4. Wing shape pairwise MANOVA comparison among subspecies of *Dione moneta*.

	D. moneta moneta	***D. moneta butleri***
D. moneta butleri	9.699*; 9.010*	-
D. moneta poeyii	15.149*; 12.017*	8.939*; 4.553*

First and second records are the *F* values for fore- (FW) and hindwing (HW), respectively. * $p < 0.001$

Additional file 6: Table S5. Cross-validation percentages of correct classification based on wing shape for the subspecies of *Dione moneta*, based on fore- (FW) and hindwing (HW).

Subspecies	**FW**	**HW**
D. moneta moneta	87.75	82.65
D. moneta butleri	83.08	64.61
D. moneta poeyii	90.59	78.82

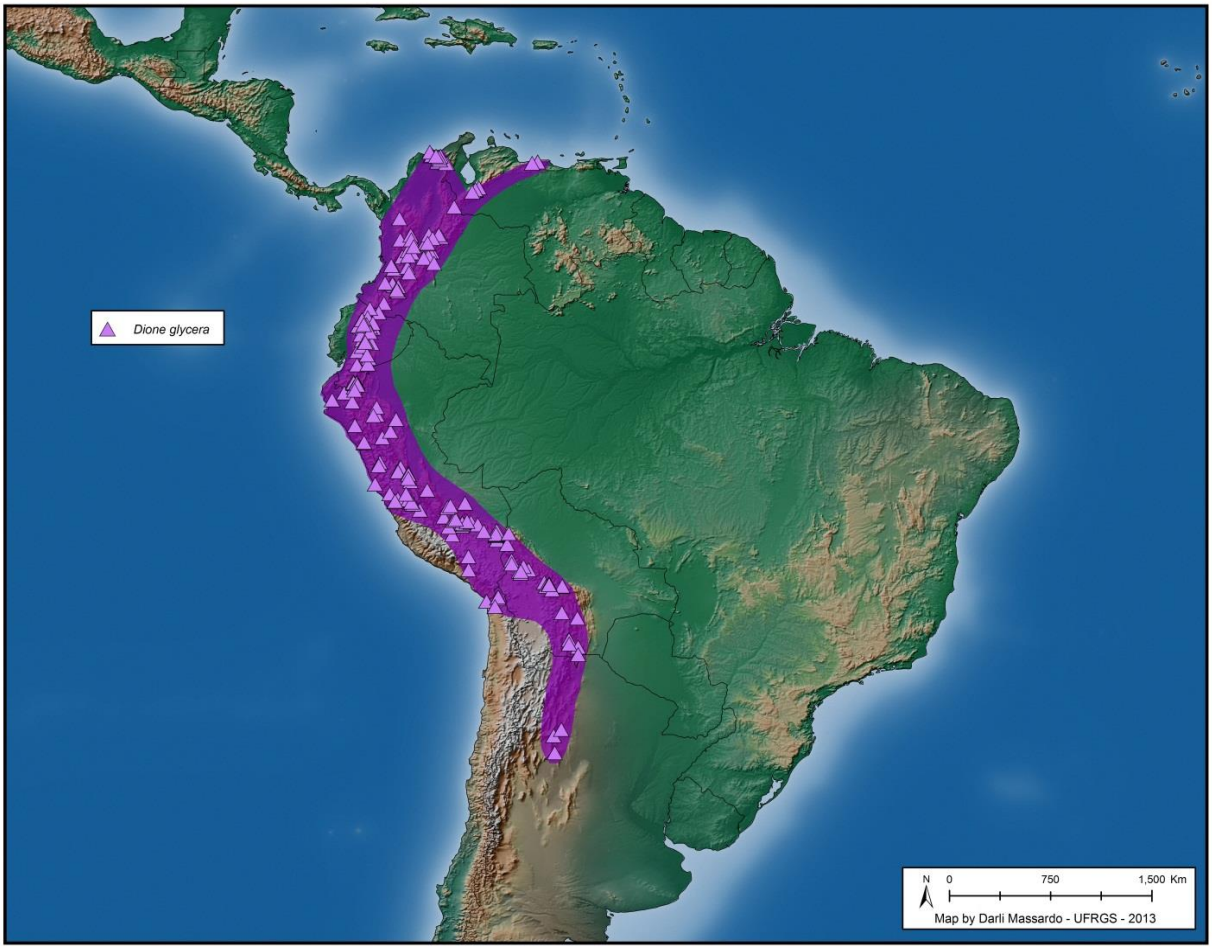

Additional file 7: Geographical distribution of *Dione glycera*, including data from Rosser et al. (2012).

Additional file 8: Geographical distributions of *Dione moneta* subspecies, including data from Rosser et al. (2012).

Additional file 9: Geographical distributions of *Dione juno* subspecies, including data from Rosser et al. (2012).

Additional file 10: Table S6. Description of primers.

Gene	Name	Sequence (5' to 3')
COI	C1-J-2183	CAACATTTATTTTGATTTTTTGG
	C1-J-2783	CCAACAGGAATTAAAATTTTTAGATGATTAGC
tRNA-Leucine	TL2-N-3014	TCCAATGCACTAATCTGCCATATTA
COII	C2-N-3812	CATTAGAAGTAATTGCTAATTTACTA
16S ribosomal (*16S*)	16Sar1	CCCGCCTGTTTATCAAAAACAT
	Ins16Sar	CCCTCCGGTTTGAACTCAGATC
Elongation factor 1alpha (*Ef-1α*)	Ef1-H-f	GAGAAGGAAGCCCAGGAAAT
	Ef1-H-r	CCTTGACRGACACGTTCTTT
Apterous (*Ap*)	ap-f35	TGAATCCTGAATACCTGGAGA
	ap-r224	GGAACCATACCTGTAAAACCC
Decapentaplegic (*dpp*)	dpp-f34	AGAGAACGTGGCGAGACACTG
	dpp-r327	GAGGAAAGTTGCGTAGGAACG
Wingless (*Wg*)	LepWG1	GARTGYAARTGYCAYGGYATGTCTGG
	LepWG2a	ACTNCGCARCACCARTGGAATGTRCA
Tyrosine Hydroxylase (*Th*)	TH2-f	ATTATACTCTGACCGAAGAAG
	TH2-r	TGTGTAGATTGGAAAACACGG

Additional file 11: Table S7. Insect collection descriptions.

Acronym*	Name	Number of records
DZUP	Coleção Entomológica "Pe. Jesus Moure", Universidade Federal do Paraná, Curitiba, Brazil	108
LMCI	Coleção de Tecidos, Laboratório de Morfologia e Comportamento de Insetos, Departamento de Zoologia, Universidade Federal do Rio Grande do Sul, Porto Alegre, Brazil	78
MCTP	Museu de Ciências, Pontifícia Universidade Católica do Rio Grande do Sul, Porto Alegre, Brazil	32
MNRJ	Museu Nacional, Universidade Federal do Rio de Janeiro, Rio de Janeiro, Brazil	75
MPEG	Museu Paraense Emílio Goeldi, Ministério da Ciência e Tecnologia, Belén, Brazil	18
MZSP	Museu de Zoologia, Universidade de São Paulo, São Paulo, Brazil	31
FSMC	Florida Museum of Natural History, Allyn Museum, University of Florida, Gainesville, USA	396
MCZ	Museum of Comparative Zoology, Harvard University, Cambridge, USA	55
MUSM	Museo de Historia Natural da Universidad Nacional Mayor de San Marcos, Lima, Peru	168
IDEA	Colección Entomológica, Facultad de Ciencias Agronómicas de Tarapacá, Arica, Chile	7
MLPA	Museo de La Plata, La Plata, Argentina	50
MACN	Museo Argentino de Ciencias Naturales "Bernardino Rivadavia", Buenos Aires, Argentina	45
IFML	Museo Miguel Lillo de Ciencias Naturales, Tucumán, Argentina	51
USNM	National Museum of Natural History, Smithsonian Institution, Washington DC, USA	292
Total		1406

* according to: Evenhuis, N.L. (1993) Abbreviations for insect and spider collections of the world. Available at: http://hbs.bishopmuseum.org/codens/codens-inst.html [Last accessed: September 18, 2013].

Additional file 12: Table S8. Landmark descriptions.

Landmark		Description
Forewing	01	Proximal extremity of the cubital vein 2 (CuA2)
	02	Proximal extremity of the cubital vein 1 (CuA1)
	03	Proximal extremity of the median vein 3 (M3)
	04	Proximal extremity of the median vein 2 (M2)
	05	Proximal extremity of the median vein 1 (M1)
	06	Proximal extremitey of the radial vein 1 (R1)
	07	Proximal extremity of the radial vein 2 (R2)
	08	Proximal extremity of the radial vein 3 (R3)
	09	Proximal extremity of the radial veins 4 and 5 (R4 e R5)
	10	Distal extremity of the radial vein 4 (R4)
	11	Distal extremity of the radial vein 5 (R5)
	12	Distal extremity of the median vein 1 (M1)
	13	Distal extremity of the median vein 2 (M2)
	14	Distal extremity of the median vein 3 (M3)
	15	Distal extremity of the cubital vein 1 (CuA1)
	16	Distal extremity of the cubital vein 2 (CuA2)
	17	Distal extremity of the anal vein 1 (A1)
Hindwing		
	18	Distal extremity of the radial sector vein (Rs)
	19	Distal extremity of the median vein 1 (M1)
	20	Distal extremity of the median vein 2 (M2)
	21	Distal extremity of the median vein 3 (M3)
	22	Distal extremity of the cubital vein 1 (CuA1)
	23	Distal extremity of the cubital vein 2 (CuA2)
	24	Distal extremity of the anal vein 2 (2A)
	25	Distal extremity of the anal vein 3 (3A)
	26	Proximal extremity of the cubital vein 2 (CuA2)
	27	Proximal extremity of the median vein 3 (M3) and cubital vein 1 (CuA1)
	28	Intersection between the radial subcostal vein (R1+Sc) and sector vein (Rs+M1+M2)
	29	Intersection between the radial sector vein (Rs) and median veins 1 and 2 (M1+M2)
	30	Proximal extremity of the median veins 1 and 2 (M1+M2)
	31	Proximal extremity of the humeral vein (H)

5. CONSIDERAÇÕES FINAIS

Dando continuidade a uma série de estudos que vem sendo desenvolvidos sobre a descrição da morfologia externa dos estágios imaturos de heliconíneos neotropicais, descreveu-se neste estudo pela primeira vez os imaturos de *Dione glycera.* Comparou-se a morfologia e a ultraestrutura tegumentar externa do ovo, das larvas de primeiro e quinto ínstar e da pupa com as demais espécies de *Dione*. Obteve-se caracteres morfológicos estáveis, com exceção do estágio de ovo, para distinguir todas as três espécies que compõem o gênero, apresentando-se assim uma chave dicotômica para os mesmas. A morfologia do ovo em *Dione* é facilmente distinguível do apresentado no grupo irmão *Agraulis*, entretanto não foram encontradas diferenças que separem *D. glycera* das espécies co-específicas. No primeiro instar larval distinguimos as espécies por meio da quetotaxia, especificamente as características do ápice das cerdas dorsais presentes no tórax e abdômen e das cerdas cefálicas póstero-dorsal P2 e lateral L1. Para o quinto instar larval utilizamos como características diagnósticas a presença/ausência de escolos na placa protorácica dorsal, bem como o tamanho do escolo cefálico em relação à cabeça. No estágio pupal distinguimos e utilizamos como características para separar as espécies na chave dicotômica a presença/ausência de manchas douradas ou prateadas e o formato da projeção cefálica.

Apesar das dificuldades do isolamento de microssatélites para Lepidoptera, obtivemos um total de 19 *loci* polimórficos para *D. moneta*, onde foram detectados de 1 a 13 alelos por locus. A maioria dos *loci* apresentou baixa heterozigosidade observada com desvio de equilíbrio de Hardy-Weinberg significativo em 12 dos 19 estudados. Tal fato pode ser explicado pela presença de alelos nulos, característica comum para microssatélites em Lepidoptera, e também pelo fato de *D. moneta* ser uma borboleta migratória causando assim uma possível mescla de indivíduos com frequências alélicas diferentes que resultam em

défice de heterozigotos nas populações. A maioria dos *loci* amplificou com sucesso também nas demais espécies e subespécies de *Dione* e de *Agraulis vanillae*, demonstrando que estes marcadores podem fornecer ferramentas eficientes para estudos de estrutura genética de populações de *D. moneta* bem como em espécies de borboletas proximamente relacionadas.

Por fim, investigou-se a história evolutiva de *Dione* através de uma abordagem integrativa utilizando dados de morfometria geométrica e marcadores moleculares, demonstrando-se que o gênero forma um clado monofilético e grupo irmão de *Agraulis*. Observamos também que as espécies de *Dione* são monofiléticas, formando grupos genéticos e fenotipicamente distinguíveis fenotipicamente, e, portanto, válidos do ponto de vista taxonômico.

Porém, ao analisarmos os padrões de diferenciação entre as subespécies de *D. juno* e *D. moneta* encontramos forte sobreposição no padrão de coloração das asas, as quais não são alopátricas em sua distribuição, e, portanto, supostamente hibridizaram ao longo de sua distribuição. Como conseqüência, uma vez que estas subespécies não são totalmente diagnosticáveis fenotípicamente, questionamos a validade e utilidade destes taxa, quer como entidades taxonômicas ou unidades evolutivas.

Estimativas do tempo de divergência entre as linhagens de Heliconiini obtidas sugerem fortemente que a especiação do gênero *Dione* coincidiu com a ascensão de Passifloraceae e o soerguimento da Cordilheira dos Andes. Tal hipótese é reforçada pelo fato de que as espécies irmãs *D. glycera* e *D. moneta* são especialistas de linhagens de passifloráceas endêmicas desta região, inferindo que as mesmas co-especiaram nos Andes. Os resultados obtidos neste estudo demonstram que a utilização de um grande número amostral ao longo de uma ampla área de cobertura da distribuição geográfica, associadas a abordagens taxonômicas integrativas, é essencial para determinar os limites de espécies e

subespécies não só em borboletas da família Nymphalidade, mas dentro de um cenário amplo de estudos taxonômicos e biogeográficos.